FABRICATION AND CHARACTERIZATION OF PIEZOELECTRIC NANOCOMPOSITE GUM SENSOR

BY

EMMANUEL ADEBAYO ADEJUMO

A thesis submitted to the faculty of Graduate Studies of the University of Manitoba in partial fulfillment of the requirements for the degree of

MASTER OF SCIENCE

Department of Mechanical Engineering,

University of Manitoba. Winnipeg

Canada

ACKNOWLEDGEMENT

I am using this medium to express my utmost and deepest appreciation to my supervisors; Dr. Nan Wu and Dr. Olarenwaju Ojo. Thank you so much for your intellectual guidance, encouragement, patience, and love towards the completion of this research work. I would also like to appreciate Dr. Stefan Cenkowski for granting access to the MTS tensile testing machine in his laboratory which was an important part of my research.

I also want to appreciate the University of Manitoba for the awards of International Graduate Student Entrance Scholarship and Manitoba Graduate Scholarship towards the support of my thesis.

I am also grateful to family, friends and colleagues, Dada Taiwo, Osho Samuel, Asala Gbenga, Aina Oluyemi, Oguntuase Oluwasanmi, Adu James, Deborah Michael, Chidima Anyawu, Ibrahim Abdulganiyu, Dr. Lina Zhang and Dr. Osoba. I also want to appreciate Sviatoslaw Karnaoukh and Trevor Smith for their technical assistance in the use of some of the facilities.

My sincere appreciation also goes to my late dad, mum, brothers, and wife for their support and prayers throughout the master's thesis. Above all, I am forever grateful to the Almighty God; the giver and the author of all things, for giving me wisdom, knowledge, and understanding to complete this program.

DEDICATION

I dedicate this master's thesis to

The Almighty God for the divine wisdom, love, and guidance throughout my master's thesis and even beyond. I also dedicate this thesis to my late father, my awesome mother and my wife who have always been there for me

List of Acronyms

List of Acronyms	Description
A_1	Area of the metal electrode
A_2	The cross-sectional area of the conductor
$BaTiO_3$	Barium Titanate
C	The capacitance of the gum sensor
CNTs	Carbon nanotubes
D	Charge density
d_{11}	Piezoelectric coefficient
F	Average force applied to the gum sensor
FOS	Fiber optics sensors
FRPC	Fiber reinforced polymer composite
GnPs	Graphene platelets
IDT	Interdigitated transducer
KCl	Potassium chloride

List of Acronyms

List of Acronyms	Description
L	Length of the conductor
MWCNTs	Multi-walled carbon nanotubes
NDT	Non-destructive testing
NW	Nanowires
PEN	Polyethylene Naphthalate
PMMA	Polymethyl methacrylate
P3OT	Poly (3-octylthiophene)
PSNF	Polystyrene nanofillers
PSS	Poly (sodium 4-styrene sulfonate)
PVA	Poly (vinyl alcohol)
PVDF	Poly Vinylidene Fluoride
PVDF-TrFe	Poly (vinylidene fluoride trifluoroethylene)
PZT	Lead Zirconate Titanate

List of Acronyms

List of Acronyms	Description
Q	Total charge generated
R	Resistance
R_o	Initial Resistance
R_f	Final Resistance
S	Stress applied to the gum sensor
SHM	Structural Health Monitoring
SWCNTs	Single-walled carbon nanotubes
TeFE	Tetrafluoroethylene
UTS	Ultimate tensile strength
V	Average voltage generated
VDF	Vinylidene Fluoride
Wt %	Wt %
ZnO	Zinc Oxide

Abstract

The initiation of cracks and the state of a structure can be monitored using a Structural Health Monitoring (SHM) techniques. Various types of sensors are used for SHM but nowadays, piezoelectric sensors are widely used for SHM and human body motion detection due to its low power requirement and production of charge output. These sensors can also be used for both static and dynamic human motion detection, artificial skin, forces, and acoustic vibration detection. In this research, the piezoelectric nanocomposites gum sensors are fabricated by direct mixing of constituent materials (ZnO and CNTs) with bubble gum. SWCNTs and MWCNTs are used in order to compare the effect of their addition to the gum sensor. The mixing process is achieved by multiple folding and stretching of the gum after the addition of the constituent materials. This is done to allow for relative homogenous distribution of the constituent materials in the gum. The result from the resilience test indicates that the constituent materials properly adhered to the surface of the gum. The piezoelectric calibration done on the gum sensor revealed that the addition of SWCNTs gives higher piezoelectric coefficient when compared to the addition of MWCNTs. The highest piezoelectric coefficient is observed with 90.9 wt % of ZnO and 9.1 wt % of SWCNTs in ZnO-SWCNTs gum sensor. The effects of two parameters (temperature and strain) are considered on the sensor resistance to further evaluate the piezoelectric performance of the gum sensors. The results show that ZnO-MWCNTs gum sensor has higher resistance as compared to ZnO-SWCNTs gum sensor, which implies that ZnO-SWCNTs gum sensor has a better piezoelectric performance. The mechanical strengths results show that ZnO-SWCNTs gum sensor has the best mechanical strength as compared to ZnO-MWCNTs gum sensor and ZnO gum sensor.

Table of Contents

LIST OF FIGURES

LIST OF TABLES

CHAPTER 1- Introduction

1.1Background Information

Failure of structures such as buildings, highway, aircraft, bridges, ships, pipelines is usually accompanied by catastrophic consequences such as loss of life and restricted commerce [1-3]. In order to prevent such catastrophic failure, it is, therefore, necessary to continuously monitor the state of the structure and identify any initiation in real time with the help of Structural Health Monitoring (SHM) technique. Damage to engineering structures are inevitable due to the load they are been subjected to but the monitoring techniques ensure that such damages are detected early enough. Through analytical methods and instrumentation system, SHM provides an independent way of tracking real-time changes in a system [4-5]. For instrumentation systems, transducers are primarily used to measure quantities such as displacement, strain, and acceleration which can give an insight of the response of the structure to deformation.

In recent times, the discovery of materials such as carbon nanotubes has led to a lot of research in the area of sensors used for SHM based on nanostructures and their composites. Strain gauges or transducers can be broadly classified into resistance-based sensors, optical sensors and piezoelectric sensors [6]. Compared to other types of sensors, piezoelectric sensors have the lowest power requirements and it produces charge output that lies within the range of measurement capabilities of commercially available digital/analog sensors. Piezoelectric sensors are based on the principle of piezoelectricity. Piezoelectricity is a phenomenon observed in non-centrosymmetric crystals in which the application of stress leads to an electric polarization (charge) been induced in the material. Conversely, with the application of an electric field, a mechanical deformation is produced [7]. Katzir [8] presented a historical background on the discovery of the piezoelectric effect. The first piezoelectric effect referred to as the direct piezoelectric effect was discovered by the Curie brothers in 1800. It was observed in certain crystals such as quartz, topaz, cane sugar, tourmaline, zincblende. The second effect known as the converse piezoelectric effect which was theoretically proven by Lippmann shortly before the Curies brothers proved it experimentally. Piezoelectricity can be induced in polymers such as nylon and copolymers of Vinylidene Fluoride (VDF) with tetrafluoroethylene (TeFE) [9]. However, most of the piezoelectric materials used for commercial sensing applications are from synthetic polycrystalline ferroelectric ceramics such as Lead Zirconate Titanate (PZT).

There are several methods used in damage detection which include optical fiber method [10,11], frequency changes [12,13], mode shape changes, ultrasonic wave method [14], dynamically measured flexibility, neural network-based methods [15], matrix update methods, acoustic emission methods, non-linear methods, piezoelectric transducers [16] and many more. These methods have been used by different researchers in the detection of damages in structures. Duggan and Ochoa [13] characterized the vibration responses of damaged fiber reinforced plates based on the effect of the material system, stacking sequence, and geometry. The research focused on the natural frequency alteration on the damage detection in structures. Al-said and Al-Qaisa [17] studied the effect of location of attached masses and crack depth on natural frequency alteration of a system. This was achieved through the free vibration of a clamped-clamped cracked beam with different attached point loads along the length of the beam. Rahman et al. [12] studied the effect of open cracks was investigated in rotor shaft using a frequency response function (FRF) phase changes. The frequency response at different points on the shaft was measured, it was observed that the vibration behavior of the shaft is extremely sensitive to crack location, crack depth and mode number.

Sensors can be classified broadly into flexible [18] and non-flexible [19]. Flexible sensors are fabricated from malleable materials without altering their properties whereas, non-flexible sensors are made from brittle and rigid materials. Although non-flexible sensors are used for different applications, they have some limitations such as intransigence, stiffness etc. These limitations become imminent when the physiological parameters of human beings are being monitored or when a large stress is required to be applied to the sensor. This led to an alternative approach of fabricating a sensor that can be used dynamically and capable of withstanding impact load without failing easily.

Nowadays, a lot of sensors used for SHM and human dynamic motions are developed from piezoelectric materials such as Zinc Oxide (ZnO), Poly Vinylidene Fluoride (PVDF), Barium Titanate ($BaTiO_3$) and Lead Zirconate Titanate (PZT); these materials have advantages and limitations for SHM applications. Lead Zirconate Titanate (PZT) is one of the most commercially used piezoelectric material which finds its application as sensors and electric actuators. When used as strain sensors, they are usually embedded inside or bonded on the surface of the matrix material for strain measurement and can only measure strain at the fixed direction and discrete points. Most pure piezoelectric materials are brittle ceramics that cannot be used for flexible applications and they are weak in tension [20].

1.2 Motivation

Due to the brittle nature of most pure piezoelectric material and due to the fact that they cannot be used in flexible application, so many studies have been done on the fabrication of flexible piezoelectric sensors or actuators. Most of these flexible sensors/actuators require special technologies, therefore, making it uneconomical for large-scale production of such sensors [21, 22]. Although other materials were also used for flexible strain sensors, they lack unique properties of piezoelectric materials or involves complicated fabrication techniques. In a research carried out by Qingliang et al [23], a piezoelectric nanogenerator was fabricated consisting of ZnO nanowires (NWs) on carbon fibers and foldable Au-coated ZnO NWs on paper using a two-step hydrothermal growth approach. Another study was carried out by Xu et al. [24] reported the fabrication of a flexible sensor by growing of ZnO Nanowires on polystyrene nanofibers (PSNF) through the immobilization of the seed onto the PSNFs followed by a hydrothermal process.

There are so many publications on the fabrication of flexible piezoelectric sensors [21-24]. In most cases, the piezoelectric materials are usually bonded to the surface or embedded inside the host structure for strain measurement- they have limitations of measuring strain at discrete points and fixed direction. Kymakis et al [25] fabricated a polymer composite by embedding single-walled carbon nanotubes (SWCNTs) in the polymer matrix. This was achieved by drop casting of the nanotube/poly (3-octylthiophene) (P3OT) mixture dissolved in chloroform. It was observed that the conductivity of the polymer composite increases with an increase in the weight percent of the SWCNTs.

There are several methods used for the fabrication of nanocomposites, the most commonly used techniques are: injection molding [26], spin coating [27][28], solvent casting [29][30], melt mixing [26], in-situ polymerization [31][32], coagulation spinning [33], latex fabrication [34][35], electrophoretic deposition [36], twin screw pulverization [37] and compression molding [38]. Each of these methods has its pros and cons; the whole essence is to achieve even distribution of the nanomaterials in the host structure or matrix.

In spite of a whole lot of contributions in the area of flexible composite sensors, they still have some limitations such as strain measurements at only discrete points and fixed direction, expensive and complex fabrication techniques, low piezoelectric output and low mechanical strength. With the recent research and advent technology in the area of strain sensors based on nanostructures [39][40] and their composite[41-45], it has accelerated the discovery of nanomaterials such as carbon nanotubes which can be used to enhanced the piezoelectric and mechanical performance of naturally occurring piezoelectric material, thereby leading to fabrication of piezoelectric nano-composites sensor. Vemuru et al. [46] developed a sensor using a multiwalled carbon nanotube film for structural health monitoring. Other studies [47] [48] also indicated the possibility of using carbon nanotubes as the major material in the fabrication of nanocomposite sensors.

As a result of technological improvement in the area of structural health monitoring (SHM), different work has been done to improve the fabrication method of piezoelectric sensors. One of the present limitations of these sensors is the complex fabrication method involved and hence an increased overall cost. Therefore, there is a need to fabricate sensors using simple fabrication technique and exhibit excellent.

1.3 Research Objective

The aim of this research is to fabricate and characterize a simple, scalable, inexpensive and mechanically flexible static and dynamic sensor that can be embedded into a material or form fitted easily into an existing structure. This sensor can be potentially used for structural health monitoring with large structural strain and also for static and dynamic human motion detection such as finger, elbow, knee and throat motions.

1.4 Research Scope

The scope of this research work is limited to the use of Zinc oxide (ZnO) nanoparticles and how its piezoelectric effect can be optimized by the addition of CNTs. Both single-walled carbon nanotubes and multi-walled carbon nanotubes were added to the ZnO nanoparticles. The reason for choosing ZnO is that it exhibits the strongest piezoelectric coefficient when compared to the piezoelectric materials apart from the PZT ceramics [49] [50]. The ZnO and CNTs nanoparticles were embedded into the gum by multiple stretching and folding technique. Two metal plates were placed on both sides of the gum sensors and were excited via static loading during the piezoelectric calibration.

1.5 Methodology

To fabricate and calibrate the piezoelectric nanocomposite sensor, bubble gum which was used as the matrix was chewed for 30 minutes and the chewed gum was washed in ethanol and distilled water overnight. The gum was left at room temperature to allow the excess water in the gum to evaporate and achieve a stable weight. Different weight percent (wt.%) of the ZnO and CNT nanoparticles were added to the surface of the gum. The gum was then stretched and folded multiple time in one direction to allow the particle to align.

The experimental procedures used in the characterization of the piezoelectric gum sensor include piezoelectric calibration, mechanical testing, temperature dependence testing. For the piezoelectric testing, the gum was placed in between two steel plate of 20mm by 20mm and was sealed round with Cantech tape. The piezoelectric calibration was done using the LMS Data Acquisition system which gives an accurate measurement of the static force applied and the voltage generated from the sensor when mechanically deformed. The mechanical properties of the piezoelectric sensor were evaluated by subjecting the gum sensor to a tensile load and at the resistance of the sensor was measured simultaneously during the mechanical testing. The temperature dependence testing was done by attaching the gum sensor to the outside of a container filled with water. The container was placed on the plate heater with magnetic bar rotating inside. The temperature of the heater was increased while the resistance was measured with a two-probe multimeter.

1.6 Major Findings

This research confirms the possibility of fabricating a stretchable, attachable and low-cost piezoelectric gum sensor by direct mixing of Zinc Oxide (ZnO) and Carbon nanotubes (CNTs) with the gum. The results validate that the piezoelectric property of nanocomposites made from ZnO can be improved by the addition of carbon nanotubes. The results obtained from the piezoelectric calibration of the gum sensor show that there is a threshold amount (9.1wt %)of CNTs that can be used for the fabrication of the piezoelectric nanocomposite gum sensor beyond which the piezoelectric coefficient of the gum sensor begins to drop. The resilience test that was carried out on the piezoelectric gum sensors confirmed that the constituent materials (ZnO and CNTs) adhered properly to the surface of the gum. The effects of temperature and strain on the sensor resistance were considered and the results indicate that ZnO-MWCNTs gum sensor has a higher resistance as compared to ZnO-SWCNTs gum sensor. This implies that ZnO-SWCNTs gum sensor has better piezoelectric property as compared to ZnO-MWCNTs gum sensor. Finally, the mechanical strengths results show that ZnO-SWCNTs piezoelectric gum sensors have the best mechanical properties when compared to ZnO piezoelectric gum sensor and ZnO-MWCNTs piezoelectric gum sensors.

1.7 Thesis Organization

This thesis consists of 6 chapters and it is organized as follows:

- **Chapter 1** contains the introduction which consists of the background information, the motivation for the work, research objectives, research scope, methodology and thesis structure.
- **Chapter 2** is the literature review which gives a general overview of the constituent materials (ZnO and CNTs), their properties and the application of nanocomposites material with ZnO and CNTs-enhanced films as the major constituent. The different methods that can be used for the fabrication of nanocomposites were discussed. Lastly, a robust literature review was done on structural health monitoring, the stages of damage growth in structures.
- **Chapter 3** provides details on the sensor fabrication and testing methodologies and instruments used in the research
- **Chapter 4** provides the results of the experimental work carried out and its analysis
- **Chapter 5** contains a summary of the major findings, conclusions and presents recommendations for future work.

CHAPTER 2-Literature Review

This section provides a robust literature review of Zinc Oxide and Carbon-nanotubes, their properties and application. It then entails a close review of the recent works on ZnO-CNT nanocomposites, nanocomposites fabrication methods and the application of piezoelectric composite materials for structural health monitoring (SHM), human motion detections and various applications.

2.1 Zinc Oxide (ZnO)

Zinc Oxide is naturally occurring n-type semi-conductor and has been used in so many researches in the past few years due to its unique and prosperous properties. The first paper on ZnO was published in the 30s, the research has been fluctuating due to the difficulty involved in obtaining a stable p-type doping [51]. However, ZnO in its nanostructured form makes it possible to integrate ZnO with other p-type materials. The possibility of integrating ZnO with other p-type materials has made the research of ZnO an intense area of research for the past few years. ZnO is an II-IV semiconductor that has a direct band gap of 3.34eV and possesses a relatively large exciton binding energy of 60meV at room temperature. Due to its high stable non-centrosymmetric hexagonal wurtzite structure, it has high piezoelectric tensor, a relatively large piezoelectric coefficient and a high modulus of elasticity. Due to these outstanding properties, it has been studied by a lot of researchers. ZnO exhibits peculiar properties most especially in its nanostructured form and it is used for applications such as photonics, sensing, and energy harvesting. It can be fabricated from different physical and chemical synthesis techniques [52].

2.2 ZnO Properties

2.2.1 Crystal Structure of ZnO

ZnO has a wurtzite structure with a hexagonal unit cell which belongs to a space group of C6mc. It has a lattice parameter of a=0.3296 and c=0.52065. The lattice parameter of any semiconductor is determined by a number of factors; (i) temperature (ii) concentration of the free electrons acting via the deformation potential of a conduction band (iii) external strain applied (iv) foreign atoms concentration, defects and the difference between ionic radii with respected to the substituted matrix ion[53]. The whole structure of the ZnO lacks a central symmetry, the cations (zinc) and the anions (oxygen) form a tetrahedral unit [54]. The crystal structure of ZnO can be seen as an alternating set of tetrahedral plane coordination of Zn^{2+} and O^{2-} ions positioned on each other along c-axis as shown in Figure 2.1.

The cryptography of ZnO is usually described in terms of the distributions of the anions and cations with cretin arrangement. A net positive or negative charge might be seen on some surfaces with the anions or cations. This leads to polar surfaces due to the positively or negatively charged surfaces. An example of polar surfaces is the basal plane. An oppositely charged ions [negatively charged O^{2-} (0 0 0 1 $^{-}$) polar surfaces and positively charged Zn^{2+} (0 0 0 1). To achieve a settled structure generally, the polar surfaces must have faces that show huge surface reconstructions [55] [56]. This process is repeated several times and leads to fast growth in the $\pm$ (0 0 0 1). ZnO also have non-polar surfaces like (1 1 20), (1 0 1 0) e.t.c. apart from the polar surfaces. Exposing the non-polar surfaces in the solution at the growth stage is the basis for one-dimensional growth. This property enables different novel ZnO nanostructures to be synthesized simply by controlling the growth condition and parameters [54].

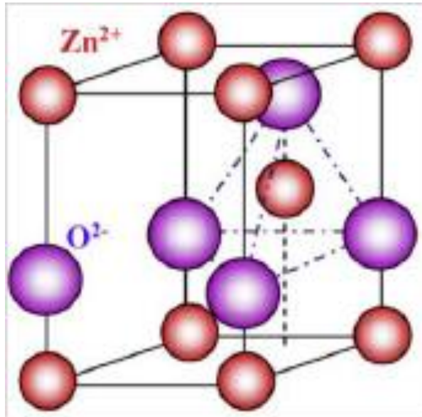

Figure 2.1: Non-central symmetry in ZnO wurtzite structure. This non-central structure is responsible for the observed piezoelectric effect for ZnO [53]

2.2.2 Mechanical Properties

Mechanical properties such as hardness, stiffness, Young's modulus, yield strength, and young modulus are so important in characterizing the behavior of any material. The strain is also an important property that describes the deformation of a material when subjected to external force. To incorporate ZnO nanoparticles as electromechanical components, it is important to investigate their mechanical properties [57]. It might be quite challenging to carry out the mechanical characterization of ZnO but due to the evolving use of ZnO in many applications, it is therefore important to study and understand their mechanical behavior. Hence the need to carry out the mechanical characterization of nanoparticle materials in order to achieve reliable and efficient piezoelectric devices and sensors.

2.2.3 Piezoelectric Properties

Piezoelectric effect was first observed by Jacques and Pierre Curie in 1888. Piezoelectric effect is defined as the ability of some materials to produce electric potential in response to applied mechanical stress. The stress applied leads to a change in the polarization density of the bulk material which is responsible for the observed potential. The piezoelectric effect is only exhibited by materials with non-centrosymmetric crystal structure [58]. Examples of piezoelectric materials that are commonly used are ZnO, Barium Titanate ($BaTiO_3$), and Polyvinylidene fluoride (PVDF). When ZnO is subjected to an applied load, there is an effective accumulation of charges which is responsible for the piezoelectric property of ZnO. ZnO is considered as a potential material for energy harvesting due to its piezoelectric and semiconducting properties.

2.2.4 Electrical Properties

As indicated above, ZnO has a potential application in optoelectronics and electronic devices. ZnO has a comparatively high breakdown voltage coupled with its electrical operation producing low noise at high temperature which is associated with the wide band gap in semiconductors. The band gap of ZnO can be tuned between 3 to 4 eV if it is alloyed with some other metal oxides such as cadmium oxide or magnesium oxide [59]. The transport properties of ZnO is affected by the strength of the electric field [59] [60]. When a relatively low electric field is applied, the thermal energy can be higher than the electron energy. This implies that the electron distribution will not be altered by the electric field [59] [60]. Therefore, the mobility of the electrons will not change; the electron scattering will not be affected, and Ohm's law still applies [59] [61]. There is a deviation of the electron distribution function from the equilibrium since the thermal energy is lower than the electron energy [60] [62].

2.2.5 Applications of Zinc Oxide films and Poly Vinylidene Fluoride films

To evaluate the state of health of a structure, physical quantities such as displacement, strain, and acceleration are used. These physical quantities provide the detailed and required information regarding the health of a structure if it is properly investigated using a different method. Strain sensors have a wide range of application in structural health monitoring. Piezoelectric materials can be used as a strain measuring device.

When piezoelectric materials are used as strain sensors, they are usually embedded inside or bonded on the surface of the matrix material for strain measurement. ZnO is a semiconducting material with a wide band gap which is electrically conductive and it is used for a wide range of piezoelectric application [63]. The detailed and ongoing research on ZnO has revealed that it has the potential of been used in many industrial applications such as nano-generators, gas sensors, solar cells, ceramics, catalysts, biosensors, ceramics, photodetectors and piezoelectric films [63]-[80].

A research was carried out by Hu et al. [81] which confirms the possibility of using ZnO as a piezoelectric material. Carbon nanotubes were coated with Zinc Oxide to produce a flexible piezoelectric generator. The flexible piezoelectric generator produced a short circuit current of $75\mu A/cm^{-2}$ and an average open-circuit current of 1.6V. Atomic layer deposition was used for coating the carbon nanotubes with zinc oxide.

Due to the limitations encountered in the use of PZT ceramics for piezoelectric applications, extensive research has been carried out and it is still on-going in the use of ZnO for piezoelectric applications. Gullapalli et al. [82] fabricated a nanocomposite material by embedding ZnO (a crystalline piezoelectric material) in a cellulose-based paper (matrix). The flexible strain sensor was fabricated using a low-temperature solvothermal process in which the paper was soaked repeatedly Zinc oxide crystal solution. Thin layers of gold coating were used as the electrode and were deposited on the surface of the flexible strain sensor using plasma sputtering. An excellent strain sensitivity was produced when the flexible strain sensor was tested under dynamic and static loading.

In order to validate the research carried out by other people on the enhanced piezoelectric property of Poly (vinylidene fluoride-trifluoroethylene) (PVDF-TrFe) polymers by the addition of ZnO, Meyer et al. [83] fabricated and characterize Zinc Oxide/PVDF-TrFe Interdigitated Transducers (IDT). The sensing and actuation performance of the transducer was characterized. The IDT electron pattern was deposited on a Kapton substrate using a photolithography process. Ultrasonication was used to suspend the zinc oxide nanoparticles in a PVDF-TrFe solution, it was then spin coated on the IDT-Kapton substrate. The ability of the substrate to detect damage was evaluated using the Lamb waves sensing and actuation validation testing technique.

Research has revealed the potential of using zinc oxide for dynamic strain sensing. One of such research was carried out by Loh and Chang [84] in which a thin film was fabricated using high-probe sonication by dispersing zinc oxide nanoparticles in Poly (vinyl alcohol) (PVA) and poly (sodium 4-styrenesulfonate) PSS. The solvent used for dispersing the nanoparticles in the polymer was dried using solution evaporation. It was observed that the thin film exhibited high dynamic strain sensitivity and good mechanical properties. The best piezoelectric property and dynamic strain sensitivity were obtained with 60wt% and 50wt% of ZnO nanoparticles in the polymer respectively.

However, some other studies have established that the piezoelectric performance of zinc oxide film can be enhanced by poling or by the addition of carbon nanotubes.

2.3 CARBON NANOTUBES (CNTs)

Carbon nanotubes (CNTs) were first discovered by Endo [85] in 1976 when he synthesized vapor-grown carbon fibers. At that time, it was not focused on, neither was it given a thought. Scientific research was globally shifted to this area after the work done by Iijma in 1991 [86] and this led to intense research on the structures, properties, and application of carbon nanotubes. It has been observed from the study of CNT that one-dimensional (1-D) nanomaterials exhibit entirely different or better properties as compared to the bulk materials. CNTs have been discovered to be the stiffest and strongest material on earth in terms of the elastic modulus and tensile strength respectively and both properties are about ten times better as compared to stainless steel [87-89]. One-dimensional nanomaterials such as CNTs are assumed to be the promising building blocks for Nano-Electromechanical System and Micro-Electromechanical Systems.

CNTs can be described as a rolling concentric graphene sheet with high aspect ratio [90]. The length of the hollow cylindrical structures could be up to a centimeter and diameter as small as up to nanometers. Several physical properties of CNTs that are associated with its electronic band structure can be studied such as the optical properties and field emission properties due to the graphene-like electronic structure of CNTs. The electronic structure of CNTs determines its application in electrical engineering either by using it for field emission effect or transistor effect. Based on the number of layers in a CNT, there are basically two types of CNTs; single wall (SWCNTs) and multi-wall CNTs (MWCNTs). SWCNTs consists of monolayer molecules which are seen as rolled-up graphene. The MWCNTs are made up of multi concentric carbon layers which are also seen as rolled-up graphene and the distance of separation between each layer is about 0.34nm. The electronic property of MWCNTs is semi-metallic as seen in graphite too while SWCNTs can be both metallic and semi-metallic. The quality of the structure will determine the behavior of SWCNTs as either metallic or semi-metallic; high-quality structure behaves as metallic SWCNTs. Metallic SWCNTs are conductive and the electrons collide and flow through the axial distance. Semi-metallic SWCNTs are semi-conductive and they have a band gap of about 0.6eV based on the diameter of the tubes [91]. The electrical properties of MWCNTs are due to the combined effect of the semi-conductive layers and the conductive layers, it has an electric property which is in between the semi-metallic and metallic. There is interaction of layers in SWCNTs and the reduction in the band gap is a result of the few nanometer sizes of the SWCNTs. Hence the conductivity difference between the metallic and semiconductor property of MWCNTs is lower than that of SWCNTs. The diameter of SWCNTs is in the range of 0.5 to 5nm while the diameter of MWCNTs varies from several nanometers up to 200nm. The concentric nanotubes of MWCNTs are bonded together by Van der Waals force [91].

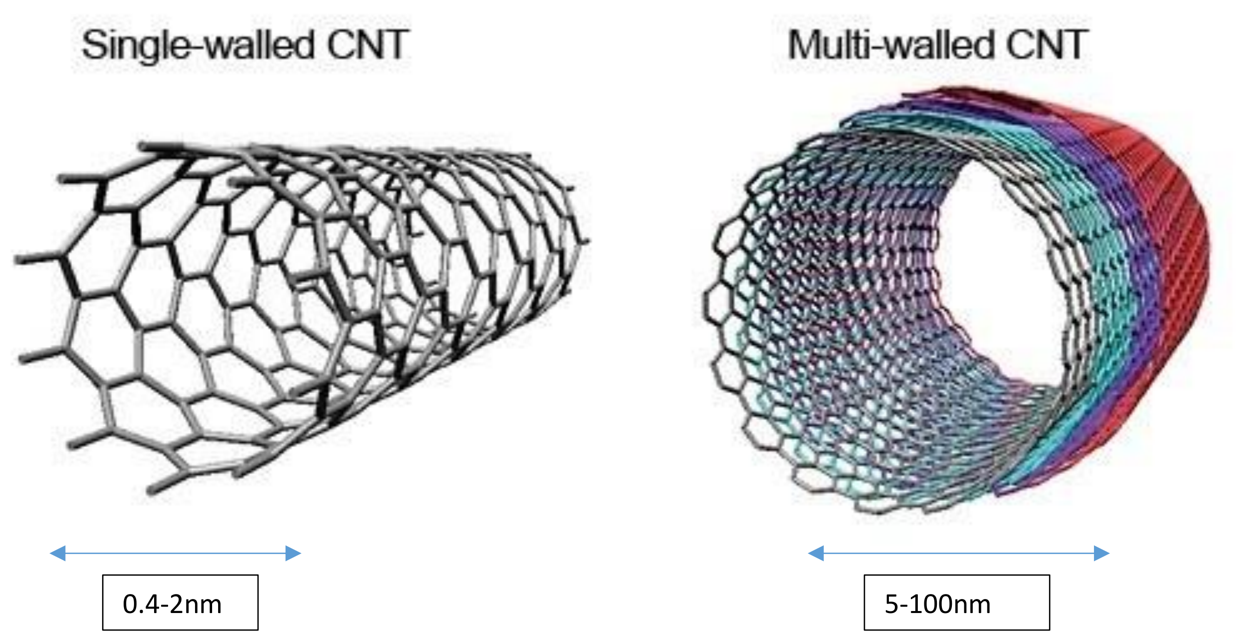

Figure 2.2: Two CNT variants: (a) SWCNTs and (b) MWCNTs [89]

2.3.1 Applications of Carbon Nanotubes enhanced films

The enhancement of the piezoelectric property of ZnO, barium titanate and PVDF polymers will lead to their improved use in most industrial application as compared to PZT. Due to some of the peculiar properties of carbon nanotubes such as high aspect ratio, high Young's modulus, excellent stiffness, chemical stability and exceptional electrical conductivity [30] [31]. Based on the theoretical calculation, Young's modulus of multi-walled carbon nanotubes (MWCNTs) ranges from 1.7-2.4 TPa and 2.8-3.6 TPa for single-walled carbon nanotubes (SWCNTs) [83]. Experimentally, Young's modulus of SWCNTs and MWCNTs were estimated to be 1470 GPa and 960 GPa respectively [34] [35]. Individual MWCNTs has an electrical conductivity ranging from $20 – 2 \times 10^7$ S/m [92].

The outstanding electrical and mechanical properties of carbon nanotubes have been leveraged on since it was discovered in 1991 by Iijima [86]. Studies have shown that CNTs and its composite can be used in a wide range of applications such as optimization of electrical performance in microelectronics, the enhancement of stiffness in coatings and films, used as components of biosensors and for increasing the capacity of lithium-ion batteries. A lot of research has confirmed the possibility of using carbon nanotubes for enhancing the electromechanical response of piezoelectric materials. The piezoelectric film was fabricated by blending of carbon nanotubes with the piezoelectric material and dispersing it into the polymer. In some cases, films were fabricated by mixing of carbon nanotubes with polymers and used for strain sensing.

The effect of the addition of carbon nanotubes to PVDF-TrFe polymers on the sensitivity of the piezoelectric polymers was studied by Ramaratnam and Jalili [93]. Two types of carbon nanotubes were used in this experiment; Single-Walled Carbon Nanotubes (SWCNTs) and Multi-walled Carbon Nanotubes (MWCNTs). The electromechanical response of the three different piezoelectric films was evaluated; PVDF-TrFe film, SWCNTs-PVDF-TrFe film and MWCNTs-PVDF-TrFe film. It was observed that the carbon nanotubes-based film yield a better piezoelectric response as compared to the plain PVDF-TrFe film. The SWCNT-PVDF-TrFe film produced a greater piezoelectric response than MWCNT-PVDF-TrFe film. The improved sensing capability of the piezoelectric polymers was as a result of an increase in Young's modulus of the elasticity of the nano-based polymer.

Some other research was done on the possibility of using carbon nanotubes for the fabrication of strain sensors by the addition of carbon nanotubes to the polymer to produce a composite. Strain gauges were designed, fabricated and characterized by Lee et al. [27] from spray-coated single-wall carbon nanotube film. It was fabricated by spray-coating of SWCNT on the polyimide film, chromium was used as the electrode. The sensitivity obtained was about eight times greater than the commercial strain gauges. Loh et al. [94] proposed a multifunctional layer-by-layer CNT-polyelectrolyte thin films for corrosion and strain sensing. The thin films were produced by dispersion of carbon nanotubes solution in poly (sodium-4-styrene-sulfonate) (PSS) and poly (vinyl alcohol) (PVA) via probe and bath sonication.

A carbon nanotube strain sensor was developed by Kang et al. [95] by dispersing of SWCNTs in polymethyl methacrylate (PMMA) for SHM purpose. Pham et al. [96] fabricated a conductive polymeric film with PMMA by solution-casting or melt-processing of the polymer matrices having a low concentration of multi-walled carbon nanotubes (MWCNTs). The composite film was used for strain sensing application.

A thin film was developed by Anand and Mahapatra [97] by dispersing of carbon nanotubes and carbon black nanoparticles in an epoxy polymer. Multi-walled carbon nanotubes of different concentrations by weight were dispersed in the epoxy matrix and it was observed that the thin film with 0.57wt% of MWCNTs gave the best and highest sensitivity were subjected to static mechanical loading. The thin films can be potentially used as accelerometers and strain sensor for structural health monitoring purposes.

Furthermore, a study was carried out by Saber et al. [98] to investigate the effect of adding MWCNTs and graphene platelets (GnPs) to three-phase nanocomposite containing epoxy and PZT. Both mechanical and electrical test was carried out to characterize the fabricated nanocomposite. It was observed from the result obtained that the addition of the GnPs to PZT and epoxy increased the dynamic response and poling behavior of the composites and yielded better results as compared to MWCNTs. This study confirmed the potential of using GnPs as an additive for enhancing the piezoelectric property of nanocomposites for SHM applications.

2.4 ZnO-CNT Nanocomposite

ZnO and CNTs nanoparticles are two important building blocks in nanotechnology and they have rarely been assembled as a hybrid structure. Dutta and Basak [99] fabricated a nanocomposite material by coating vertically grown ZnO nanowires with a solution of MWCNTs which were dispersed in 2-propanol. It was observed that with an increased coating of the ZnO nanowires with a solution of MWCNTs, the ultraviolet emission is enhanced and also the ultraviolet photoresponse increased. These improved properties were attributed to the faster electron response and surface plasmon resonance effect of MWCNTs.

A piezoelectric composite nanotube was fabricated by Jin et al. [100] by coating of the carbon nanotubes with zinc oxide nanocrystals. The nanocomposite was subjected to both electrical voltage and axial strain and the corresponding mechanical responses were observed. Euler beam model was used to investigate the axial buckling of the nanocomposite accounting for the piezoelectricity of the coating layer. It was observed that a tensile radial stress is generated in the nanocomposite prior to buckling.

Furthermore, Venugopal et al. [101] fabricated a ZnO/CNT nanocomposite electrode by mixing ZnO nanopowder with MWCNTs in different proportions. The nanocomposite was characterized electrochemically by cyclic voltammetry in 0.1, 0.5 and 1M of potassium chloride (KCl) aqueous solutions using a scan rate of $100mVs^{-1}$. The result obtained from the electrochemical experiment indicated that ZnO-CNT combination with ratio 2:1 gave a better specific capacitance value than ZnO-CNT combination with 1:1 and 1:2. The ZnO-CNT combination with a ratio of 2:1 has a stable cycle life with characteristics charging-discharge straight lines whereas the ZnO-CNT combination with ratio 1:2 shows a less capacitance values with a small IR drop as a result of the resistance on the surface of the MWCNTs in contact with the electrolyte.

2.5 Nanocomposites fabrication methods

Depending on the polymer material to be used, two or more materials are mixed together at different proportions using different techniques in order to fabricate a nanocomposite. The nanocomposites are usually made up of carbon nanotubes, piezoelectric materials, and polymers. The ability of the nanoparticles to be uniformly distributed in the polymer depends on the procedures of fabrication and the mixing methods.

There are basically three factors that affect the piezoelectric performance of nanocomposites [26]: the uniform distributions of the piezoelectric particles in the polymeric matrix, the interfacial bond between the main constituent materials and the polymer, and the alignment of the piezoelectric particles in the composites. These factors ensure a uniform transfer of load and the generation of charges in the nanocomposites.

2.5.1 Direct mixing of Polymer and Nanofillers

Direct mixing of the polymeric material with the nanoparticles is a step-wise approach in the fabrication of nanocomposites. This depends on the ability of the nanoparticles to mix homogeneously with the polymer during the process of mixing. This method is suitable for the fabrication of polymer matrix nanocomposites. There are two ways of mixing the polymer and nanoparticles; the first way is mixing of the polymer without solvent with the nanoparticles above their glass transition temperature (T_g), this is referred to as melt compounding method [102] [103]. The second way involves using a solvent to mix the polymer and the nanoparticles together and it is referred to as solution mixing/solvent method [103]. This method was used in this thesis for the fabrication of the piezoelectric nanocomposite gum sensors.

2.5.2 Melt Mixing

Melt melting is one of the common methods used in the fabrication of nanocomposites. This method is used for manufacturing nanocomposites that contain thermoplastics as the polymeric material since there is a decrease in the hardness of the material when heat is applied to it. This method requires a high temperature in order to reduce the viscosity of the polymeric material and this produces a high shear force which perturbates the bundle of the nanotubes. Different sizes of nanocomposites are fabricated using techniques such as injection molding, compression molding or extrusion [25]. Andrews et al. [104] fabricated a nanocomposite thin films and fibers using melt mixing from MWCNTs and industrial polymers such as polypropylene, acrylonitrile-butadiene-styrene (ABS) and polystyrene. The uniform distribution of carbon nanotubes in the polymers was achieved at elevated temperature and with high impact force. The thin film composites were manufactured using compression molding. The fabrication of nanocomposites using compression molding and shear mixing was studied by other researchers [37]

2.5.3 Solvent Casting

This is the commonest method used in the fabrication of nanocomposites, although it depends on the solubility of the constituent materials. Due to the energetic nature of the agitation, there is a homogenous distribution of the nanotube dispersion and the composite. The agitation of the constituent materials is achieved by reflux, magnetic stirring, sonication, and shear mixing.

The carbon nanotubes, piezoelectric materials, and the polymer are all dispersed in a solvent and are agitated together for some time.

There are some other methods used in the production of nanocomposites apart from direct mixing, melt mixing, and solvent casting. They include twin screw pulverization [37], in-situ polymerization [31] [32], coagulation spinning [33], electrophoretic deposition [36] and latex fabrication [34] [35].

2.5.4 Materials and Fabrication Techniques for Flexible Nanocomposite Sensors

There are different factors that determine the materials used for the fabrication of flexible sensors and these include the application of the sensor, manufacturing cost, the availability of the material etc. Organic electronics are one of the key aspects of materials science which has been developed substantially for the fabrication of flexible sensors [105]. These types of sensors have been used for the manufacturing polymer electrodes, ionic pumps, thin film transistors etc. Electronic devices that are printed on thin layers are developed from a process known as Organic and large area electronics (OLAE) [106]. Polyethylene Terephthalate (PET) and Polyethylene Naphthalate (PEN) are the main substrates that are used for this operation due to their transparency and lower cost compared to other organic polymers. OLAE process is popularly used for the fabrication of wearable medical and health devices.

Flexible sensors are commonly developed from PEN [107], PDMS [108] [109], Polyimide (PI)[110], PVDF-TrFe [111], Polypyrrole [112] and Parylene [113] for different applications. Different conducting materials such as metallic nanoparticles and carbon-based nanoparticles have used as the electrode part of the sensor. Among the metallic nanoparticles, gold [114] [115], silver [116][117] and nickel [118] are some of the most widely used ones in flexible wearable sensors. The carbon compound include graphene [119]-[121], CNTs [122] [123],carbon fibers[124] etc.

Different techniques such as screen printing [125], photolithography [126], laser cutting [127], and inkjet printing [128] are used for the fabrication of flexible sensors. The dimensions of the final product determine the procedure used to manufacture the prototype of the sensor. The commonly used insulating substrate for developing flexible sensors are PEN [129], PET [130], PI [131], PDMS [132] etc.

2.6 Piezoelectric Composite Materials Applications

In structural health monitoring, sensors and actuators are used for monitoring the failure of structures. Most of the actuators and sensors are manufactured from smart materials that possess piezoelectric properties. Piezoelectricity is an inherent property of a material and its importance cannot be overemphasized.

2.6.1 Smart Materials

With the present-day advance in technology, there are some special group of materials referred to as smart materials. Smart materials are materials that can significantly alter one or more of their inherent properties owing to the application of external stimuli in a controlled fashion. The several external stimuli to which smart materials are sensitive to are; stress, moisture, temperature, pH, electric fields and magnetic fields. Smartness denotes self-sensing, self-adaptability, multiple functionalities and memory of the structures or materials [133]. The materials can be used in a wide range of applications such as manufacturing, aerospace, civil engineering, and biomechanics.

The recent advance and growth in technology have led to the discovery of smart technology. The aim was to achieve a faster and easier result of specified tasks using smart materials. Smart or intelligent materials are materials with both intrinsic and extrinsic properties; they are able to respond to environmental and stimuli changes, they are able to achieve their functions based on these changes [134].

There are different types of smart materials and these include; piezoelectric materials, Magneto-resistive materials, Thermo-responsive materials, Chromogenic materials, Polymer gels and pH sensitive materials [133]. For piezoelectric material, the input stimulus is in form of mechanical stress and the output response is an electric charge, they also exhibit an inverse piezoelectric effect that makes them under mechanical deformation upon application of electrical charge. The input stimulus for electro-rheological fluid is an electric field and the response is viscosity change (internal damping). When the magneto-restrictive material is subjected to a magnetic field, it experiences mechanical deformation. When shape memory alloys are heated, it returns to its original memorized shapes. Changes in pressure, temperature and mechanical strain in optical fibers cause a change in the optoelectronic signals.

Smart materials are categorized into two: active and passive [133]. Active smart materials are materials that are capable of changing their shapes or their properties when subjected to magnetic, thermal or electrical fields and in the process acquiring an intrinsic capacity of energy conversion. They include magneto-restrictive materials, shape memory alloys and piezoelectric materials. Active smart materials are used basically as actuators and force transducers. Passive smart materials do not have the intrinsic capability of energy conversion. They are used as sensors and cannot be used as actuators or force transducers [133].

The peculiar property of piezoelectric material makes it an important part of this research work. The material produces an electric charge when subjected to mechanical deformation and also exhibit a reverse effect- it is able to undergo mechanical deformation when an electric field is applied to it. It exhibits the electromechanical effect. Piezoelectric materials have mechanical properties; they have Young's Modulus and obey Hooke's law. It simply means that the application of a mechanical load on the piezoelectric material will produce an electrical charge which can be measured using an electrical device. Conversely, when an electric charge is passed through it, it experiences a mechanical deformation.

However, from the constitutive equation of piezoelectric, the whole concept of piezoelectricity was better understood. It should be understood that when a piezoelectric material is subjected to mechanical deformation, it is anticipated that there with be some changes in the mechanical properties accompanying the electric charge produced. Also, with the application of electric charge, it is expected that the material will experience an electrical response simultaneously with the mechanical deformation. A lot of piezoelectric materials has been used by different researchers for structural health monitoring applications.

There are lots of research work published on SHM applications and piezoelectric materials have been used for the acquisition of data which are thereafter using different algorithms such as wavelet analysis and neural networks. The neural network was used by Islam and Craig [15] for the detection of damage in a composite using a piezoelectric material; the response was analyzed. Yan and Yam [135] used wavelet analysis to develop an online damage detection method for structures based on the generated data from the embedded piezoelectric materials.

Dib et al. [136] monitored the health of a structure using PZT ceramics as the sensing device. The health of the structure was measured using guided wave technique while the health of the PZT ceramics was monitored using the impedance method. From the study, it was concluded that PZT ceramics are good for sensing the damage of a structure when they are 80mm from the impact point.

A study was carried out by Dziendzikowski et al. [137] to compare the use of mounting surface and embedded PZT transducers for the damage detection of hardly noticeable impact crack confined in a composite structure. When the PZT transducers were embedded in the composite structure, it was observed that there was a change in the electrical properties of the transducers. However, the sensing ability of the embedded transducer can be immensely enhanced even when it is embedded. It was concluded from the research that the surface mounted PZT transducers have a better ability for damage detection of hardly noticeable impact crack confined in a composite structure as compared to embedded transducers.

Piezoelectric materials could be naturally occurring or artificial (manufactured). Some examples of piezoelectric materials include tourmaline, Zinc oxide (ZnO), quartz, lithium sulfate, Rochelle salt, Lead Zirconate Titanate (PZT), barium titanate ($BaTiO_3$) and Poly Vinylidene Fluoride (PVDF). Each of these materials has their limitations for structural health monitoring application.

Despite the peculiar piezoelectric property of PZT ceramics, it cannot be used in applications that require flexibility due to its brittle nature. Piezoelectric materials have been widely used in the monitoring of the health and crack growth of a structure.

2.6.2 Flexible sensors

Different types of flexible wearable sensor are fabricated based on the parameters that are to be monitored which invariably determines the fabrication method that would be used for the sensors. For example, monitoring of parameters such as respiration [138], cardiorespiratory signal [139] and heart rate [140] would require sensors that are sensitive and subtle. For monitoring of physiological parameters of a human being such as gait analysis [141], limb movement [142] and motions such as running and walking [143], sensor patches that are bigger and more flexible are used. Flexible wearable sensors are used as glucose sensor through different medium such as immobilization of glucose oxidase [144] [145], tear [146]. To mimic the function of a natural skin and the changes in pressure, temperature or even the health condition of human beings, electronic skins were developed [147][148]. Thermal actuators and organic displays were integrated into these sensors [149]. One of such development is the fabrication of wearable skin sensors [150] that could be used as non-volatile memory, physiological sensors, and therapeutic actuators and for drug release [151]-[153]

Artificial skins [154], human motion detection [155] [156], forces and acoustic vibrations [115] are some of the application of flexible sensors. Due to their high bendability and flexibility, flexible sensors are widely used as pressure sensors [115] [157] [158]. They can also be used potentially in the field of aviation and robotics.

From the literature review, it was observed that most of the sensors were fabricated from brittle materials and complex techniques which invariably affects the cost of fabrication. Furthermore, existing flexible sensors usually measure static or low frequency dynamic strain based on the resistant variation with different strain levels [159]. Hence, there is a need to fabricate the gum sensors from a stretchable and foldable materials that can measure both static and dynamic motions by introducing piezoelectricity and using a simple method in a cost effective way.

CHAPTER 3- MATERIALS AND EXPERIMENTAL PROCEDURE

This chapter gives a description of the steps involved in the fabrication of the piezoelectric nanocomposite gum sensor. It provides detail of the experiments that were carried out to characterize the gum sensor. The electrical, mechanical and temperature dependency properties of the piezoelectric nanocomposite gum sensor were characterized. All the methods involved in the fabrication and characterization of the piezoelectric gum sensor are discussed.

3.1 Materials

The piezoelectric nanocomposite gum sensors were fabricated with double mint bubble gum, dispersed Zinc oxide (ZnO) in water, and dispersed Carbon Nanotubes (CNTs) in water. ZnO acts as piezoelectric functional particles sensing dynamic signals with high sensitivity and speed of reaction, while the gum with CNTs works as static strain gauge with variable resistance under different strain. Both Single-walled carbon nanotubes (SWCNTs) and Multi-walled carbon nanotubes (MWCNTs) were used. The Zinc Oxide (ZnO) nanopowder suspension was supplied by Sigma Aldrich. As mentioned in chapter 2, due to the non-centrosymmetric crystal structure of ZnO, it exhibits piezoelectric effect [58]. Both the SWCNTs and MWCNTs were supplied by US Research Nanomaterials. Inc. The properties of the materials used for the fabrication of the piezoelectric nanocomposite gum sensor and their sources are shown in Table 3.1.

Bubblegum was selected as the matrix material due to its ability to be folded and stretched into different shapes and sizes. It is also cheap, commercially available and most importantly used as a proof of concept. The use of nanotube and nanostructures such as CNTs and ZnO have shown to be quite promising in the advancement of flexible and stretchable strain sensor [160]-[164]. Figure

3.1 shows the images of the materials used in the fabrication of piezoelectric nanocomposite gum sensor.

Table 3.1: The properties and source of the materials used in the fabrication of the piezoelectric nanocomposite gum sensor

Name	**Properties**	**Source**
Double- mint bubble gum	Foldable and Stretchable elastic-plastic material	Super-Store, Canada
Dispersed Zinc Oxide (ZnO) nanoparticle in water	<100 nm particle size (DLS), ≤ 40 nm avg. part size (APS), 20 wt % in water.	Sigma Aldrich®, St. Louis, Missouri, United States of America.
Dispersed Single-Walled Carbon Nanotubes (SWCNTs) in water	1wt%, >95%, OD: 1-2 nm, length: 1-3μm.	US Research Nanomaterials. Inc., Houston, Texas, United States of America
Dispersed Multi-Walled Carbon Nanotubes (MWCNTs) in water	1wt%, >95+%, OD: 5-15 nm, ID: 3-5 nm, length: around 50μm.	US Research Nanomaterials. Inc., Houston, Texas, United States of America

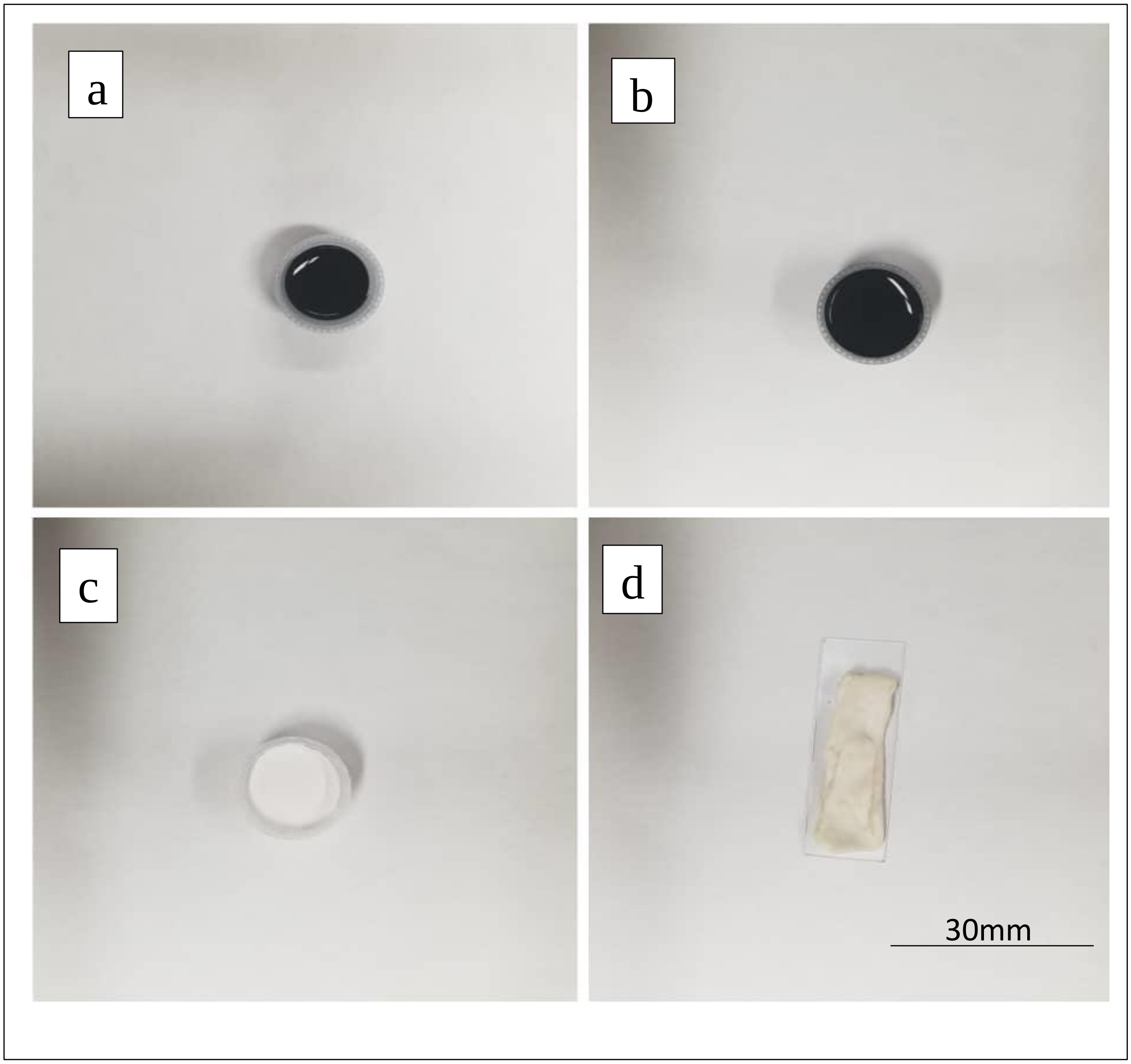

Figure 3.1: Images of the materials used in the fabrication of the piezoelectric nanocomposites gum sensor a) SWCNTs dispersion b) MWCNTs dispersion c) ZnO dispersion d) bubble gum

3.2 Fabrication of the Piezoelectric Nanocomposite Gum Sensor

The piezoelectric gum sensor was fabricated by using Carbon Nanotubes, Zinc Oxide and Bubble gum with bubble gum serving as the matrix.

The following steps were adopted in the fabrication of piezoelectric nanocomposite gum sensor.

1. The bubble gum was chewed for 30 minutes and it was immersed in ethanol for 24 hours to remove the saliva.
2. The bubble gum was removed from the ethanol and then immersed in distilled water for 24 hours.
3. The bubble was removed from the distilled water and placed on the glass slide. The gum was left at room temperature overnight in order to allow the excess water to dry out and also attain a stable weight.
4. The gum was weighed using a weighing balance, 3.5±0.5g of the gum was weighed.
5. ZnO nanoparticle dispersion was added to the surface of the weighed gum, it was stretched and folded for 20 times in one direction. The reason for folding and stretching is to allow for better alignment and more evenly distribution of the ZnO particles in the bubble gum.
6. CNTs dispersion was added to the surface of the ZnO-gum mixture. The gum mixture was then stretched and folded for like 20 times in the same direction to ensure the alignment of the CNTs along the stretched direction [159].
7. The ZnO-CNT gum mixture was allowed to dry for 24 hours.
8. The piezoelectric gum sensor was thereafter characterized.

Different volumes of ZnO nanoparticle dispersion and CNTs dispersion were mixed by direct mixing method with the bubble gum resulting in different weight percentage (wt %) of ZnO and CNTs in the final dried gum sensor for the fabrication process. The mixing method was selected because it is one of the most suitable methods for the fabrication of polymer matrix nanocomposite and it is believed that the direct mixing method helps to achieve a homogenous mixture of the nanoparticles with the polymer after multiple times of stretching and folding [103] [159]. The flow-chart of the steps involved in the fabrication of the piezoelectric nanocomposites gum sensor is shown in Figure 3.2.

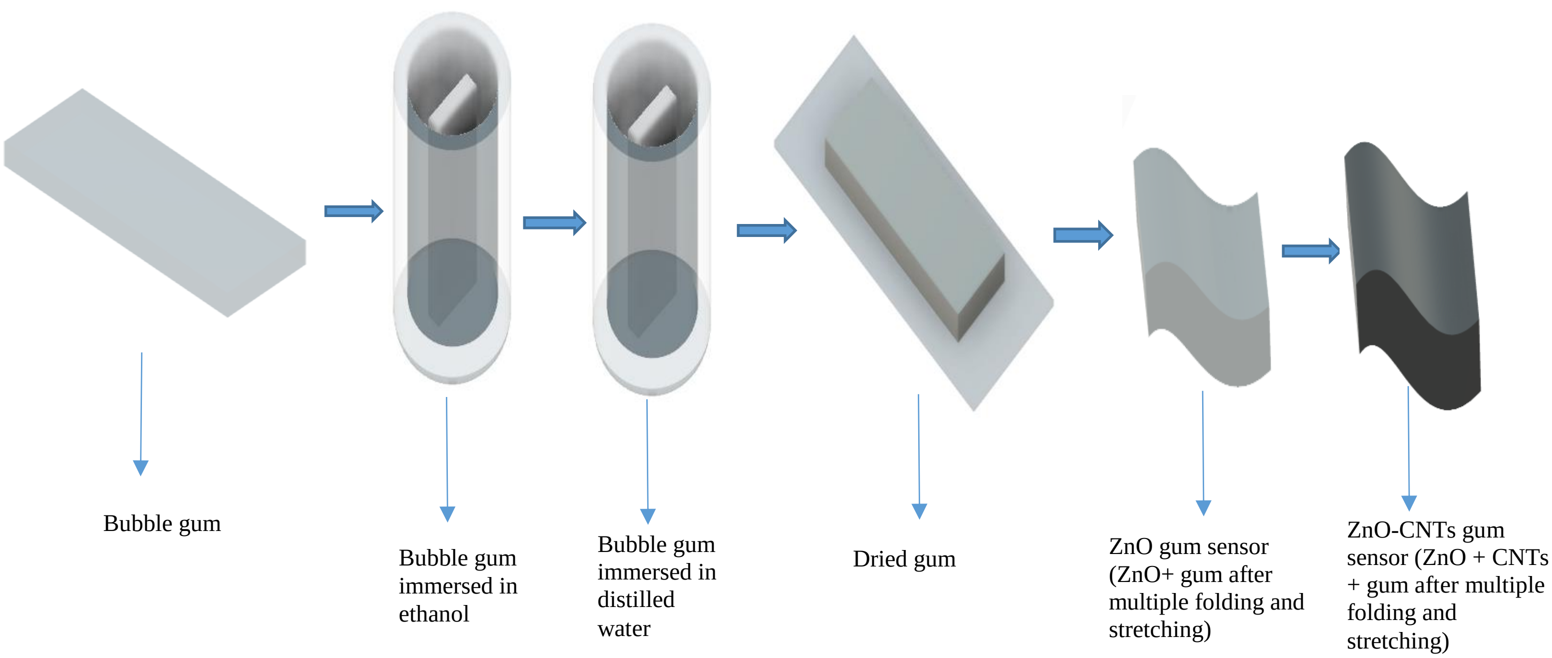

Figure 3.2: Flow-chart of the fabrication process

In order to determine the wt % of CNTs that is required to be added to ZnO to give an optimum piezoelectric property, different wt % of SWCNTs was added to ZnO in the gum to fabricate ZnO-SWCNTs gum sensors as shown in Table 3-2 and Table 3-3. Furthermore, to evaluate if the addition of MWCNTs to ZnO in the gum sensor would give better enhanced piezoelectric property as compared to ZnO-SWCNTs gum sensors, ZnO-MWCNTs gum sensors were fabricated by adding different wt % of MWCNTs to ZnO as shown in Table 3-4. The piezoelectric coefficient of ZnO-SWCNTs and ZnO-MWCNTs gum sensor were compared. ZnO gum sensor was also fabricated because ZnO is the base material and responsible for the piezoelectric property. Figure 3.3 shows the images of the prepared ZnO gum sensor, ZnO-SWCNTs gum sensor, and the ZnO-MWCNTs gum sensor. It costs less than $20 CAD to fabricate the piezoelectric gum sensors considering the cost of ZnO and CNTs which were around $50CAD/100g and $120/50g respectively.

Some other tests such as resilience test, mechanical test and temperature and strain dependency effect were carried out on ZnO-SWCNTs, and ZnO-MWCNTs gum sensors to ascertain if the addition of the CNTs to the ZnO did not impair other properties of the gum sensors.

Table 3.2: The varying composition (weight percent) of the SWCNTs in the ZnO-SWCNTs piezoelectric nanocomposites gum sensor for optimization purpose

Piezoelectric Nanocomposite gum sensor	SWCNTs (wt %)
Sample 1	2.44
Sample 2	2.92
Sample 3	3.61
Sample 4	3.70
Sample 5	4.22
Sample 6	4.76
Sample 7	6.98
Sample 8	9.1
Sample 9	11.11
Sample 10	13.07
Sample 11	23.07

Table 3.3: The varying composition (weight percent) of the SWCNTs in the ZnO-SWCNTs piezoelectric nanocomposites gum sensor

Piezoelectric Nanocomposite gum sensor	SWCNTs (wt %)	ZnO (wt %)
Sample 1	3.6	96.4
Sample 2	4.2	95.8
Sample 3	4.8	95.2
Sample 4	7.0	93.0
Sample 5	9.1	90.9

Table 3.4: The varying composition (weight percent) of the MWCNTs in the ZnO-MWCNTs piezoelectric nanocomposites gum sensor

Piezoelectric Nanocomposite gum sensor	MWCNTs (wt %)	ZnO (wt %)
Sample 1	3.6	96.4
Sample 2	4.2	95.8
Sample 3	4.8	95.2
Sample 4	7.0	93.0
Sample 5	9.1	90.9

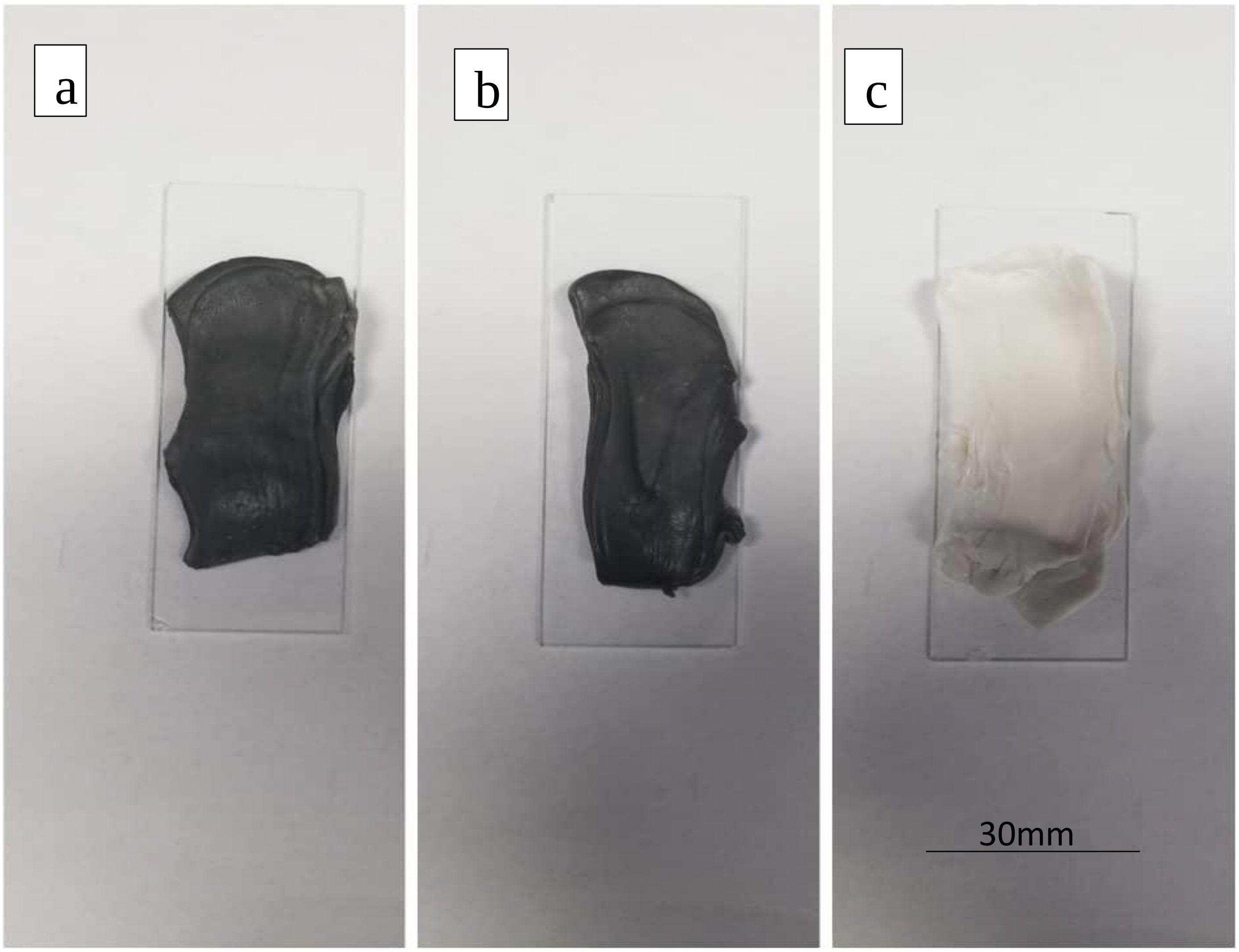

Figure 3.3: Images showing the raw samples of fabricated piezoelectric gum sensors a) ZnO-SWCNTs piezoelectric nanocomposite gum sensor b) ZnO-MWCNTs piezoelectric nanocomposite gum sensor c) ZnO piezoelectric gum sensor

3.3 Resilience Test

Resilience tests were carried out on three types of piezoelectric gum sensors (ZnO gum sensor, ZnO-SWCNTs gum sensor, and ZnO-MWCNTs gum sensor) to evaluate the ability of the constituent materials (ZnO and CNTs) to bond and adhere to the surface of the gum. It was also used to evaluate the mix-ability of the constituent materials with the gum. This is also important because sensors are also used in the neutral environment with pH of 6.5-7.0. It is therefore imperative to test the ability of the piezoelectric gum sensors to withstand neutral environments.

To evaluate the adherence and bond-ability of the constituent material to the gum and to also evaluate the ability of the gum sensor to withstand the neutral environment, the three different piezoelectric gum sensors were immersed in both distilled water and a buffer solution of pH of 7 for 1 week. A pH meter (Mettler Toledo EL2-Basic Portable Education pH Meter) as shown in Figure 3.4 was immersed in the distilled water and buffer solution before and after the leaving the piezoelectric gum sensors into the media for a certain period. This was done to evaluate if there was a change in the pH of the media which would indicate that the media have been contaminated by the constituent materials (ZnO and CNTs) of the gum sensor.

3.4 Piezoelectric Calibration

The calibration of the piezoelectric coefficients of the samples of the piezoelectric gum sensors was done using the LMS data acquisition system. The LMS data acquisition system has different channels for measuring force via the use of a force transducer input and other time-dependent functions. The data acquisition system generates accurate data of these quantities within microsecond intervals.

Figure 3.4: Mettler Toledo EL2-Basic Portable Education pH Meter

The gum sensor was placed in between a 20mm by 20mm sheet metal which served as the electrode and was sealed round with Cantech tape as shown in Figure 3.5. The figure also shows the data acquisition system and the captured signal during the testing of the gum sensor along the 1-1 direction where the ‘1’ denotes the direction of the applied force and measure electrical field as shown in Figure 3.6. Direction 3 indicate the CNTs alignment direction.

The force transducer was connected to one of the channels of the LMS data acquisition system to monitor the force applied to the gum sensor. Copper tapes were attached to both sides of the sealed gum sensor. A signal cable which was used to monitor the voltage generated as one of its ends connected to the copper tapes and the other end was connected to one of the channels of the LMS data acquisition system. The LMS data acquisition system records both the force applied, and the corresponding voltage generated when a compressive force is applied to the sealed piezoelectric gum sensor via the force sensor. Eleven (11) compressive loading cycles was done in 8 seconds period.

To ensure an accurate reading, the piezoelectric calibration for each gum sensor was done four times and the average value of the force applied and the voltages generated were used for the piezoelectric calibration. The readings obtained from the force applied and corresponding voltage from one of the tests carried out are plotted as shown in Figure 3.7 and Figure 3.8 respectively.

The capacitance of the gum sensors was measured using a two-probe multimeter (U1242B Handheld Digital Multimeter). The piezoelectric coefficients were calculated from the capacitance, the peak value of the forces applied and the corresponding voltages. The following formulas were used for the calculation of the piezoelectric coefficients of the piezoelectric gum sensors;

$$Q = C * V \tag{3-1}$$

where Q is the total charge generated on the surface of the gum sensor covered by the metal electrode, C is the capacitance of the gum sensor at a particular point, and V is the average of the corresponding voltage generated as a result of the force applied at a particular point.

$$D = Q/A \tag{3-2}$$

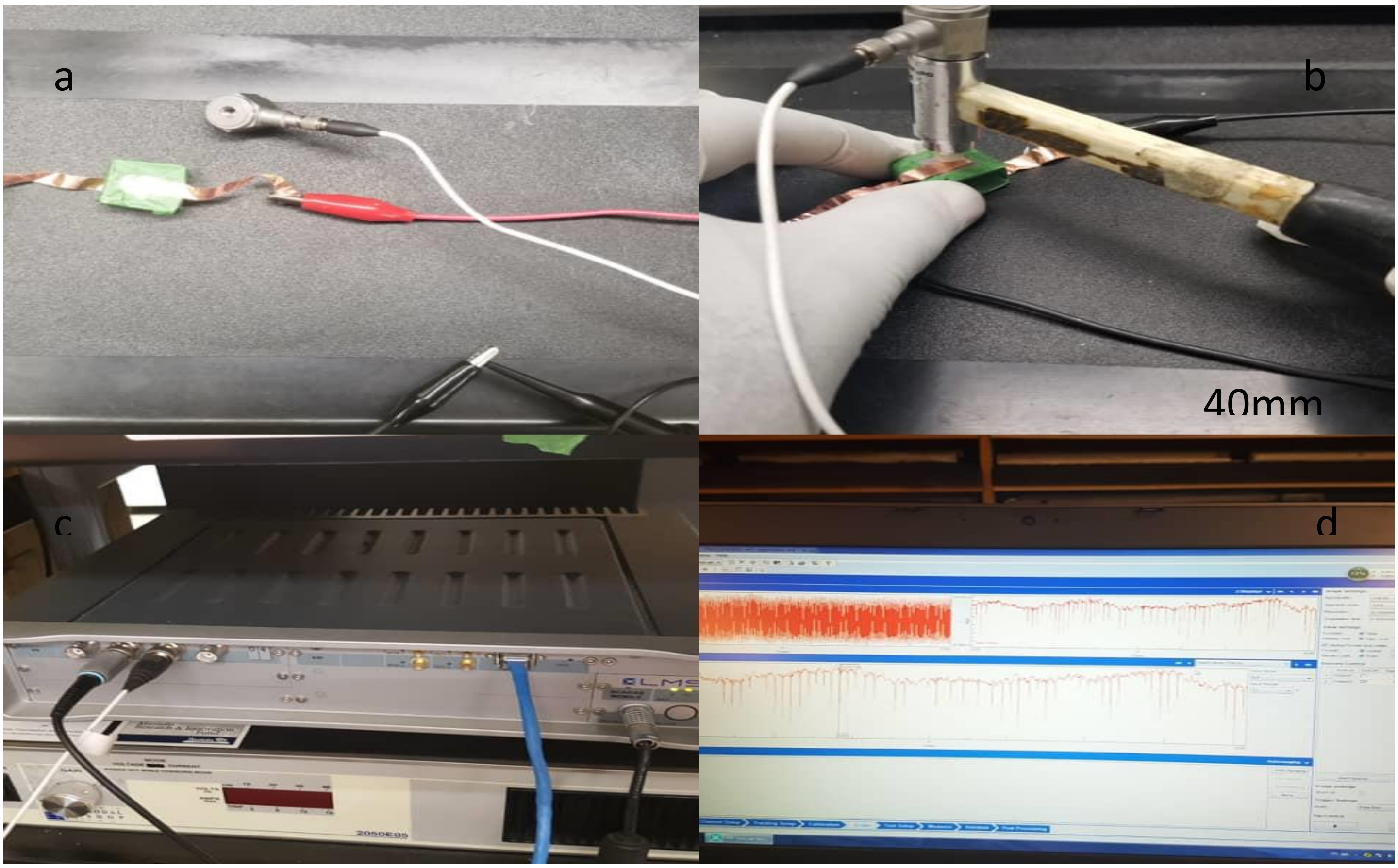

Figure 3.5: (a) The piezoelectric calibration setup showing the force transducer and the gum sensor (b) The piezoelectric calibration setup showing the force transducer with the hammer used to apply force on the gum sensor (c) The image of the front view of the LMS data acquisition with two channels for the applied force and subsequent voltage generated (d) The image of the signal responses of the reading during the excitation of the gum sensor

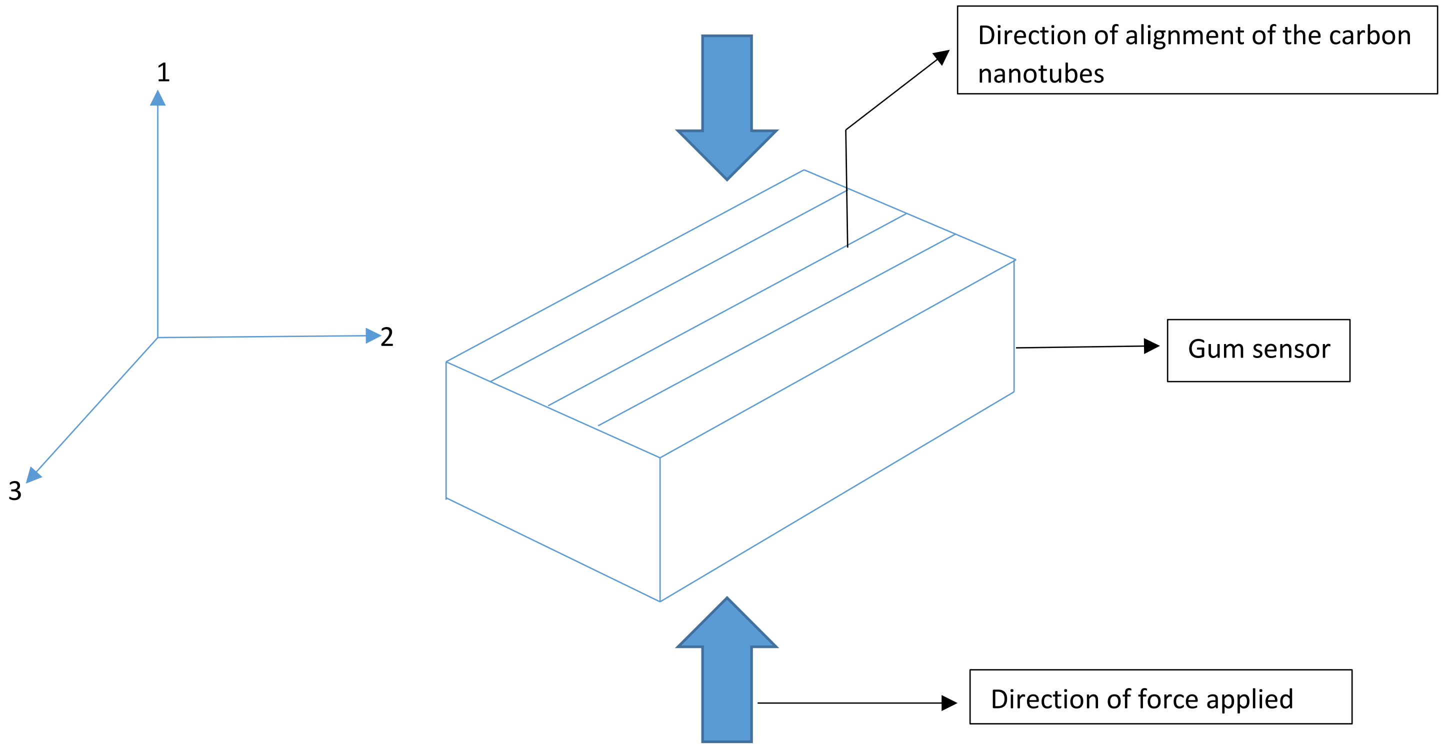

Figure 3.6: Direction of alignment of carbon nanotube and force applied

where D is the charge density and A is the area of the metal electrode.

$$d_{11} = D/S \qquad (3\text{-}3)$$

where d_{11} is the piezoelectric coefficient and S is the stress applied on the gum sensor.

$$S = F/A \qquad (3\text{-}4)$$

where F is the average force applied to the gum sensor.

Force Applied During Piezoelectric Calibration (N)

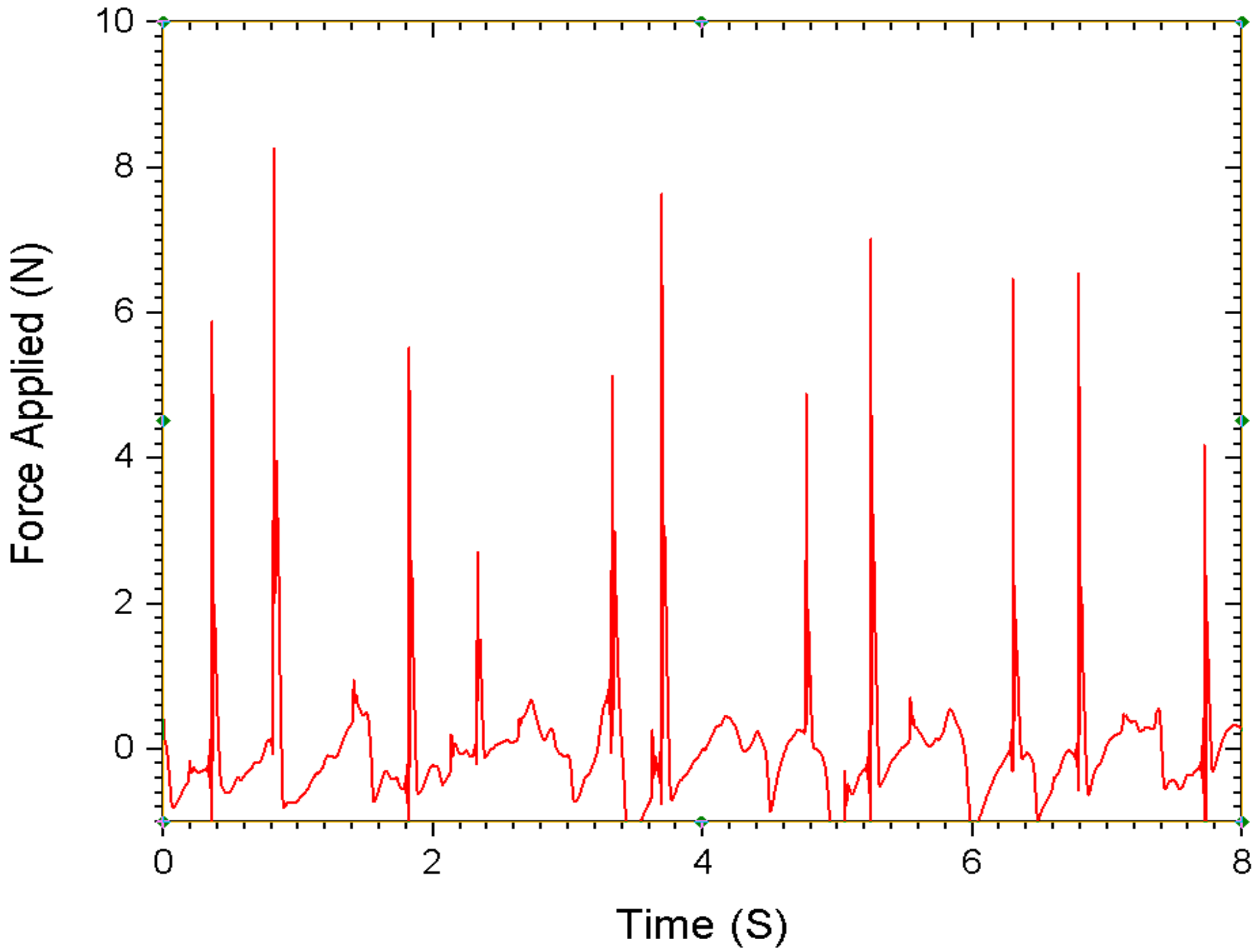

Figure 3.7: The plot of force applied against time during the piezoelectric calibration of the piezoelectric gum sensor

Voltage Generated During Piezoelectric Calibration (mV)

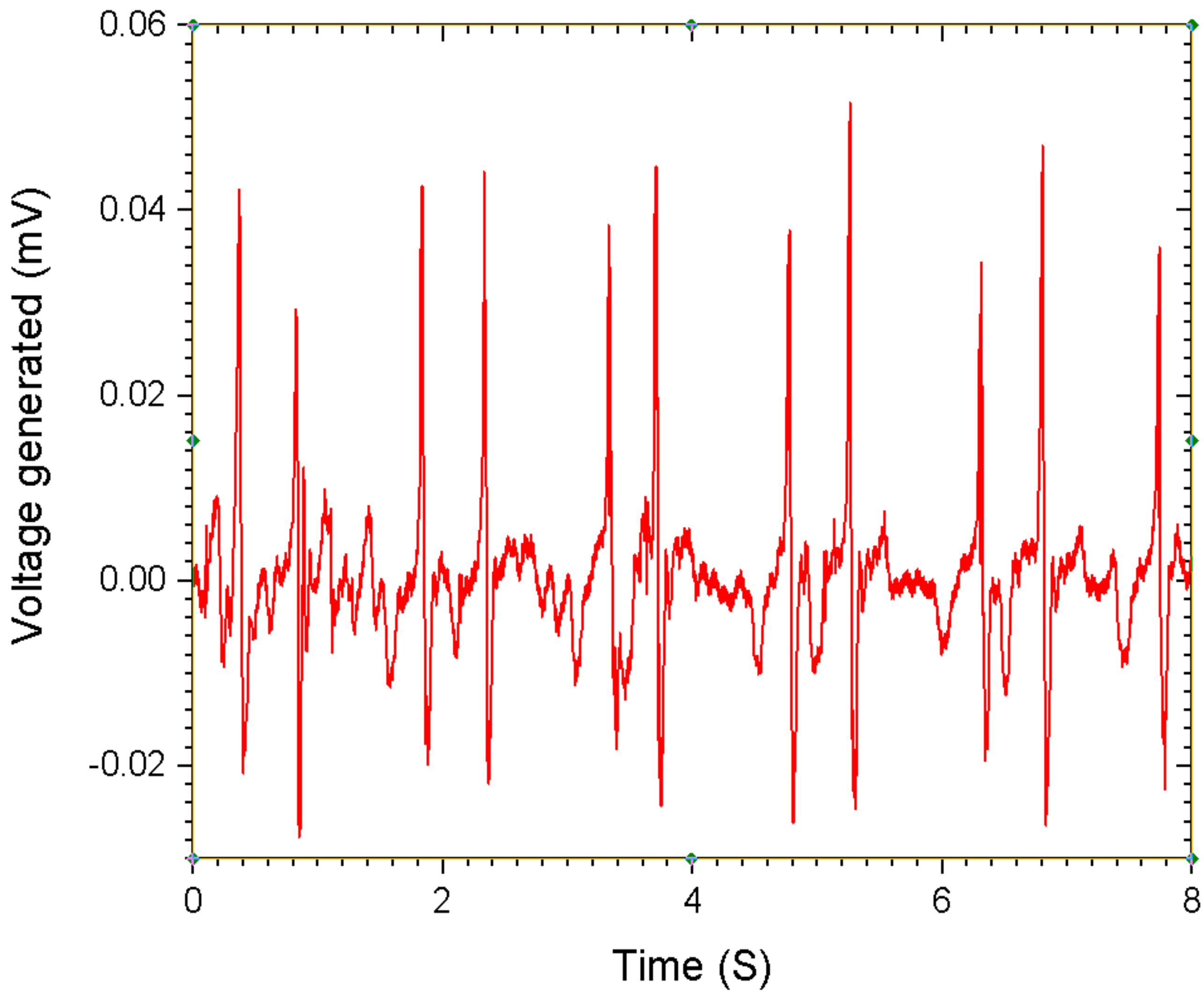

Figure 3.8: The plot of the voltage generated against time during the piezoelectric calibration of the piezoelectric gum sensor

3.5 Mechanical Testing

Tensile tests were conducted to evaluate the mechanical properties of the piezoelectric gum sensors using an Instron 3366 Universal Testing Machine equipped with a static load range of ± 2KN as shown in Figure 3.9. This load cell was chosen so that the Instron machine can detect the smallest force applied to the sample. The ends of the piezoelectric gum sample with a 65mm length, 15mm width, and 0.65mm thickness were attached to flat metal plates with a universal glue and attached to the grips of the Instron machine operating at a constant speed rate of 5mm/mins.

To determine the effect of strain on the sensor resistance, the resistance was measured with a two probes digital multimeter (HYELEC MS8236, data-logging multimeter) simultaneously during the tensile testing. Two-sided copper tapes were used to connect the ends of the sample to the probes of the multimeter.

3.6 Temperature Dependency Test

The performance of a polymer-based nanocomposite piezoelectric sensor can be affected by the electrical resistance of the sensor. The resistance of the CNTs in the gum sensor can change due to temperature changes which invariably would affect the piezoelectric property of the sensor. In order to ensure that the CNTs can effectively connect and transport the charges produced by the ZnO nanoparticles in the sensor, it is important to carry out a temperature dependency test on the sensor.

The piezoelectric gum sensor with 50mm length, 2mm width and 0.5 mm thickness was affixed to the outer part of the container filled with water. Copper tape was connected to both ends of the piezoelectric gum sensor and connected to the digital multimeter (HYELEC MS8236, data-logging multimeter). The container was placed on a plate heater (Barnstead Thermolyne Cimarec heater) with a magnetic bar rotating inside the container. The temperature of the heater was increased from 20°C-80°C in the step of twenty while the resistance of the piezoelectric gum sensor was measured at the same time using a two-probe digital multimeter. The temperature range was selected because it was noticed that the gum was melting above 80°C.

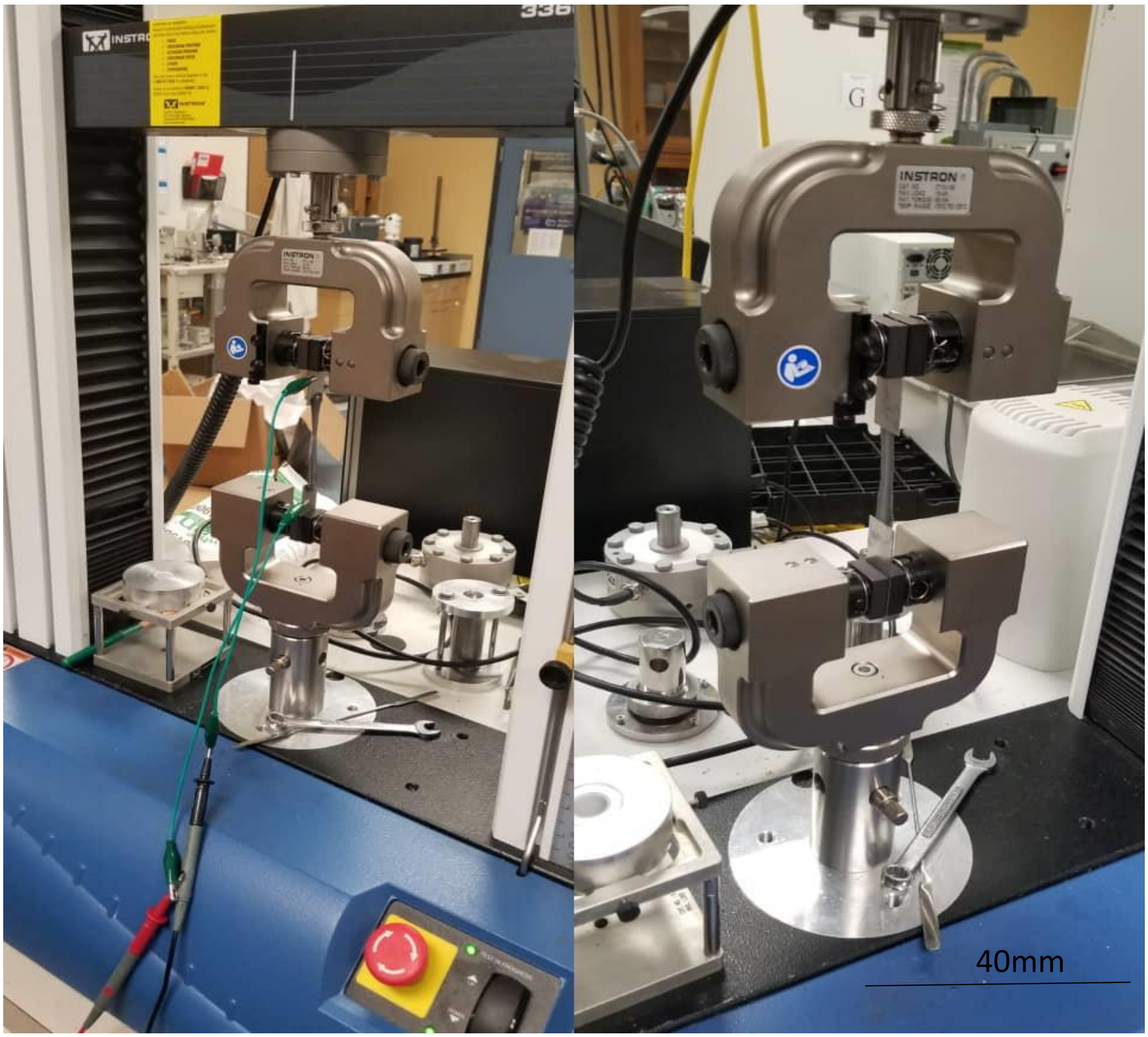

Figure 3.9: Instron 3366 Universal Testing Machine with the sample attached to the jaws.

CHAPTER 4- RESULTS AND DISCUSSION

This chapter contains the results and explanation of the results obtained from the resilience test, piezoelectric calibration, mechanical test, and temperature dependency test.

4.1 Resilience Test Results

In order for a sensor to function properly, it is important to consider different environments in which the sensor would be used. It is crucial to carry out this test to evaluate the ability of the constituent materials (ZnO and CNTs) to bond and adhere to the surface of the gum for use as bio-sensor for example. This test is also used to evaluate the ability of the gum sensor to be used in neutral environments of pH of 6.5-7.5.

The pH of the buffer solution and the distilled water were measured using the pH meter before immersing the piezoelectric gum sensors (ZnO gum sensor, ZnO-SWCNTs gum sensor, and ZnO-MWCNTs gum sensor). The pH of both media is 7 as expected. The pH was measured after the piezoelectric gum sensors have been immersed in these media for 7 days, and it is seen that there is no significant change in the pH of the media. It, therefore, means that the constituent materials are well bonded to the gum surface and the piezoelectric gum sensor can withstand a neutral environment. The media are clear with no traces of the constituent materials in the media as shown in Figure 4.1 and Figure 4.2. This also validates the ability of the constituent materials to bond perfectly to the gum matrix and the ability of the piezoelectric gum sensor to withstand the environment.

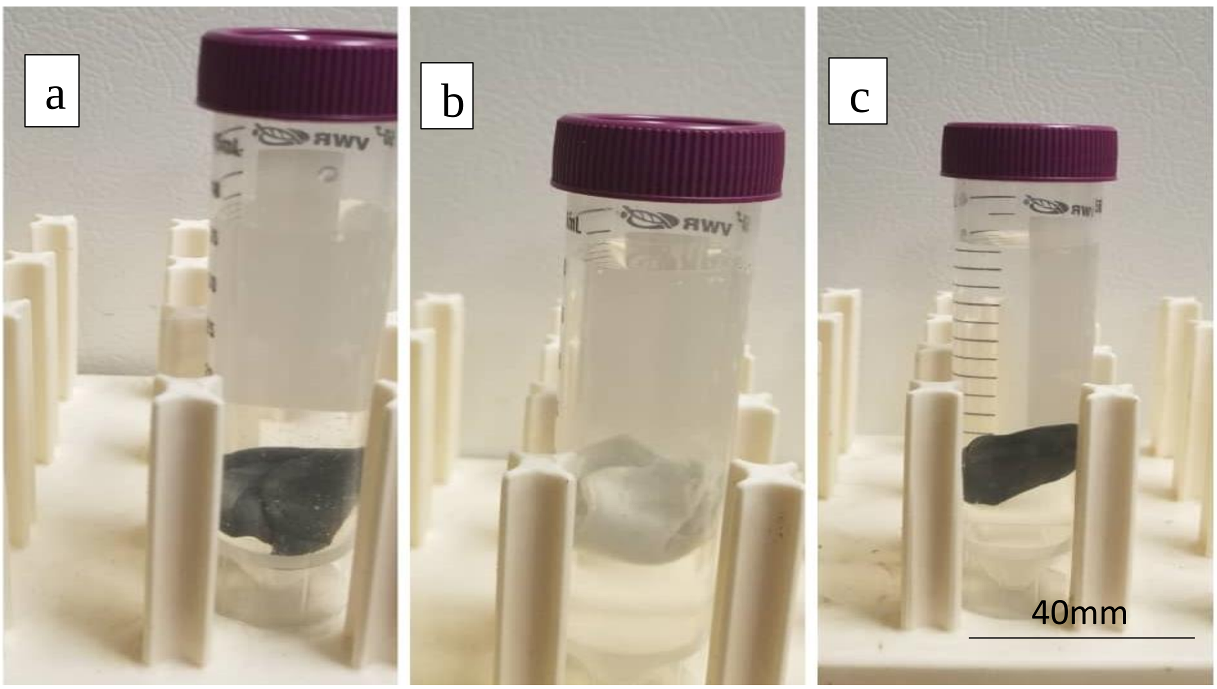

Figure 4.1: Clear solution of the piezoelectric gum immersed in distilled water after 7 days a) ZnO-SWCNTs gum sensor immersed in distilled water b) ZnO gum sensor immersed in distilled water c) ZnO-MWCNTs gum sensor immersed in distilled water

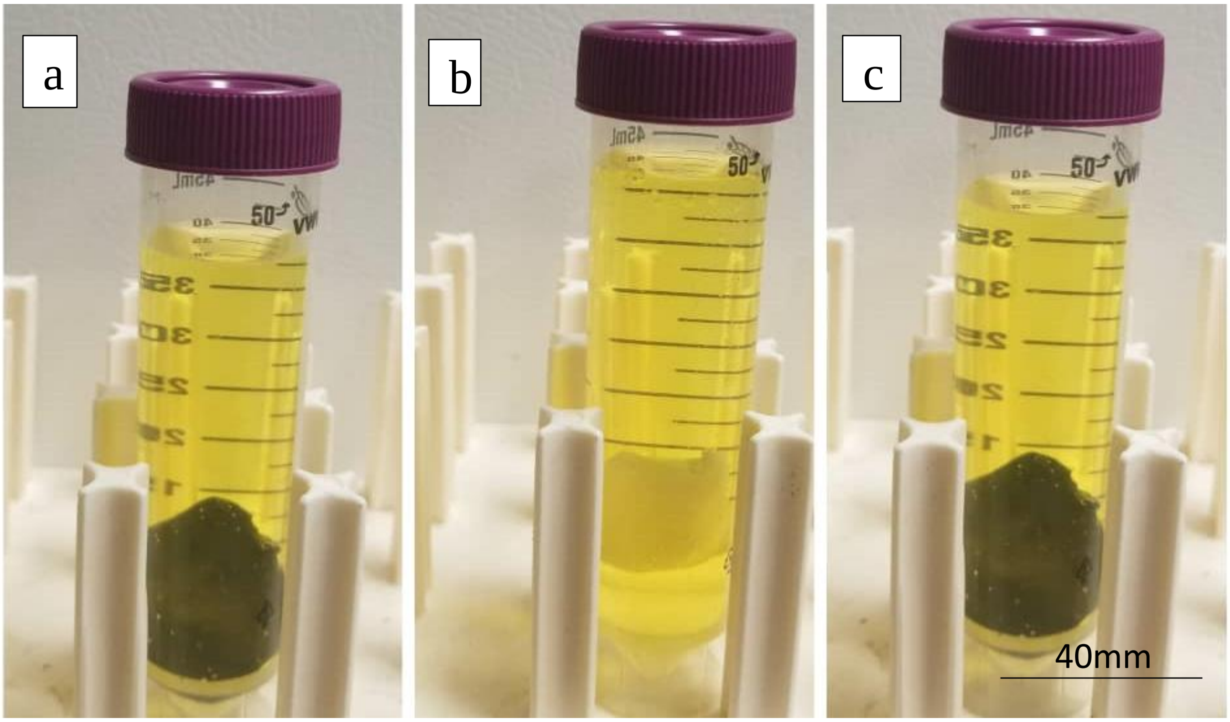

Figure 4.2: Clear solution of the piezoelectric gum immersed in a buffer solution of pH 7 after 7 days a) ZnO-SWCNTs gum sensor immersed in buffer solution b) ZnO gum sensor immersed in buffer solution c) ZnO-MWCNTs gum sensor immersed in a buffer solution

4.2 Optimization of CNTs in the gum sensor by the use of Piezoelectric Calibration

Several literatures [99]-[101] have shown that the piezoelectric property of ZnO can be enhanced by the addition of CNTs. It is, however, important to determine the wt % of CNTs that is required to be added to the ZnO in order to achieve an optimum piezoelectric property of the gum sensor. Based on this, different piezoelectric gum sensors were fabricated by adding different wt %s of SWCNTs to ZnO (base material) in the gum sensor. The piezoelectric properties of these gum sensors were evaluated using the piezoelectric coefficient (d11) calculated from piezoelectric calibration of the gum sensor gotten from LMS data acquisition system. The piezoelectric coefficient (d11) was calculated using equation (3-1) – (3-4). The values of the piezoelectric coefficient for the different wt % of CNTs added to ZnO in the gum sensors are shown in Table (4.1).

The optimization plot as seen in Figure 4.3 shows the plot of the piezoelectric coefficient of the piezoelectric gum sensor against increasing varying wt % of CNTs. It can be observed from Figure 4.3 that there is an increase in the piezoelectric coefficient of the gum sensor with an increase in the wt % of CNT to a threshold value followed by a sharp decline. The highest piezoelectric coefficient occurs when 90.9 wt % of ZnO and 9.1 wt % of CNTs solutions were used for the fabrication of the gum sensor. The CNTs were optimized within the limitation of the preparation and test procedures. There is a drastic drop in the piezoelectric coefficient of the gum sensor when the wt % of SWCNTs was increased from 9.1% to 11.1%. The piezoelectric coefficient dropped by approximately 339% from the threshold value of 27.05 pC/N to 5.43pC/N when the wt% of SWCNTs was increased from 9.1% to 11.1%. This shows that excess of SWCNTs in the gum sensor is detrimental to the piezoelectric property of the gum sensor. However, if added in a little amount, the piezoelectric property of the ZnO in the gum sensor would not be optimally enhanced.

The piezoelectric coefficient of the gum sensor increases with increase in the addition of CNTs to the ZnO in the gum sensor as shown in Figure 4.3 and this suggest that there is an enhanced electrical bridging and connectivity between the ZnO nanoparticles with increase in CNTs addition [165] [166]. The presence of CNTs in the piezoelectric gum sensor perhaps leads to the formation of electrically connected networks providing a continuous pathway for the electric current to be transmitted [167]. The application of force on the gum sensor can cause the CNTs to flex and bend against adjacent ZnO nanoparticles. This leads to the deformation of the structure which in effect induces electrical potential. Due to cross-linking of the ZnO and CNTs nanoparticles, there can be inhomogeneity in the gum domain creating a potential difference across the gum resulting in the change in voltage [165].

The same behavior is also reported in some research carried out on energy storage and conversion device [168]-[170]. Researchers reported that the addition of CNTs to lithium-ion batteries helped in the enhancement of the electrical properties of the batteries. It enhanced the electrical connectivity of the Lithium-based active materials in the battery, decreases the electrolyte absorption time and subsequently increases the lifetime of the batteries. The uniform introduction of CNTs into the batteries resulted in an increased electrical connectivity and hence, provides a pathway linking the nanoparticles in the battery [169].

However, because the CNTs nanoparticles are in water suspension, with more addition of CNTs dispersion (> 9.1 wt. %) to ZnO, this can lead to excess voids in the gum sensor after the water dries up. This can affect the electrical connections between the ZnO nanoparticles [165]. The electrical charges produced by the ZnO nanoparticles when subjected to external load cannot be connected due to these voids causing a low voltage output from the gum sensor and hence a low piezoelectric coefficient.

Piezoelectric Coefficient (pC/N) with increasing wt % of CNTs

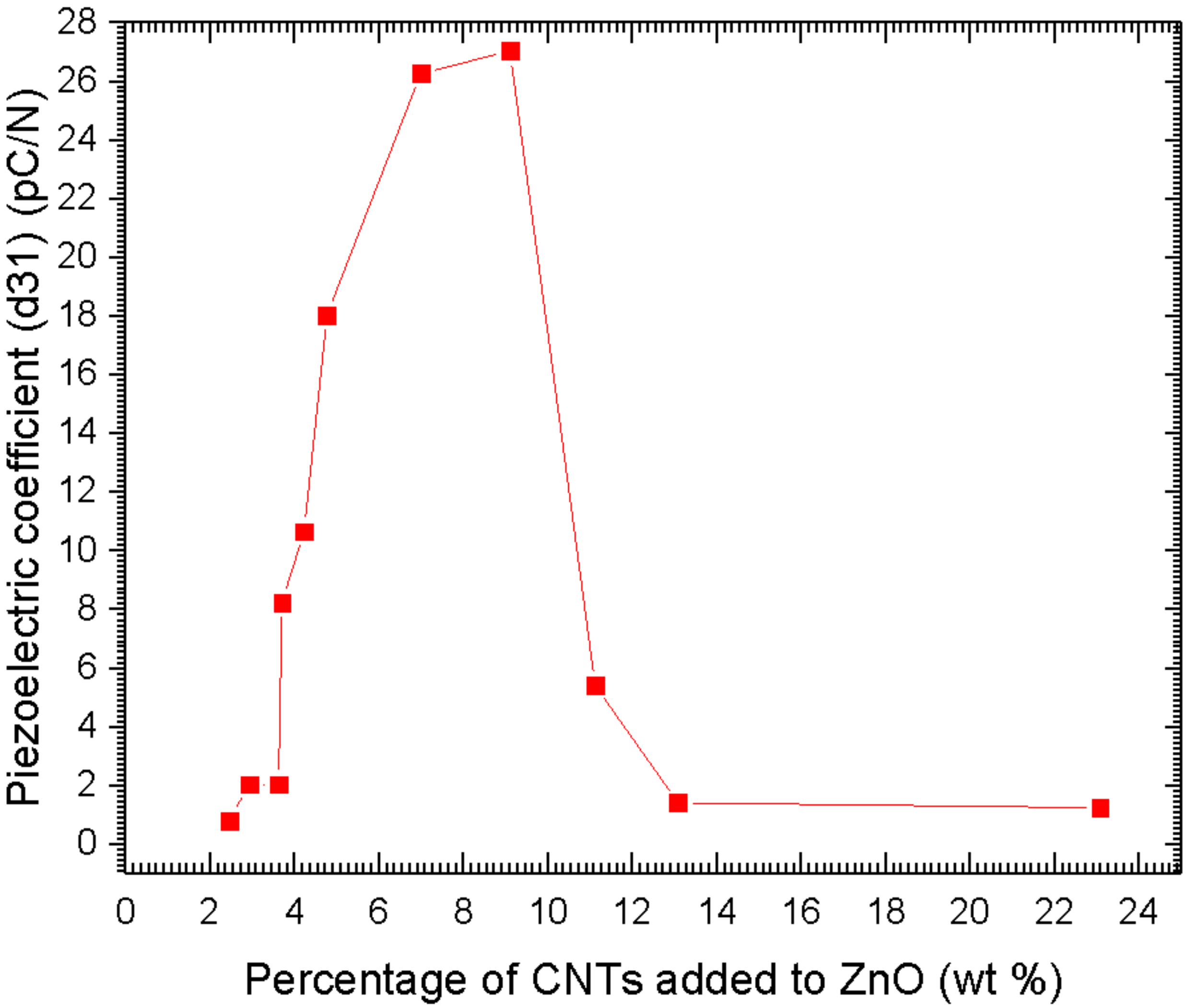

Figure 4.3: The effect of increase in CNTs addition to the ZnO in the gum

Table 4.1: The piezoelectric coefficients of ZnO-SWCNTs with varying wt %s of SWCNTs in the gum sensor

SWCNTs (wt %)	Piezoelectric Coefficient (pC/N)
2.4	0.81
2.9	2.05
3.6	2.06
3.7	8.26
4.2	10.67
4.8	18.04
6.9	26.27
9.1	27.05
11.1	5.43
13.1	1.43
23.1	1.26

4.2.1 Comparison of the Piezoelectric Coefficient of ZnO-SWCNTs and ZnO-MWCNTs Gum Sensor

In order to evaluate if the addition of MWCNTs to ZnO in the gum will further enhance the piezoelectric property of the gum sensor as compared to the addition of SWCNTs to ZnO, ZnO-MWCNTs and ZnO-SWCNTs gum sensors were fabricated with the same wt %s of CNTs (SWCNTs and MWCNTs) and ZnO. The effects of the increase in the wt % of CNTs (SWCNTs and MWCNTs) on the piezoelectric coefficients of ZnO-SWCNTs gum sensor and ZnO-MWCNTs gum sensor respectively are shown in Figure 4.4. It shows that for both piezoelectric nanocomposite gum sensors, the piezoelectric coefficients increased with increase in the wt % of SWCNTs and MWCNTs. Both ZnO-SWCNTs and ZnO-MWCNTs gum sensors have almost the same piezoelectric coefficient values when the wt %s of the CNTs were increased from 3.61% to 4.22%. Further increase in the wt % of SWCNTs and MWCNTs in the gum sensors indicate that ZnO-SWCNTs gum sensor has a higher piezoelectric coefficient as compared to ZnO-MWCNTs gum sensor. The highest piezoelectric coefficient is obtained at 9.1 wt.% each of SWCNTs and MWCNTs.

Better piezoelectric property is observed for ZnO-SWCNTs gum sensor as compared to ZnO-MWCNTs gum sensor as seen in Figure 4.4. This is probably because the shorter SWCNTs were able to provide a better conduction path for the ZnO nanoparticles in the gum sensor than MWCNTs. SWCNTs are known to have fewer defects as compared to MWCNTs [171]. The presence of more defects in MWCNTs could reduce the ease of connection and transportation of the charges produced by the ZnO nanoparticles. The same behavior was reported by Ramaratnam and Jalili [21]. The SWCNT-PVDF-TrFe film produced a greater piezoelectric response than MWCNT-PVDF-TrFe film.

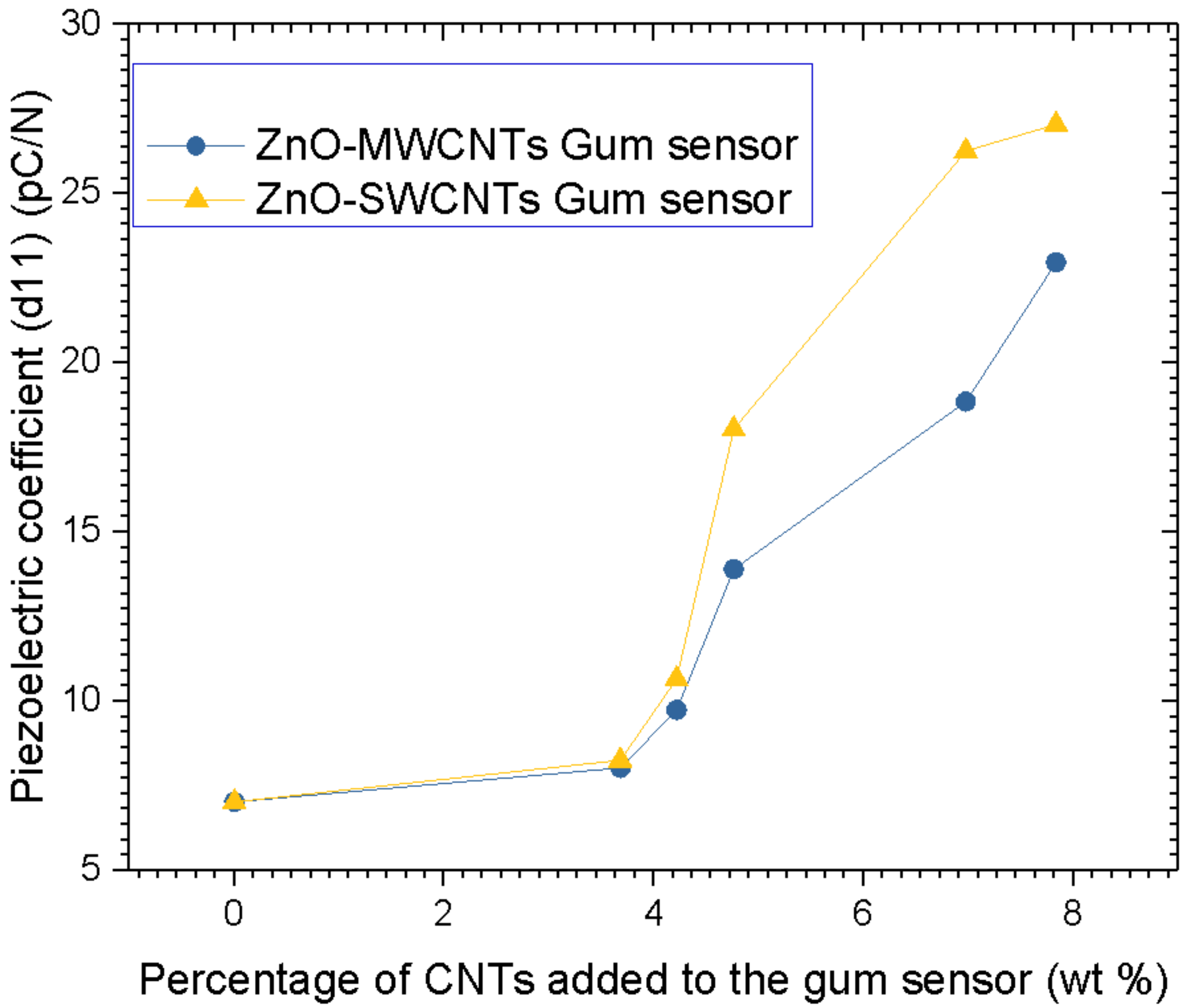

Figure 4.4: The effect of an increase in CNT addition on the piezoelectric coefficient of ZnO/SWCNTs gum sensor and ZnO/MWCNTs gum sensor.

4.3 Effect of Strain on Sensor Resistance

The performance of a polymer-based nanocomposite sensor can be affected by the electrical resistance of the sensor. The resistance of the CNTs in the gum sensor can change due to strain application which invariably affects the piezoelectric property of the sensor. Several researches [99]-[101] however, have shown that carbon nanotubes are responsible for connecting the charges produced by the ZnO nanoparticles. It is therefore important to consider the effect of strain on the sensor resistance to ensure that the CNTs can effectively connect and transport the charges produced by the ZnO nanoparticles.

Two piezoelectric gum sensors; optimized ZnO-SWCNTs and ZnO-MWCNTs gum sensors were subjected to tensile loading and the resistance change was measured simultaneously as explained in chapter 3. The resistance versus strain plots for ZnO-SWCNTs gum sensor and ZnO-MWCNTs sensor when they were subjected to tensile loading is shown in Figure 4.5 and Figure 4.6 respectively. The resistance increases with increase in the applied load even unto the fracture for the two gum sensors. The change in resistance of the piezoelectric gum sensors with applied load could be due to the loss of contacts among the CNTs and tunneling resistance variation due to rearrangement of neighboring CNTs and intrinsic resistance due to deformation [171-178].

The increase in the resistance of both the ZnO-SWCNTs gum sensor and ZnO-MWCNTs gum sensor suggests that the electrical properties of piezoelectric gum sensors are greatly affected by the tunneling effect in which it is required that the tunneling distance is close enough for appreciable electron flow to occur [179] [180]. Tunneling is a plausible concept that is greatly influenced by the gap between two neighboring tubes. The electrical conductivity vanishes slowly as the gap between these CNTs increases thereby leading to an increase in the tunneling resistance or, proportionately, a reduction in electrical conductivity is observed [171].

Due to the applied load, there is every likelihood that changes occur in the tunneling resistance between neighboring CNTs because of inter-tube distance enlargement and/or decrease in the electrical contact areas. Both concepts can lead to an increase in the resistance of both the ZnO-SWCNTs gum sensor and ZnO-MWCNTs gum sensor with applied load [179].

The increase in the resistance of both gum sensors with an increase in applied load can also be explained using the geometric effect. The resistance of the gum sensor is given as;

$$R = \frac{\rho l}{A} \tag{4-1}$$

where ρ is the electrical resistivity

L is the length of the conductor

A is the cross-sectional area of the conductor.

The resistance of the gum sensor increases upon elongation in length and reduction in cross-sectional area.

Furthermore, as observed in Figure 4.5 and Figure 4.6, the initial and final resistance values obtained for ZnO-MWCNTs gum sensor are quite higher than that obtained for ZnO-SWCNTs gum sensor with increase in load application. The introduction of more contacts and tunneling points between neighboring CNTs possibly can lead to a reduction in electrical conductivity which subsequently causes an increase in the electrical resistance and percolation threshold [181]. More contacts points and tunneling points are likely to be introduced due to the wavy and multiconcentric layers of the MWCNTs as compared to SWCNTs which has a single contact point. Large interface and contact resistance are built up due to the contact between the multiconcentric layer MWCNTs which acts as a barrier to the flow of electric current [182] and therefore responsible for higher resistance in ZnO-MWCNTs gum sensor as compared to ZnO-SWCNTs gum sensor.

Moreover, the mechanical strength of the ZnO-SWCNTs gum sensor is found to be much higher than ZnO-MWCNTs gum sensor, while the ZnO-SWCNTs gum sensor fails at around 40% strain and ZnO-MWCNTs gum sensor is broken at only 22% strain as shown in Figures 4.5 and 4.6. SWCNTs are known to have fewer defects as compared to MWCNTs [171]. The presence of more defects or voids in the ZnO-MWCNTs gum sensor is believed to be responsible for the higher resistance and lower strain capacity as compared with ZnO-SWCNTs gum sensor with fewer defects. These results confirm that ZnO-SWCNTs gum sensor has a better piezoelectric property as compared to ZnO-MWCNTs gum sensor.

Resistance vs Strain Plot for ZnO-SWCNTs gum sensor

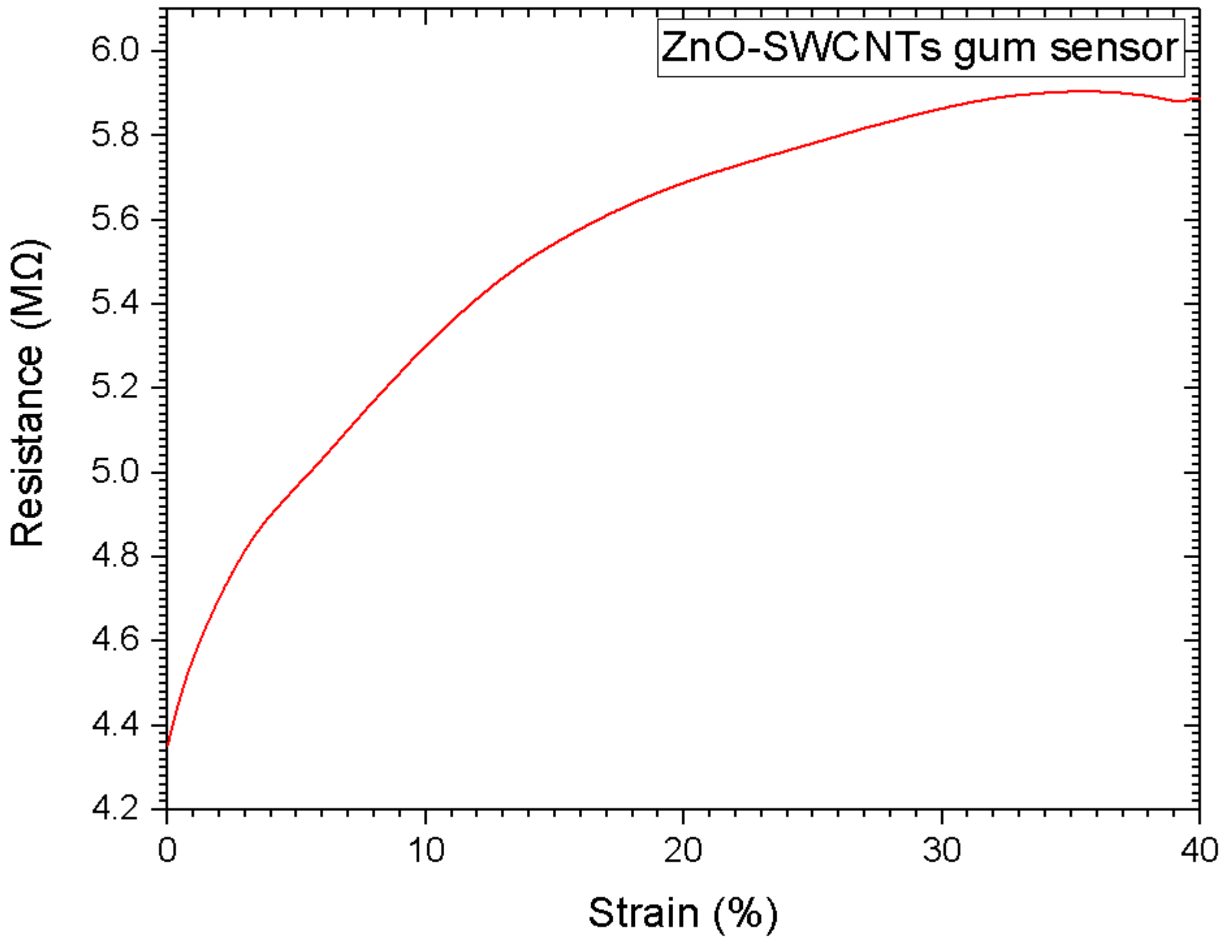

Figure 4.5: Resistance vs Strain Plot for ZnO-SWCNTs gum sensor with 9.1 wt % of SWCNTs

Resistance vs Strain Plot for ZnO-MWCNTs gum sensor

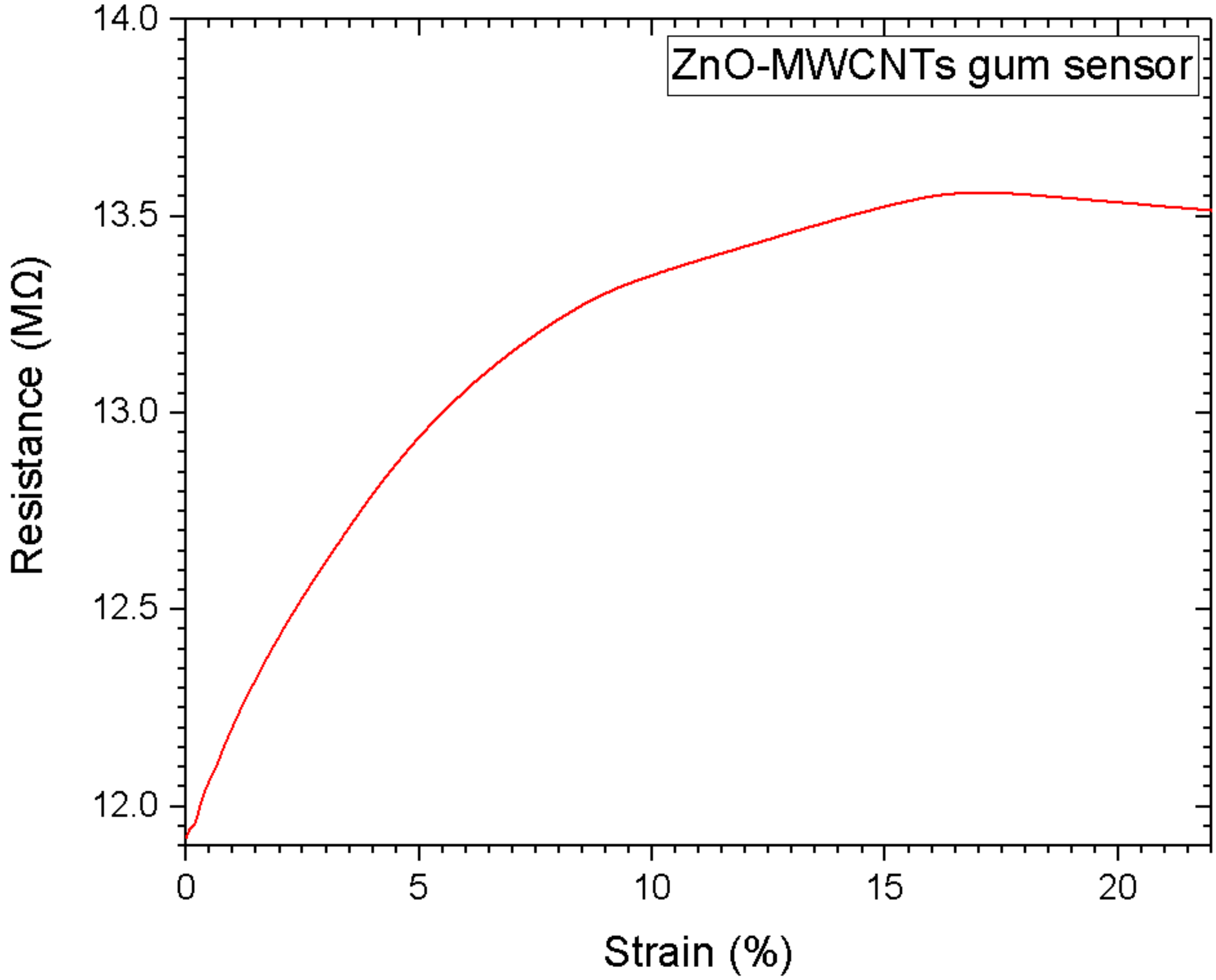

Figure 4.6: Resistance vs Strain Plot for ZnO-MWCNTs gum sensor with 9.1 wt % of MWCNTs

4.4 Effect of Temperature on Sensor Resistance

The performance of a polymer-based nanocomposite piezoelectric sensor can be affected by the electrical resistance of the sensor. The resistance of the CNTs in the gum sensor can change due to temperature changes which invariably affects the piezoelectric property of the sensor. In order to further confirm that the CNTs can effectively connect and transport the charges produced by the ZnO nanoparticles, it is important to consider the effect of temperature on the resistance of the sensor.

The resistance vs temperature plots for ZnO-SWCNTs (9.1 wt % of SWCNTs) and ZnO-MWCNTs (9.1wt % of MWCNTs) is as shown in Figure 4.7. The resistance increases with increase in temperature from 20^{o}C to 80^{o}C for the piezoelectric nanocomposites gum sensors as expected as shown in Figure 4.7. The temperature range was selected because it was noticed that the gum was melting above 80^{o}C. The mechanism of the increase in resistance with increase in temperature has been explained in several kinds of literature using several theories such as conduction pathway theory, percolation phenomenon, thermal expansion theory, electric field emission theory and tunnel effect theory [183-188].

The increase in the resistance of the piezoelectric gum sensor with increase in temperature is believed to be due to the difference in the thermal expansion between nanoparticles and the gum which can cause an increase in the interparticle gap width of the conductive path [189]-[192].

ZnO-MWCNTs piezoelectric gum sensor has a higher resistance as compared to ZnO-SWCNTs piezoelectric gum sensor for each temperature. The result shows that at 20 ^{o}C, the resistance of ZnO-MWCNTs piezoelectric gum sensor is 173% higher than the resistance of ZnO-SWCNTs piezoelectric gum sensor while at 80 ^{o}C, the resistance of ZnO-MWCNTs piezoelectric gum sensor is 42% higher than the resistance of ZnO-SWCNTs piezoelectric gum sensor.

Effect of temperature on the resistance

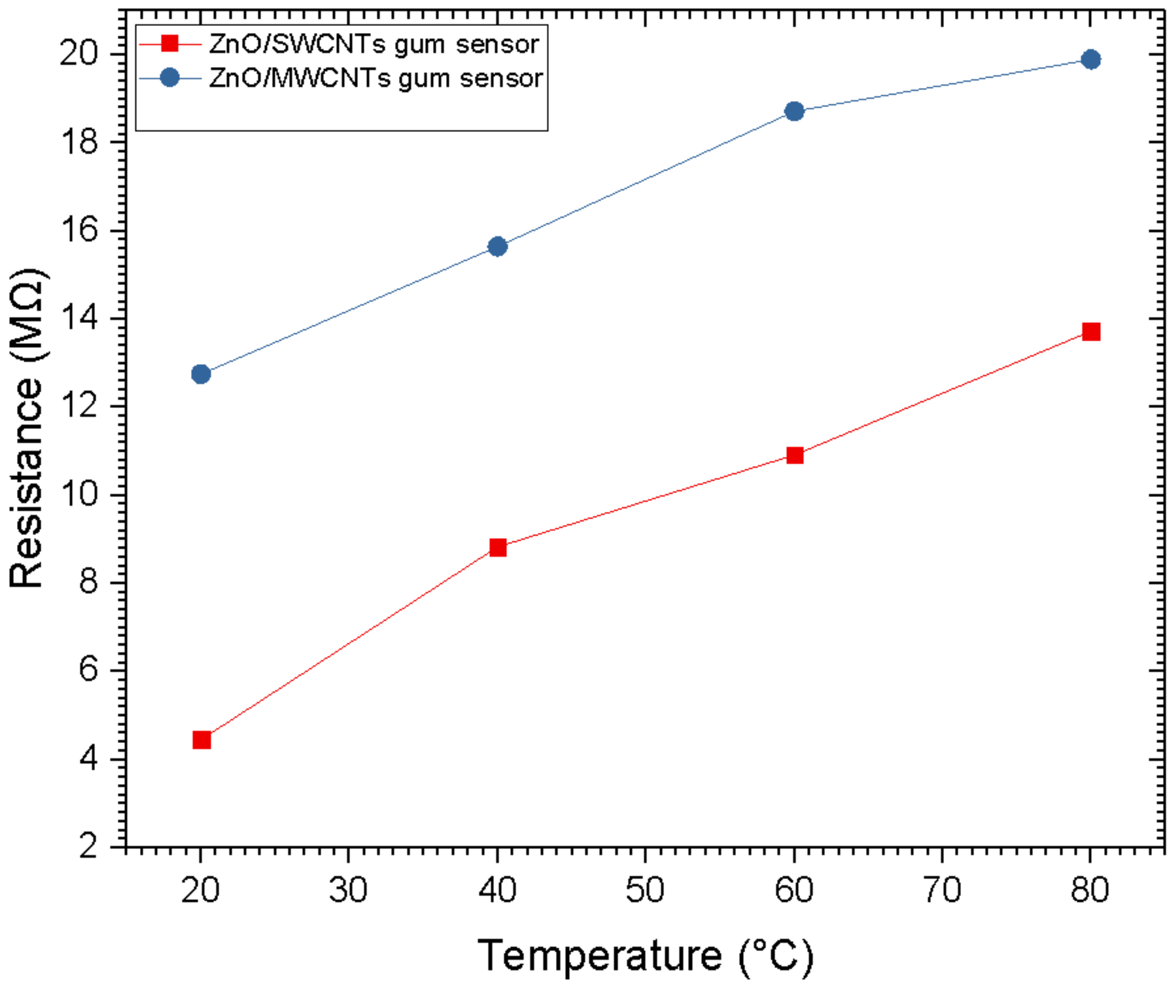

Figure 4.7: Comparison of the effect of temperature on the resistance of the piezoelectric gum sensors

The interparticle gap width between the CNTs perhaps increased with increase in temperature. It, therefore, implies that the smaller the interparticle gap width, the lower the resistance of the piezoelectric sensor [38] [182]. This suggests that the interparticle gap width between SWCNTs nanoparticles in the ZnO-SWCNTs piezoelectric gum sensor is smaller than the interparticle gap width between MWCNTs in the ZnO-MWCNTs piezoelectric gum sensor. This can explain the reason for the lower resistance obtained for ZnO-SWCNTs piezoelectric gum sensor as compared to ZnO-MWCNTs piezoelectric gum sensor and this confirms that ZnO-SWCNTs gum sensor has a better piezoelectric property as compared to ZnO-MWCNTs gum sensor.

4.5 Effect of CNT addition on the mechanical properties of the gum sensor

Traditionally, carbon nanotubes are used as nanofillers for polymeric material to enhance their mechanical properties. Enhanced mechanical property is important as the sensor would be subjected to load and it is important for the sensor to have significant load-bearing capacity in application.

The stress vs strain plots as shown in Figure 4.8, 4.9 and 4.10 obtained during the tensile testing of the three piezoelectric gum sensors show the values of the strain to failure, yield strength, ultimate tensile strength (UTS), and the failure strength for each of the piezoelectric gum sensors. The bar charts in Figure 4.11, Figure 4.12, Figure 4.13 and Figure 4.14 gives the comparison of the different mechanical properties that are obtained from the stress-strain curve for the three piezoelectric gum sensors. The stress vs strain plot shows that ZnO-SWCNTs piezoelectric gum sensor can withstand more load as compared to ZnO piezoelectric gum sensor and ZnO-MWCNTs piezoelectric gum sensor.

Stress-strain plot

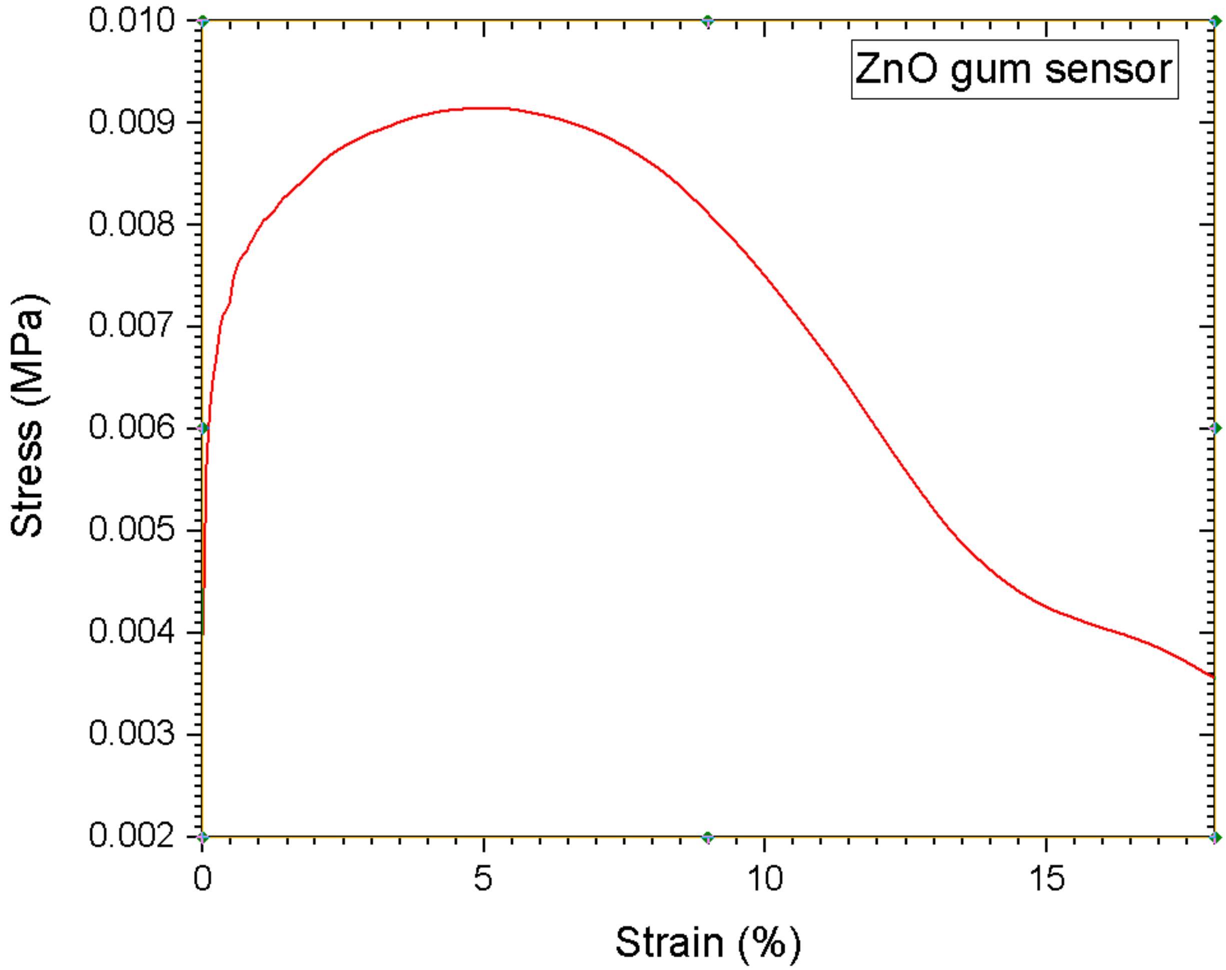

Figure 4.8: Stress-Strain Plot for ZnO piezoelectric gum sensors

Stress-strain plot

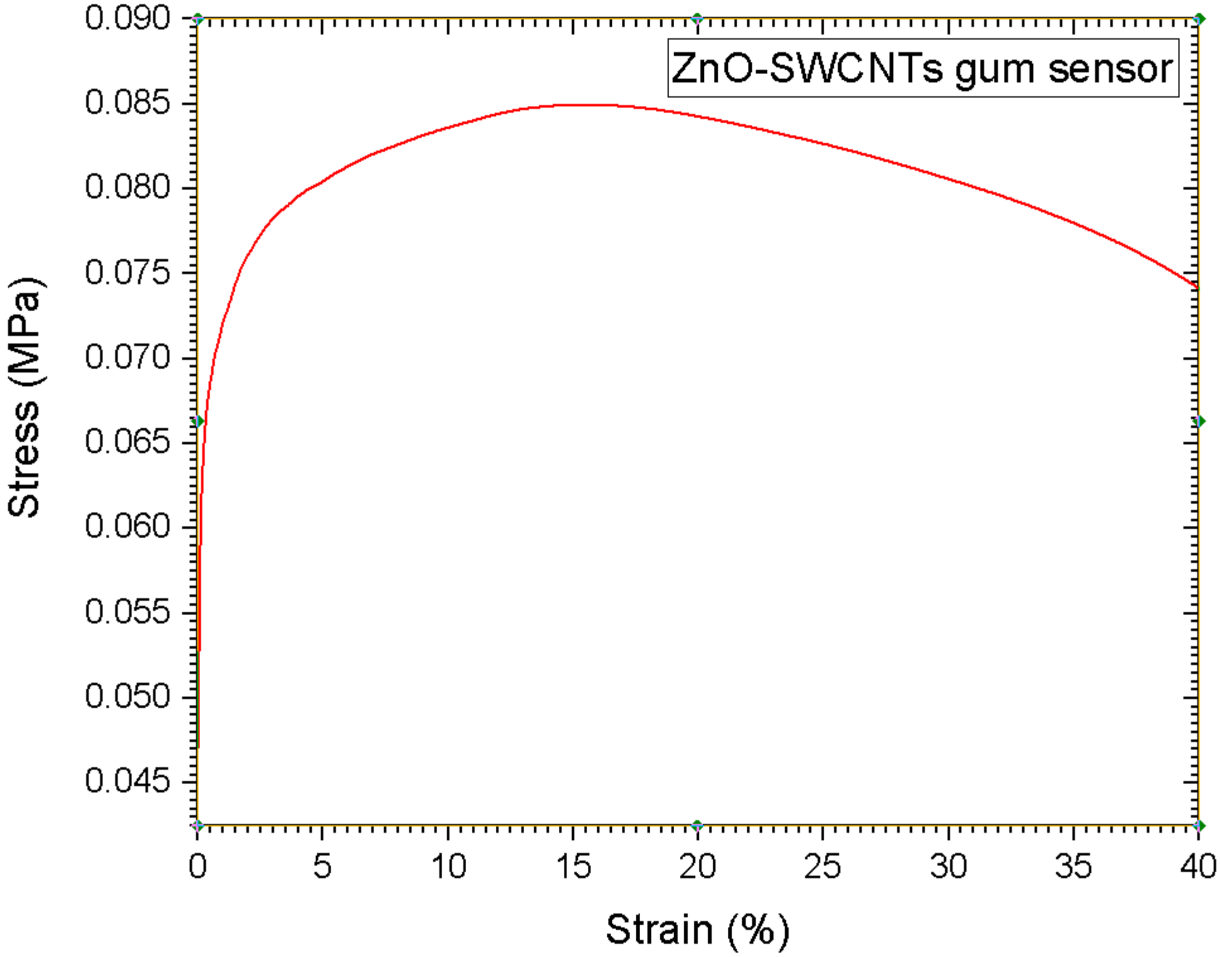

Figure 4.9: Stress-Strain Plot for ZnO-SWCNTs the piezoelectric gum sensors

Stress-strain plot

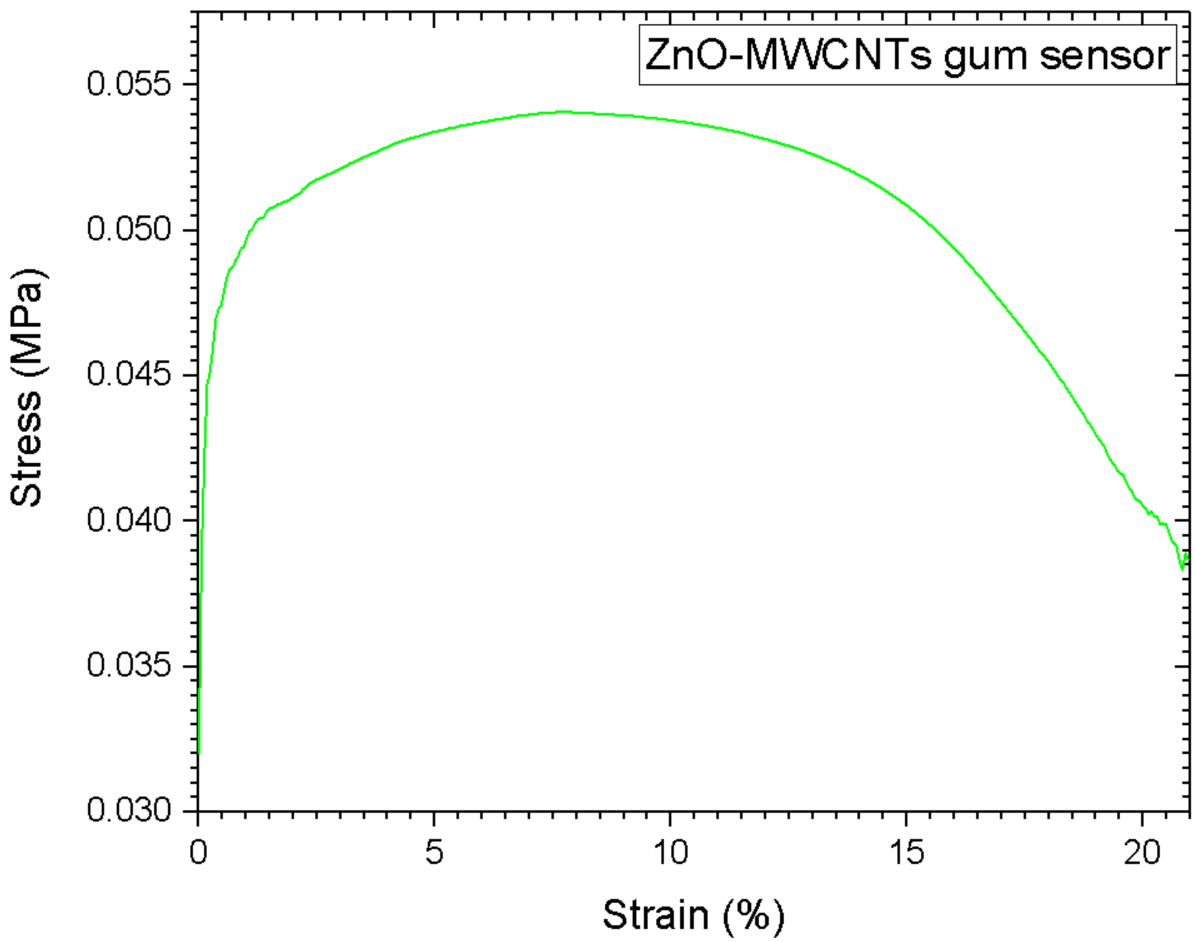

Figure 4.10: Stress-Strain Plot for ZnO-MWCNTs the piezoelectric gum sensors

Strain to failure

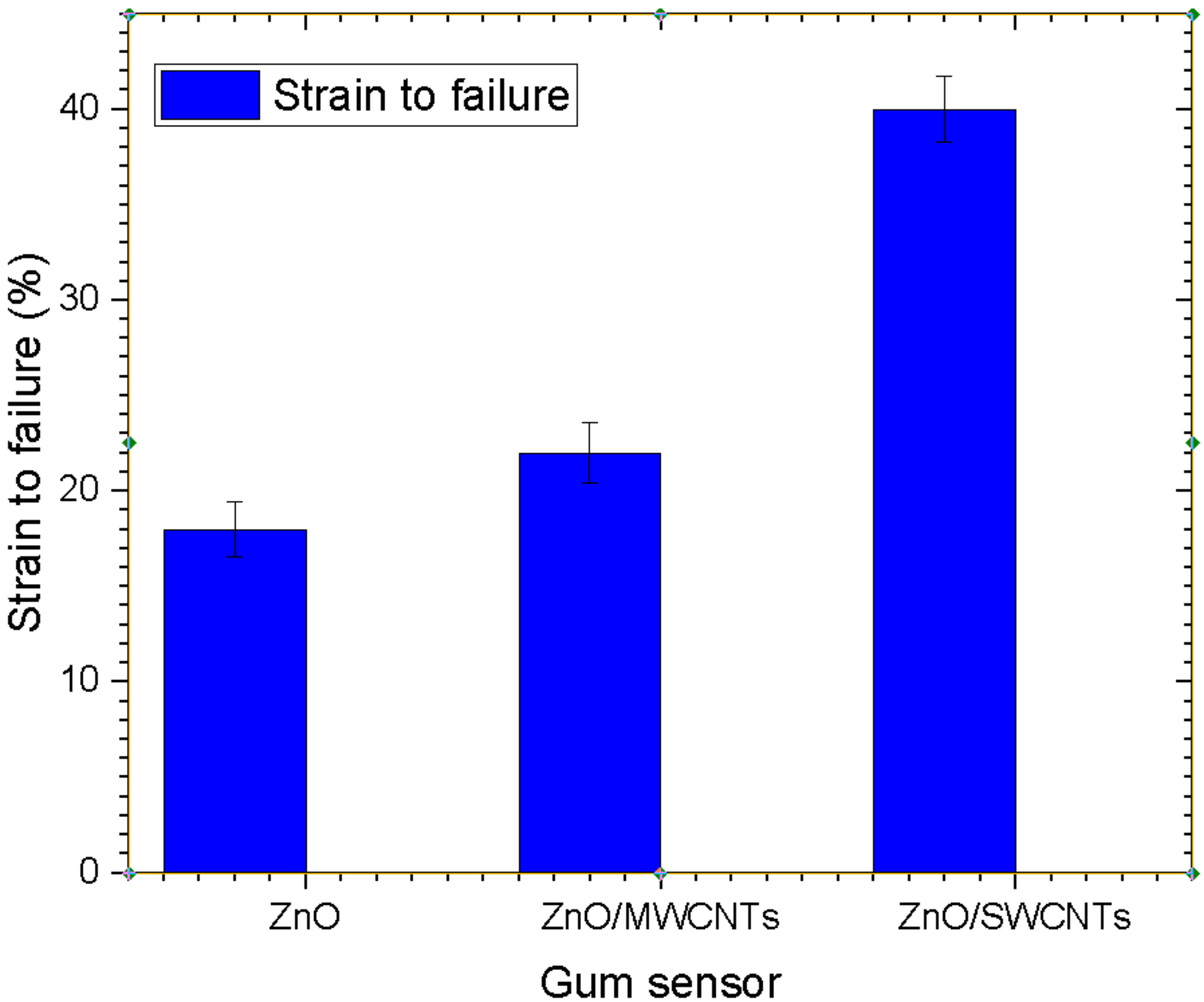

Figure 4.11: The comparison of the strain to failure for the mechanical testing of the piezoelectric gum sensors

The strain to failure values obtained for the three piezoelectric gum sensors; ZnO, ZnO-SWCNTs, and ZnO-MWCNTs show that the strain to failure of ZnO-SWCNTs piezoelectric gum sensor is more than twice that of ZnO piezoelectric gum sensor and almost twice the strain to failure of ZnO-MWCNTs piezoelectric gum sensor. Also, as shown in Figure 4.12, the yield strength for ZnO-SWCNTs piezoelectric gum sensor is almost 2 times greater than the yield strength of ZnO piezoelectric gum sensor and close to the value obtained for ZnO-MWCNTs piezoelectric gum sensor. In order to evaluate the maximum stress that the three piezoelectric gum sensors can withstand when subjected to loading before breaking, the ultimate tensile strength (UTS) is obtained from the stress vs strain plot and the results indicate that the UTS for ZnO-SWCNTs piezoelectric gum sensor is almost ten times greater than that of ZnO piezoelectric gum sensor and has a close but greater value as compared to UTS obtained for ZnO-MWCNTs piezoelectric gum sensor. The failure strength of ZnO-SWCNTs piezoelectric gum sensor is more than 20 times greater than that of ZnO piezoelectric gum sensor and almost twice the UTS obtained for ZnO-MWCNTs piezoelectric gum sensor.

The enhancement of the mechanical properties of nanocomposites can be attributed to the transfer of stress from the polymer matrix to the nanoparticles. It is, therefore, necessary to have strong interfacial adhesion between the polymer and CNTs for improved mechanical properties. However, the presence of voids, agglomerates, defects, and other inclusions of MWCNTs reduces the strength of a nanocomposites [193]. Better mechanical properties are observed in ZnO-SWCNTs piezoelectric gum sensor as compared to ZnO-MWCNTs piezoelectric gum sensor and this is could be because SWCNTs have fewer defects as compared to MWCNTs [171]. The internal layer of MWCNTs possibly slide over each other thereby reduces the load-bearing capacity of the nanotubes; only the outer shells of MWCNTs tend to carry loads.

Yield strength

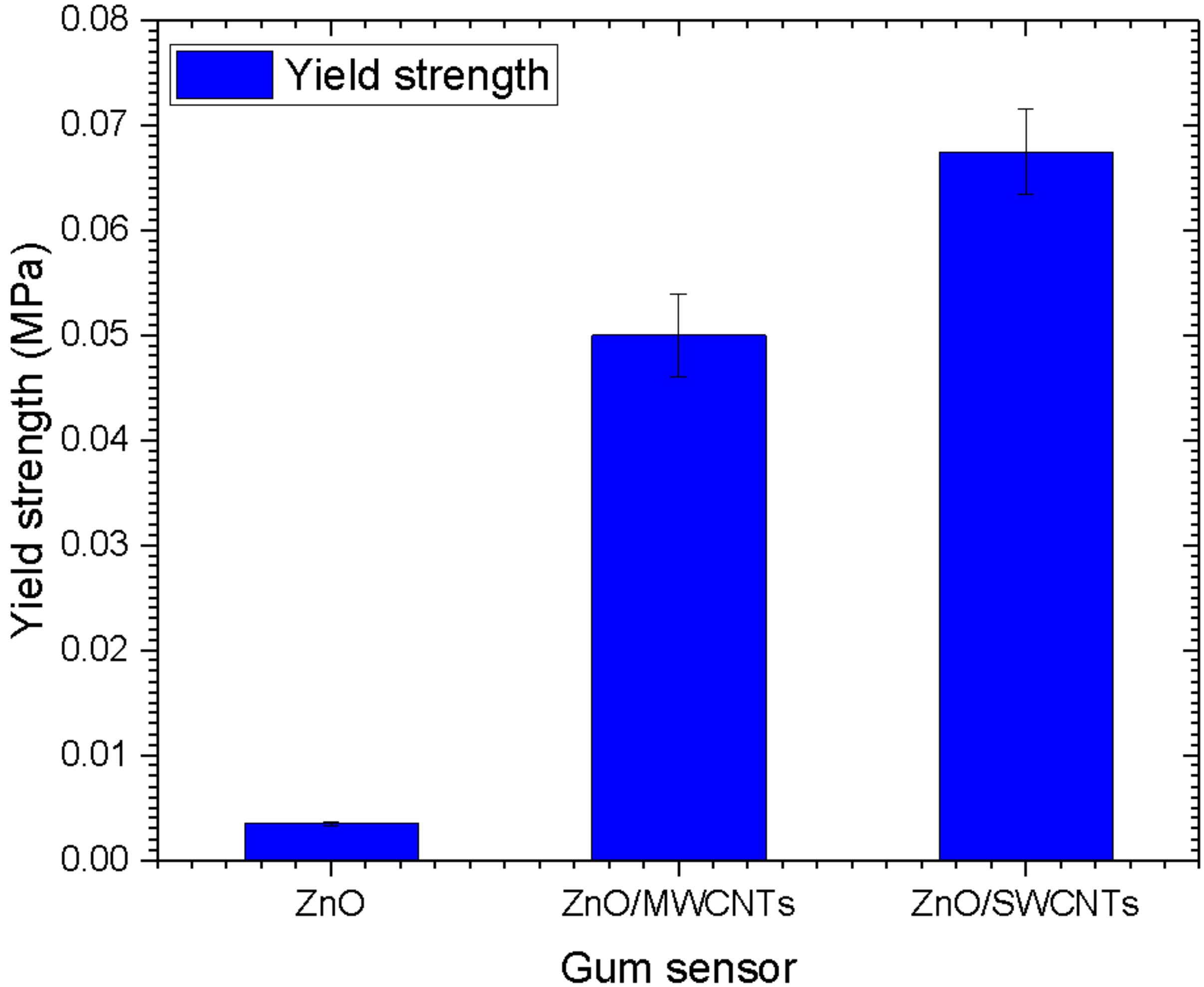

Figure 4.12: The comparison of the yield strength for the mechanical testing of the piezoelectric gum sensors

This suggests that only weak van der Waals force interaction is responsible for transferring the loads between the shells, the resulting aggregates act as a defect site rather than reinforcing the nanocomposites, and inner shells are hence able to slide and rotate freely [193].

SWCNTs are made from a single rolled-up graphene and there is the absence of multiple nesting in SWCNTs as found in MWCNTs and as a result, it is believed to have better mechanical properties due to curvature effect. In addition, SWCNTs are made up of close-packed stacking ropes and form self-assembled cables on nanometer scales [89] and therefore provides strength to the piezoelectric nanocomposites gum sensor. It is also possible that agglomeration occurs at a higher concentration of MWCNTs in the piezoelectric nanocomposite gum sensor which could reduce the strength of the piezoelectric nanocomposite gum sensor [171].

A similar trend was observed in a research carried out by Gojny et.al [194], where the mechanical properties of epoxy reinforced with varying wt % of Double-walled carbon nanotubes (DWCNTs), SWCNTs and MWCNTs. It was observed that the epoxy reinforced with SWCNTs has a higher UTS and young modulus than the epoxy reinforced with MWCNTs. SWCNTs is believed to have provided better mechanical properties due to its large surface area and aspect ratio as compared to epoxy reinforced with MWCNTs. It was also attributed to the agglomeration of MWCNTs with local stress concentration and thus reduces the strength of the nanocomposites.

Ultimate tensile strength

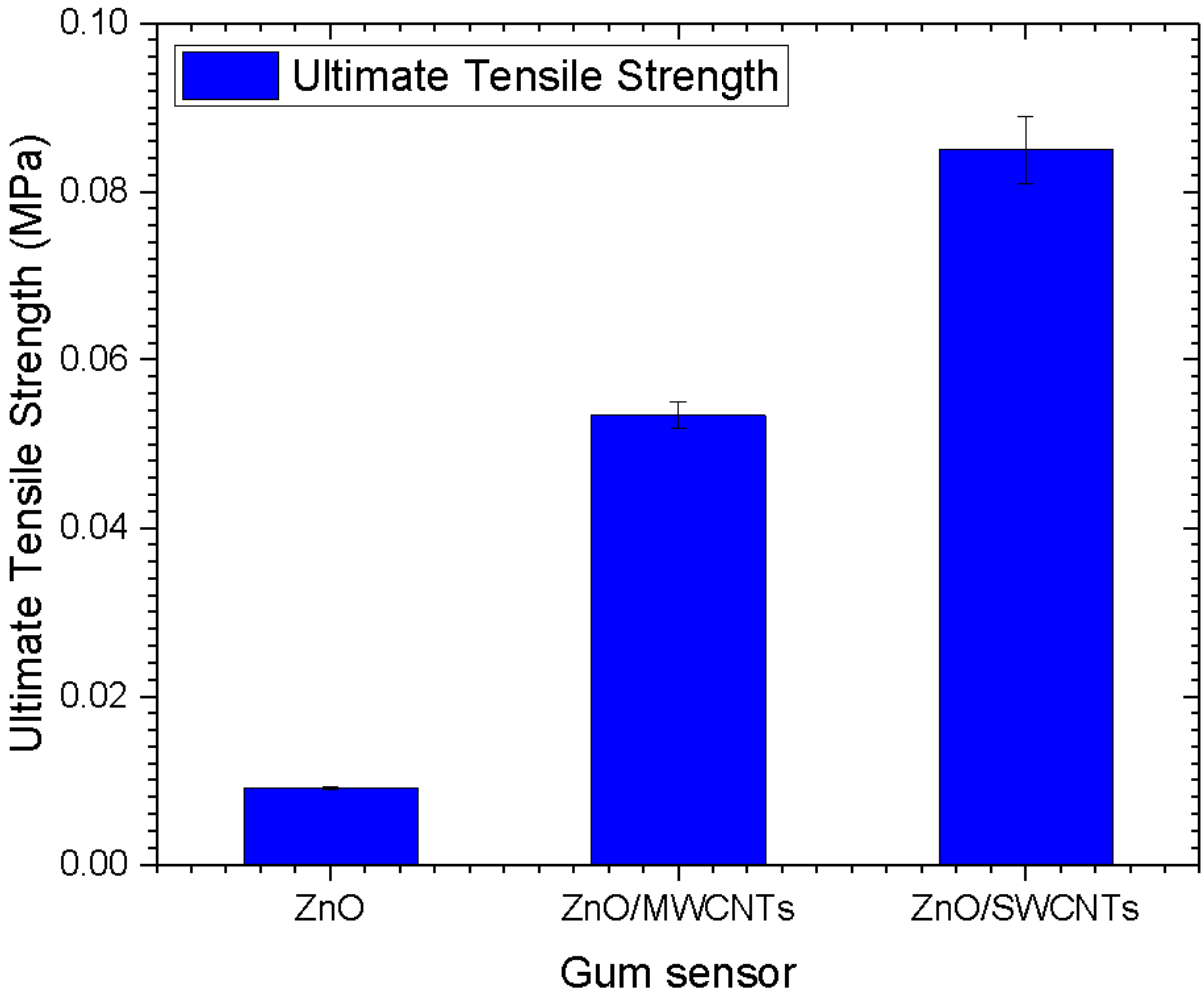

Figure 4.13: The comparison of the ultimate tensile strength for the mechanical testing of the piezoelectric gum sensor

Failure strength

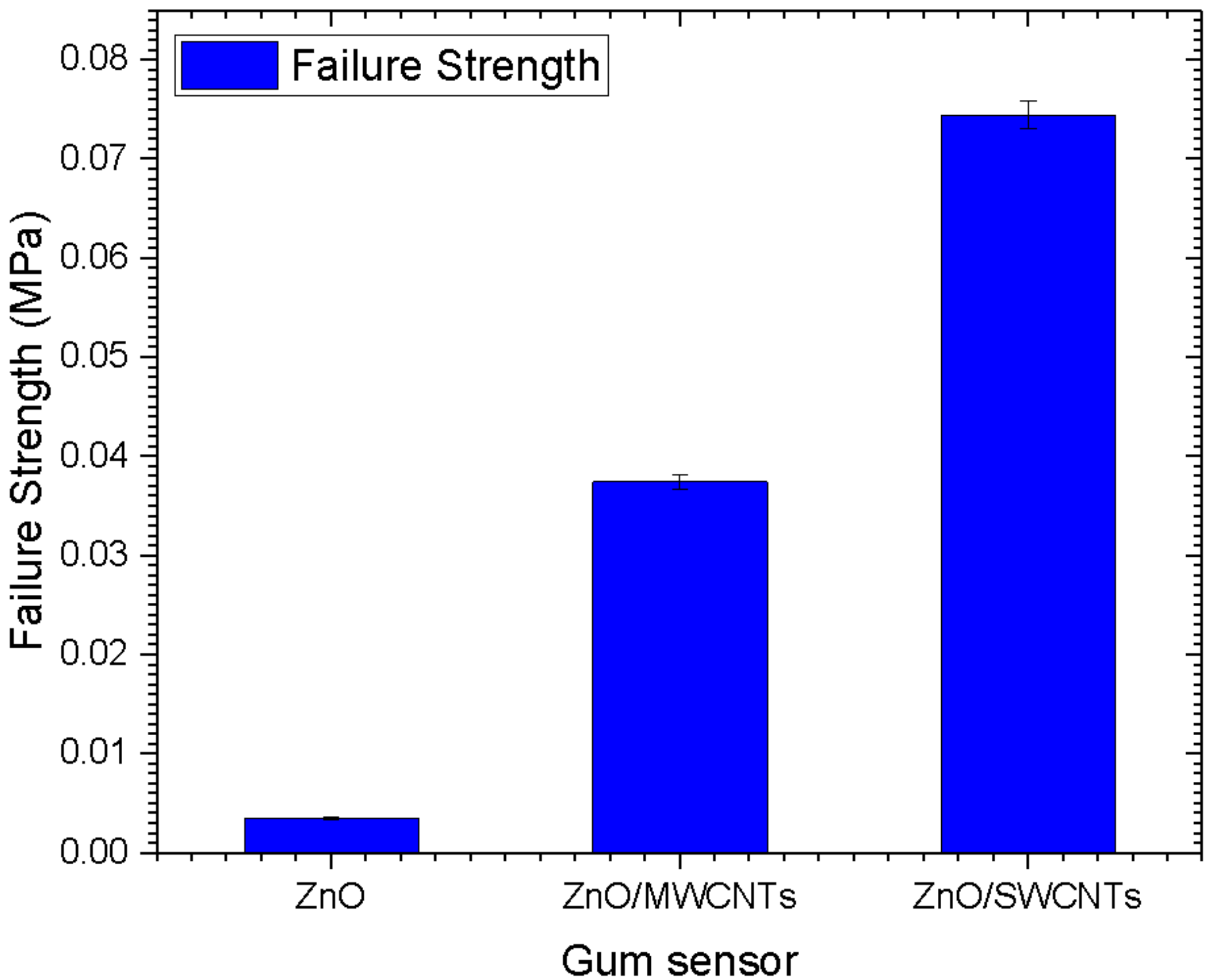

Figure 4.14: The comparison of the failure strength for the mechanical testing of the piezoelectric gum sensors

CHAPTER 5- Conclusions and Recommendation

5.1 Summary and Conclusions

The purpose of this research was to fabricate a piezoelectric nanocomposite gum, which can serve as both static and dynamic sensor, by direct mixing of the constituent materials (ZnO and CNTs) with gum. The piezoelectric gum sensor was characterized using the LMS data acquisition to obtain the piezoelectric coefficient, resilience test was done to determine the ability of the constituent materials to adhere properly to gum and the ability of the gum sensor to withstand the environment, the effects of temperature and strain on the sensor resistance were considered to further evaluate the performance of the gum sensors. Finally, a mechanical test was done to evaluate the mechanical properties of the gum sensors. The results from the experiments show that;

- Piezoelectric nanocomposites gum sensor can be effectively fabricated by direct mixing of ZnO and CNTs with the gum.
- The constituent materials (ZnO and CNTs) adhered properly to the surface of the gum and were able to withstand the environment without been dissolved in the solution.
- The piezoelectric property of nanocomposite made from ZnO embedded in the gum can be enhanced by the addition of CNTs.
- There is a threshold for the weight % of CNTs (9.1 wt %) required for the fabrication of the piezoelectric nanocomposites gum sensor beyond which the piezoelectric coefficient of gum sensor would decrease.
- The addition of SWCNTs to ZnO provide a better piezoelectric property enhancement as compared to MWCNTs possibly because SWCNTs are able to form a better electrical bridges and connection between the ZnO nanoparticles as compared to MWCNTs

- ZnO-MWCNTs gum sensor has a higher resistance with increase in strain as compared to ZnO-SWCNTs gum sensor. The presence of multiconcentric layer in MWCNTs as compared to single contact point in SWCNTs could be responsible for higher resistance in strain observed in ZnO-MWCNTs gum sensor as compared to ZnO-SWCNTs gum sensor.
- ZnO-MWCNTs gum sensor has a higher resistance with increase in temperature as compared to ZnO-SWCNTs gum sensor. This could be due to interparticle gap width of SWCNTs which is smaller than that of MWCNTs with increase in temperature.
- The mechanical strength of the piezoelectric nanocomposite gum sensor is significantly enhanced by introducing CNTs. ZnO-SWCNTs piezoelectric gum sensor has higher strength than the ZnO-MWCNTs and this could be possibly due to fewer defects in SWCNTs as compared to MWCNTs.
- The results obtained from this research shows that the optimized ZnO/SWCNTs piezoelectric nanocomposite gum sensor can be fabricated with 9.1 wt% of SWCNTs and 90.9 wt% of ZnO. This combination has a better piezoelectric property, mechanical property and temperature and strain dependency effect as compared to ZnO/MWCNTs piezoelectric nanocomposite gum sensor with the same composition of MWCNTs and ZnO.

5.2 Recommendations for Future Work

- One of the main limitations of this research was the inability to measure the piezoelectric coefficient of the piezoelectric nanocomposite gum sensor along other directions i.e. along the direction of alignment of the nanotubes. If this can be measured, it would give rise to a better piezoelectric property.

- Attempts were made to carry out the microscopic examination of the piezoelectric nanocomposite gum sensor but due to the soft nature of the matrix material (bubble gum), it was quite difficult to get a microtomed section on the TEM grid. If the microscopic examination of the gum sensor was possible, it would help to reveal the arrangement of the constituent materials (ZnO and CNTs) in the gum.
- The effect of temperature on the piezoelectric coefficient of the piezoelectric nanocomposite gum sensors should be investigated.
- Gum was used as the matrix material for the fabrication of the sensor and as a proof of concept. The temperature range of application without damage of the gum sensor is limited. Other flexible matrix materials should hence be considered for the fabrication process
- Further studies are required to be carried out on the field testing of the piezoelectric nanocomposite gum sensor.

References

[1] Estes, A. C., and Frangopol, D. M. “Bridge lifetime system reliability under multiple limit states.” J. Bridge Eng., 10.1061/ (ASCE) 1084-0702(2001)6:6(523), pp. 523–528, 2001.

[2] LeBeau, K. H., and Wadia-Fascetti, S. J. “Fault tree analysis of Schoharie Creek Bridge collapse.” J. Perform. Constr. Facil., 10.1061/ (ASCE) 0887-3828(2007)21:4(320), pp. 320–326, 2007.

[3] Xie, F., and Levinson, D. “Evaluating the effects of the I-35 W Bridge collapse on road-users in the twin cities metropolitan region.” Transp. Plann. Technol., vol. 34, no. 7, 691–703, 2011.

[4] C. R. Farrar, S. W. Doebling, A. D. Nix, “Vibration–based structural damage identification,” *Philos. Trans. R. Soc. London*, vol. 359, pp. 131–149, 2001.

[5] S. W. Doebling, C. R. Farrar, M. B. Prime, “A Summary Review of Vibration-Based Damage Identification Methods,” *Shock Vib. Dig*., no. 30, pp. 91–105, 1998.

[6] G. Park, T. Rosing, M. D. Todd, C. R. Farrar, W. Hodgkiss, “Energy Harvesting for Structural Health Monitoring Sensor Networks” *ASCE J.Infrastruct. Syst*, vol. 14, pp. 64–79, 2008.

[7] James F. Tressler, Sedat Alkoy and Robert E. Newnham. ”Piezoelectric Sensors and Sensor Materials”. Jour. of Electroceramics, vol. 2, no. 4, pp 257-272 1998.

[8] Katzir, S. The discovery of the piezoelectric effect, In KATZIR S. (eds) The beginnings of piezoelectricity. Boston Studies in Philosophy of Science, vol 246. Springer, Dordrecht, 2008.

[9] T. Furukawa "Structure and Properties of Ferroelectric Polymers", Key Engineering Materials, Vols. 92-93, pp. 15-30, 1994

[10] D. Barazanchy, M. Martinez, B. Rocha, and M. Yanishevsky, “A hybrid structural health monitoring system for the detection and localization of damage in composite structures,”*J. Sensors*, vol. 2014, 2014.

[11] K. S. C. Kuang, “Distributed damage detection of offshore steel structures using plastic optical fiber sensors,” *Sensors Actuators A Phys.*, vol. 229, pp. 59–67, 2015.

[12] A. G. A. Rahman, Z. Ismail, S. Noroozi, and O. Z. Chao, “Study of open crack in rotor shaft using changes in frequency response function phase,” *Int. J. Damage Mech.*, vol. 22, no. 6, pp. 791–807, 2013.

[13] M. B. Duggan and O.O. Ochoa, “Natural Frequency Behavior of Damaged Composite Materials,” *J. Sound Vib.*, vol. 158, no. 3, pp. 545–551, 1992.

[14] G. J. Sylvester, “Electronic Theses and Dissertations Damage Detection in Plate Structures using Guided Ultrasonic Waves,” 2013.

[15] A. S. Islam and K. C. Craig, “Damage detection in composite structures using piezoelectric materials,” vol. 318, 1994.

[16] P. P. Kumar, B. V. Soma Sekhar, K. Balasubramaniam, C. V. Krishnamurthy, and B. Maxfield, “In-situ damage detection in plate structures using PWAS and non-contact Laser Doppler Velocimeter,” *AIP Conf. Proc.*, vol. 894, pp. 1509–1515, 2007.

[17] S. A. M. Al-Said and A. A. Al-Qaisia, “Influence of crack depth and attached masses on beam natural frequencies,” *Int. J. Model. Simul.*, vol. 28, no. 3, pp. 239–247, 2008.

[18] M. Segev-Bar and H. Haick, “Flexible sensors based on nanoparticles,” *ACS Nano*, vol. 7, no. 10, pp. 8366–8378, Sep. 2013

[19] Y. Unno *et al.*, “Development of n-on-p silicon sensors for very high radiation environments,” *Nucl. Instrum. Methods Phys. Res. A, Accel., Spectrometers, Detectors Assoc. Equip.*, vol. 636, no. 1, pp. S24–S30, 2011.

[20] A. G. A. Rahman, Z. Ismail, S. Noroozi, and O. Z. Chao, “Study of open crack in rotor shaft using changes in frequency response function phase,” *Int. J. Damage Mech.*, vol. 22, no. 6, pp. 791–807, 2013.

[21] L. Fixter, C. Williamson, State of the Art Review—Structural Health Monitoring, Smart Materials, Surfaces, and Structures Network (Smart.Mat) Report, 2006.

[22] Cass RB, Khan A, Mohammadi, F. “Innovative ceramic-fiber technology energizes advanced cerametrics”. *Am Ceram Soc Bull,* vol. 82, pp. 14-15, 2003.

[23] Qingliang Liao, Zheng Zhang, Xiaohui Zhang, Markus Mohr, Yue Zhang and Hans-Jorg Fecht “Flexible piezoelectric nanogenerators based on a fiber/ZnO nanowires/paper hybrid structure for energy harvesting” Journ. Of Nano Research, 2014.

[24] Xu Xiao, Longyan Yuan, Jumoen Zhong, Tiapeng Ding, Yu Liu, Zhixiang Cai, Yaogang Rong, Hongwei Han, Jun Zhou and Zhonglin Wang “High-Strain Sensor Based on ZnO Nanowire/Polystyrene Hybridized Flexible Films” Journ. Of Advanced Materials, vol. 23, pp. 5440-5444, 2011.

[25] E.Kymakis and G.A.J. Amaratunga “Single-wall Carbon nanotube/ conjugated polymer Photovoltaic devices”. Journ of Appl. Phys. Lett, vol. 80, no. 1, pp. 110-114, 2002.

[26] V. Choudhary, B. P. Singh, and R. B. Mathur, “Carbon Nanotubes and Their Composites,” *Synth. Appl. Carbon Nanotub. Their Compos.*, pp. 193–222, 2013.

[27] S. Xu, Y.-W. Yeh, G. Poirier, M. C. Mcalpine, R. A. Register, and N. Yao, "Flexible Piezoelectric PMN−PT Nanowire-Based Nanocomposite and Device." *Nano. Lett.* vol. 13, pp 2393-2398.

[28] R. P. Ummer, R. B, C. Thevenot, D. Rouxel, S. Thomas, and N. Kalarikkal, "Electric, magnetic, piezoelectric and magnetoelectric studies of phase pure (BiFeO 3 –NaNbO 3)–(P(VDF-TrFE)) nanocomposite films prepared by spin coating," *RSC Adv.*, vol. 6, no. 33, pp. 28069–28080, 2016

[29] J.-M. Benoit, B. Corraze, S. Lefrant, W. J. Blau, P. Bernier, and O. Chauvet, "Transport properties of PMMA-Carbon Nanotubes composites," *Synth. Met.*, vol. 121, pp. 1215–1216, 2001.

[30] R. B. Mathur, S. Pande, B. P. Singh, and T. L. Dhami, "Electrical and Mechanical Properties of Multi-Walled Carbon Nanotubes Reinforced PMMA and PS Composites, "*Polym. Polym. Compos.* vol. 16, no. 2, pp. 101–113, 2008.

[31] P. Saini, V. Choudhary, B. P. Singh, R. B. Mathur, and S. K. Dhawan, "Polyaniline-MWCNT nanocomposites for microwave absorption and EMI shielding," *Mater. Chem.Phys.*, vol. 113, no. 2–3, pp. 919–926, 2009.

[32] Q. Xiao and X. Zhou, "The study of multiwalled carbon nanotube deposited with conducting polymer for supercapacitor," *Electrochim. Acta*, vol. 48, no. 5, pp. 575–580, 2003.

[33] B. Vigolo *et al.*, "Macroscopic Fibers and Ribbons of Oriented Carbon Nanotubes," *Am.Assoc. Adv. Sci.*, vol. 290, no. 5495, pp. 1331–1334, 2000.

[34] T. M. Wu and E. C. Chen, "Preparation and characterization of conductive carbon nanotube-polystyrene nanocomposites using latex technology," *Compos. Sci. Technol.*, vol. 68, no. 10–11, pp. 2254–2259, 2008.

[35] O. Regev, P. N. B. ElKati, J. Loos, and C. E. Koning, "Preparation of Conductive Nanotube–Polymer Composites Using Latex Technology," *Adv. Mater.*, vol. 16, no. 3, pp. 248–251, 2004

[36] C. Dhand, S. K. Arya, S. P. Singh, B. P. Singh, M. Datta, and B. D. Malhotra, "Preparation of polyaniline/multiwalled carbon nanotube composite by novel electrophoretic route," *Carbon N. Y.*, vol. 46, no. 13, pp. 1727–1735, 2008.

[37] H. Xia, Q. Wang, K. Li, and G. H. Hu, "Preparation of polypropylene/carbon nanotube composite powder with a solid-state mechanochemical pulverization process," *J. Appl. Polym. Sci.*, vol. 93, no. 1, pp. 378–386, 2004.

[38] J. N. Coleman, U. Khan, W. J. Blau, and Y. K. Gun'ko, "Small but strong: A review of the mechanical properties of carbon nanotube-polymer composites," *Carbon N. Y.*, vol.44, no. 9, pp. 1624–1652, 2006.

[39] Dharap, P., Li, Z., Nagarajaiah, S., and Barrera, E. V. "Nanotube film based on single-wall carbon nanotubes for strain sensing," *Nanotechnology*, vol. 15, no 3, pp. 379–382, 2004.

[40] Li, Z., Dharap, P., Nagarajaiah, S., Barrera, E. V., and Kim, J. "Carbon nanotube film sensors," *Advanced Materials*, vol. 16, no. 7, pp 640–643.

[41] Kang, I., Schulz, M. J., Kim, J. H., Shanov, V., and Shi, D. "A carbon nanotube strain sensor for structural health monitoring," *Smart Mater. and Struct.*, vol. 15, no. 3, pp. 737, 2006.

[42] K. J. Loh, J. P. Lynch, B. S. Shim, "Tailoring piezoresistive sensitivity of multilayer carbon nanotube composite strain sensors," *J. Intell. Mater. Syst. Struct.*, vol. 19, no. 7, pp. 747–764, 2008.

[43] Zhang, W., Suhr, J., and Koratkar, N. “Carbon nanotube/polycarbonate composites as multifunctional strain sensors*,” J. Nanosci. Pand Nanotechnol*, vol. 6, no. 4, pp 960-964, 2006.

[44] M. K. Tiwari, A. L. Yarin, C. M. Megaridis, “Electrospun Fibrous Nanocomposites as Permeable, Flexible Strain Sensors,” *J. Appl. Phys.*, 103, 044305–10, 2008.

[45] O.J. *Aldraihem*, *W.N. Akl*, and *A.M. Baz*, "Nanocomposite functional paint sensor for vibration and noise monitoring," *Sensors* and *Actuators* A, vol. *149*, pp. *233-240*, 2009.

[46] S. M. Vemuru, R. Wahi, S. Nagarajaiah, and P. M. Ajayan, “Strain sensing using a multiwalled carbon nanotube film,” Journal of Strain Analysis for Engineering Design, vol. 44, no. 7, pp. 555–562, 2009.

[47] D. Lee, H. P. Hong, C. J. Lee, C. W. Park, and N. K. Min, Microfabrication and characterization of spray-coated single-wall carbon nanotube film strain gauges, *“Nanotechnology*, vol. 22, p. 455301, 2011.

[48] K. J. Loh, J. Kim, J. P. Lynch, N. W. S. Kam, and N. a Kotov, Multifunctional layer-by-layer carbon nanotube–polyelectrolyte thin films for strain and corrosion sensing,” *Smart Mater. Struct.*, vol. 16, no. 2, pp. 429–438, 2007.

[49] M. Laurenti *et al.*, “Evaluation of the piezoelectric properties and voltage generation of flexible zinc oxide thin films,” *Nanotechnology*, vol. 26, no. 21, p. 215704, 2015.

[50] S. Kessler and S. Spearing, “Design of a piezoelectric-based structural health monitoring system for damage detection in composite materials,” *Proc. SPIE*, vol. 4701, pp. 86–96, 2002.

[51] M. Willander, O. Nur, Q. X. Zhao, L. L. Yang, M. Lorenz, B. Q. Cao, J. Z. P_erez, C. Czekalla, G. Zimmermann, M. Grundmann, A. Bakin, A. Behrends, M. Al-Suleiman, A. El-

Shaer, A. C. Mofor, B. Postels, A. Waag, N. Boukos, A. Travlos, H. S. Kwack, J. Guinard, D. L. S. Dang, Nanotech., 20 (2009) 332001.

[52] Z. L. Wang, "ZnO nanowire and nanobelt platform for nanotechnology," *Mat. Sci. and Eng*. vol. 64, no. 3-4, pp 33-71, 2009.

[53] H.Morkoc and U.Ozgur, "Zinc Oxide; Fundamental, Materials and Device Technology", *Wiley-VCh Verlag GmbH & Co. KGaA, Weinheim*, chapter 3, pp. 131, 2009.

[54] O. Dulub, L.A. Boatner, U. Diebold, "Surface Chemistry and Surface Electronic Properties of ZnO single crystals nanorods," *Surf. Sci*., vol. 27, no. 2, pp. 328, 2002.

[55] *B. Meyer*, *D. Marx*, "Density-functional study of the structure and stability of ZnO surfaces". *Phys. Rev. B, vol. 67,035403*, 2003.

[56] P. W. Tasker, "The stability of ionic crystal surfaces "J. *Phys. C: Sol. Sta. Phys*., vol. 12, pp. 49-77, 1979.

[57] Y. Ding, X.Y. Kong, Z. L. Wang, "Doping and Planar defects in the formation of single crystal ZnO nanorings", *Phys. Rev. B*, vol. 70, pp. 235-408, 2004.

[58] Eiman satti Nour, "Development of Zinc Oxide Piezoelectric Nanogenerator for low-frequency applications," Department of Science and Technology, Linkoping University, Sweden, 2016.

[59] Ü. Özgür, Ya. I. Alivov, C. Liu, A. Teke, M. A. Reshchikov, S. Doan, V. Avrutin, S. J. Cho, and H. Morkoç, "A comprehensive review of ZnO materials and devices," *J. Appl. Phys*, vol. 98, no. 4, pp. 41-301, 2005.

[60] K. Subannajui, D. S. Kim, M. Zacharias, "Electrical analysis of individual ZnO nanowires," *J. Appl. Phys*, vol 104, no. 1, pp 014308-014314, 2008.

[61] D.G Thomas, “The exciton spectrum of zinc oxide,” *J. Phys. And Chem. Of Solids,* vol. 15, no 1-2, pp 89-96, 1960.

[62] F. Jones, F. Léonard, A. A. Talin, N. S. Bell, “Electrical conduction and photoluminescence properties of solution-grown ZnO nanowires”, *J. Appl. Phys*. vol. 102, no. 1 pp. 014305,2007.

[63] Z. L. Wang and W. Zhong Lin, “Zinc oxide nanostructures: growth, properties, and applications,” *J. Phys. Condens. Matter*, vol. 16, no. 25, pp. R829–R858, 2004.

[64] S. Hingorani, V. Pillai, P. Kumar, M. S. Multani, and D. O. Shah, “Microemulsion Mediated Synthesis of Zinc-Oxide Nanoparticles for Varistor Studies,” *Mater. Res. Bull.*, vol. 28, no. 12, pp. 1303–1310, 1993.

[65] H. Rodríguez-Tobías, G. Morales, O. Rodríguez-Fernández, and P. Acuña, “Mechanical and UV-shielding properties of in situ synthesized poly(acrylonitrile-butadiene styrene)/ zinc oxide nanocomposites,” *J. Appl. Polym. Sci.*, vol. 127, no. 6, pp. 4708–4718, 2013.

[66] H.N. Chandrakala, B. Ramaraj, Shivakumaraiah, Joong Hee Lee, Siddaramaiah, “Polyvinyl alcohol-carbon coated zinc oxide nanocomposites: Electrical, optical, structural and morphological characteristics,” vol. 580, no. 1, pp. 392-400, 2013.

[67] P. Jood *et al.*, “Al-doped zinc oxide nanocomposites with enhanced thermoelectric properties,” *Nano Lett*, vol. 11, no. 10, pp. 4337–4342, 2011.

[68] H.-M. Lin, S.-J. Tzeng, P.-J. Hsiau, and W.-L. Tsai, “Electrode effects on gas sensing properties of nanocrystalline zinc oxide,” *Nanostructured Mater.*, vol. 10, no. 3, pp. 465–477, 1998.

[69] J. A. Rodriguez, T. Jirsak, J. Dvorak, S. Sambasivan, and D. Fischer, “Reaction of NO with Zn and ZnO: Photoemission, XANES, and Density Functional Studies on the Formation of NO3,” no. 2, pp. 319–328, 2000.

[70] P. X. Gao, Y. Ding, W. Mai, W. L. Hughes, C. Lao, and Z. L. Wang, "Conversion of zinc oxide nanobelts into superlattice-structured nanohelices," *Science (80-.).*, vol. 309, no. 5741, pp. 1700–4, 2005.

[71] L. Gao, Q. Li, W. Luan, H. Kawaoka, T. Sekino, and K. Niihara, "Preparation and Electric Properties of Dense Nanocrystalline Zinc Oxide Ceramics," *Am. Ceram. Soc.*, vol. 85, no. 4, pp. 1016–1018, 2002.

[72] N. F. C. Ooray, K. K. Ushiya, A. F. Ujimaki, and D. O. Kumura, "Optimization of Al-doped ZnO Window Layers for Large-Area Cu (InGa) Se 2 -Based Modules by RF / DC / DC Multiple Magnetron Sputtering," *Jpn. J. Appl. Phys.*, vol. 38, no. 11, pp. 6213–6218,1999.

[73] A. Becheri, M. Durr, P. Lo Nostro, and P. Baglioni, "Synthesis and characterization of zinc oxide nanoparticles: Application to textiles as UV-absorbers," *J. Nanoparticle Res.*, vol. 10, no. 4, pp. 679–689, 2008.

[74] H. K. Yadav and V. Gupta, "A comparative study of ultraviolet photoconductivity relaxation in zinc oxide (ZnO) thin films deposited by different techniques," *J. Appl. Phys.*, vol. 111, no. 10, 2012.

[75] M. D. Spring, "Design of Zinc Oxide Tetrapod Devices," 2007.

[76] B. Kumar, K. Smita, L. Cumbal, and A. Debut, "Green approach for fabrication and applications of zinc oxide nanoparticles," *Bioinorg. Chem. Appl.*, vol. 2014, 2014.

[77] F. Verbakel, S. C. J. Meskers, and R. A. J. Janssen, "Electronic memory effects in diodes of zinc oxide nanoparticles in a matrix of polystyrene or poly(3-hexylthiophene)," *J. Appl. Phys.*, vol. 102, no. 8, 2007.

[78] A. Yadav, Virendra Prasad. A.A. Kathe, Sheela Raj, Deepti Yadav, C. Sundaramoorthy, N. Vigneshwaran., “Functional finishing in cotton fabrics using zinc oxide nanoparticles, *“Bull. Mater. Sci.*, vol. 29, no. 6, pp. 641–645, 2006.

[79] S. Talam, S. R. Karumuri, and N. Gunnam, “Synthesis, Characterization, and Spectroscopic Properties of ZnO Nanoparticles,” *ISRN Nanotechnol.*, vol. 2012, pp. 1–6, 2012.

[80] A. Moezzi, A. M. McDonagh, and M. B. Cortie, “Zinc oxide particles: Synthesis, properties, and applications,” *Chem. Eng. J.*, vol. 185–186, pp. 1–22, 2012.

[81] C. J. Hu, Y. H. Lin, C. W. Tang, M. Y. Tsai, W. K. Hsu, and H. F. Kuo, “ZnO-coated carbon nanotubes: Flexible piezoelectric generators,” *Adv. Mater.*, vol. 23, no. 26, pp. 2941–2945, 2011

[82] H. Gullapalli *et al.*, “Flexible piezoelectric ZnO-paper nanocomposite strain sensor, ”*Small*, vol. 6, no. 15, pp. 1641–1646, 2010.

[83] F. N. Meyers, K. J. Loh, J. S. Dodds, and A. Baltazar, “Active sensing and damage detection using piezoelectric zinc oxide-based nanocomposites., *Nanotechnology*, vol.24, no. 18, p. 185501, 2013.

[84] K. J. Loh and D. Chang, “Zinc oxide nanoparticle-polymeric thin films for dynamic strain sensing,” *J. Mater. Sci.*, vol. 46, no. 1, pp. 228–237, 2011.

[85] Endo, M., Vapor-Grown Carbon Fibers, *Ph.D. Thesis*, Nagoya: Nagoya Univ., 1978

[86] lijima, S.; "Helical Microtubules of Graphitic Carbon", *Nature* 354 (6348), pp. 56- 58,1991.

[87] Philippe Poncharal, Z. L. Wang, Daniel Ugarte, Walt A. de Heer, “Electrostatic Deflections and Electromechanical Resonances of Carbon Nanotubes”, Science, vol 283, no.5407, pp 1513-1516, 1999.

[88] Min-Feng Yu, Oleg Lourie, Mark J. Dyer, Katerina Moloni, Thomas F. Kelly, Rodney S. Ruoff, "Strength and Breaking Mechanism of Multiwalled Carbon Nanotubes Under Tensile Load", Science, vol 287, no. 5508, pp 637-640, 2000.

[89] Jean-Paul Salvetat, G. Andrew D. Briggs, Jean-Marc Bonard, Revathi R. Bacsa, Andrzej J. Kulik, Thomas Stöckli, Nancy A. Burnham, and László Forró, "Elastic and Shear Moduli of Single-Walled Carbon Nanotube Ropes'', *Physical Review Letters*, vol. 82, no. 5, pp 944-947, 1991.

[90] Jayaprakash Khanderi, Rudolf C. Hoffmann, Aleksander Gurlo and Jörg J. Schneider, "Synthesis and sensory response of ZnO decorated carbon nanotubes", *Journal of Materials Chemistry*, vol 19, no 28, pp 5039-5046, 2009.

[91] L. Hu, Y. Zhao, K. Ryu, C. Zhou, J. F. Stoddart, and G. Grüner, "Light-induced charge transfer in pyrene/CdSe-SWNT hybrids". *Adv. Mater*. vol 20, pp. 939, 2008.

[92] T. T. Ebbesen, T. W., Lezec H. J., Hiura H., Bennett J. W., Ghaemi H. F, "Electrical conductivity of individual carbon nanotubes," *Nature*, vol. 382. pp. 54–56, 1996.

[93] N. Ramaratnam, Arun, and Jalili, "Reinforcement of Piezoelectric Polymers with Carbon Nanotubes: Pathway to Next-generation Sensors," *J. Intell. Mater. Syst. Struct.*, vol. 17, no. 3, pp. 199–208, 2006.

[94] K. J. Loh, J. Kim, J. P. Lynch, N. W. S. Kam, and N. a Kotov, Multifunctional layer-by-layer carbon nanotube–polyelectrolyte thin films for strain and corrosion sensing," *Smart Mater. Struct.* vol. 16, no. 2, pp. 429–438, 2007.

[95] I. Kang, M. J. Schulz, J. H. Kim, V. Shanov, and D. Shi, "A carbon nanotube strain sensor for structural health monitoring," *Smart Mater. Struct*, vol. 15, pp. 737–748, 2006.

[96] G. T. Pham, Y. Bin Park, Z. Liang, C. Zhang, and B. Wang, “Processing and modeling of conductive thermoplastic/carbon nanotube films for strain sensing,” *Compos. Part B Eng.*, vol. 39, no. 1, pp. 209–216, 2008.

[97] S. V Anand and D. Roy Mahapatra, “Quasi-static and dynamic strain sensing using carbon nanotube/epoxy nanocomposite thin films,” *Smart Mater. Struct.* vol. 18, no. 4, p. 45013, 2009.

[98] N. Saber *et al.*, “Superior piezoelectric composite films: taking advantage of carbon nanomaterials,” *Nanotechnology*, vol. 25, no. 4, p. 45501, 2014.

[99] M. Dutta and D. Basak, “Multiwalled carbon nanotubes/ZnO nanowires composite structure with enhanced ultraviolet emission and faster ultraviolet response,” *Chemical Physics Letters*, vol. 48, pp. 253-257, 2009.

[100] Zhang Jin, Ruijie Wang and C.Y. Wang, “Piezoelectric ZnO-CNT nanotubes under axial strain and electrical voltage, *Jour. of Low-dimensional systems and nanostructures*, vol. 46, pp. 105-112, 2012.

[101] N. Venugopal, B.C. Yang and T. Ko, “ZnO/CNT nanocomposite electrode for aqueous electrochemical supercapacitor,” *Jour. of Materials Research Innovators*, vol. 16, no. 2, pp 96-100, 2013.

[102] Takadama, H.; Hashimoto, M.; Takigawa, Y.; Mizuno, M.; Kokubo, T. Effect of melt flow rate of polyethylene on bioactivity and mechanical properties of polyethylene/titania composites. In *Bioceramics 16, Key Engineering Materials: Proceedings of the 16th International Symposium on Ceramics in Medicine*; Barbosa, M.A., Monteiro, F.J., Correia, R., Leon, B., Eds.; Trans Tech Publications Inc.: Uetikon-Zurich, Switzerland, vol. 254–256, pp. 569–572, 2004.

[103] Jankong, S. Srikulkit. “Preparation of polypropylene/hydrophobic silica nanocomposites.” *Jour. Met. Mater. Miner.* vol *18*, pp. 143–146, 2008.

[104] R. Andrews, D. Jacques, D. Qian, and T. Rantell, “Multiwall carbon nanotubes: Synthesis and application,” *Acc. Chem. Res.*, vol. 35, no. 12, pp. 1008–1017, 2002.

[105] C. Liao, M. Zhang, M. Y. Yao, T. Hua, L. Li, and F. Yan, “Flexible organic electronics in biology: Materials and devices,” *Adv. Mater.*, vol. 27, no. 46, pp. 7493–7527, 2015.

[106] J. van den Brand *et al.*, “Flexible and stretchable electronics for wearable health devices,” *Solid-State Electron.*, vol. 113, pp. 116–120, Nov. 2015.

[107] T. Someya and T. Sekitani, “Bionic skins using flexible organic devices,” in *Proc. ESSDERC*, Sep. 2014, pp. 68–71.

[108] C.-Y. Chen, C.-L. Chang, T.-F. Chien, and C.-H. Luo, “Flexible PDMS electrode for one-point wearable wireless bio-potential acquisition,” *Sens. Actuators A, Phys.*, vol. 203, pp. 20–28, Dec. 2013.

[109] J.-H. Moon, D. H. Baek, Y. Y. Choi, K. H. Lee, H. C. Kim, and S.-H. Lee, “Wearable polyimide–PDMS electrodes for intrabody communication,” *J. Micromech. Microeng.*, vol. 20, no. 2, p. 025032, 2010.

[110] Y. Qin *et al.*, “Lightweight, superelastic, and mechanically flexible graphene/polyimide nanocomposite foam for strain sensor application,” *ACS Nano*, vol. 9, no. 9, pp. 8933–8941, 2015.

[111] T. Fujita, S. Shiono, K. Kanda, K. Maenaka, H. Hamada, and K. Higuchi, “Flexible sensor for human monitoring system by using P(VDF/TrFE) thin film,” in *Proc. ICETET*, Nov. 2012, pp. 75–79.

[112] A. P. Tjahyono *et al.*, “A five-fingered hand exoskeleton driven by pneumatic artificial muscles with novel polypyrrole sensors,” *Ind. Robot, Int. J.*, vol. 40, no. 3, pp. 251–260, 2013.

[113] D. Ha, W. N. de Vries, S. W. M. John, P. P. Irazoqui, and W. J. Chappell, “Polymer-based miniature flexible capacitive pressure sensor for intraocular pressure (IOP) monitoring inside a mouse eye,” *Biomed. Microdevices,* vol. 14, pp. 207–215, Feb. 2012.

[114] Y. Hasegawa, M. Shikida, D. Ogura, Y. Suzuki, and K. Sato, “Fabrication of a wearable fabric tactile sensor produced by artificial hollow fiber,” *J. Micromech. Microeng.*, vol. 18, no. 8, p. 085014, 2008.

[115] S. Gong *et al.*, “A wearable and highly sensitive pressure sensor with ultrathin gold nanowires,” *Nature Commun.*, vol. 5, Feb. 2014, Art. no. 3132.

[116] M. Amjadi, A. Pichitpajongkit, S. Lee, S. Ryu, and I. Park, “Highly stretchable and sensitive strain sensor based on silver nanowireelastomer nanocomposite,” *ACS Nano,* vol. 8, no. 5, pp. 5154–5163, 2014.

[117] J. Wang *et al.*, “A highly sensitive and flexible pressure sensor with electrodes and elastomeric interlayer containing silver nanowires,” *Nanoscale*, vol. 7, no. 7, pp. 2926–2932, 2015.

[118] S. L. P. Tang, “Recent developments in flexible wearable electronics for monitoring applications,” *Trans. Inst. Meas. Control*, vol. 29, nos. 3–4, pp. 283–300, 2007.

[119] S.-H. Bae, Y. Lee, B. K. Sharma, H.-J. Lee, J.-H. Kim, and J.-H. Ahn, “Graphene-based transparent strain sensor,” *Carbon*, vol. 51, pp. 236–242, Jan. 2013.

[120] H. Tian, Y. Shu, Y.L Cui, W.T. Mi, Y.Yang, D. Xie and T.L Ren "Scalable fabrication of high-performance and flexible graphene strain sensors," *Nanosc.*, vol. 6, no. 2, pp. 699–705, 2014.

[121] K. K. Sadasivuni, A. Kafy, L. Zhai, and J. Kim, "Transparent and flexible cellulose nanocrystal/reduced graphene oxide film for proximity sensing," *Small*, vol. 11, no. 8, pp. 994–1002, 2015.

[122] B. S. Shim, W. Chen, C. Doty, C. Xu, and N. A. Kotov, "Smart electronic yarns and wearable fabrics for human biomonitoring made by carbon nanotube coating with polyelectrolytes," *Nano Lett.*, vol. 8, no. 12, pp. 4151–4157, 2008.

[123] D. J. Cohen, D. Mitra, K. Peterson, and M. M. Maharbiz, "A highly elastic, capacitive strain gauge based on percolating nanotube networks," *Nano Lett.*, vol. 12, no. 4, pp. 1821–1825, 2012.

[124] K. Jost, D. Stenger, C.R. Perez, J.K. McDonough, K. Lian, Y. Gogotsi and G. Dion., "Knitted and screen printed carbon-fiber supercapacitors for applications in wearable electronics," *Energy, Environ. Sci.*, vol. 6, no. 9, pp. 2698–2705, 2013.

[125] I. Locher and G. Tröster, "Screen-printed textile transmission lines," *Textile Res. J.*, vol. 77, no. 11, pp. 837–842, 2007.

[126] W. Haung, T.J. Albert, K. Nuwaysir, A. Pitas, T. Richmond, T. Gorski, J.P. Berg, J. Ballin, M. McCornick, J. Norton, T. Pollock, T. Sumwalt, L. Butcher, D. Porter, M. Molla, C. Hall, F. Blattner, M.R. Sussman, R.L. Wallace, F. Cernina, R.D. Green "Gene expression analysis using oligonucleotide arrays produced by maskless photolithography," *Genome Res.*, vol. 12, no. 11, pp. 1749–1755, 2002.

[127] A. J. Birnbaum, H. Kim, N. A. Charipar, and A. Piqué, “Laser printing of multi-layered polymer/metal heterostructures for electronic and MEMS devices,” *Appl. Phys. A, Mater. Sci. Process.*, vol. 99, no. 4, pp. 711–716, 2010.

[128] C.-T. Wang, K.-Y. Huang, D. T. W. Lin, W.-C. Liao, H.-W. Lin, and Y.-C. Hu, “A flexible proximity sensor fully fabricated by Inkjet printing,” *Sensors*, vol. 10, no. 5, pp. 5054–5062, 2010.

[129] L. Wang, J. Yin, H. Zhang, J. Wu, X. Shi, E. Crew, Z. Xu, Q. Rendeng, S. Lu, M. Poliks, B. Sammakia and C.J. Zhong., “Flexible chemiresistor sensors: Thin film assemblies of nanoparticles on a polyethylene terephthalate substrate,” *J. Mater. Chem.*, vol. 20, no. 5, pp. 907–915, 2010.

[130] B. Hu, W. Chen, and J. Zhou, “High performance flexible sensor based on inorganic nanomaterials,” *Sens. Actuators B, Chem.*, vol. 176, pp. 522–533, Jan. 2013.

[131] K.-P. Yoo, L.-T. Lim, N.-K. Min, M. J. Lee, C. J. Lee, and C. W. Park, “Novel resistive-type humidity sensor based on multiwall carbon nanotube/polyimide composite films,” *Sens. Actuators B, Chem.*, vol. 145, no. 1, pp. 120–125, 2010.

[132] K. F. Lei, K.-F. Lee, and M.-Y. Lee, “Development of a flexible PDMS capacitive pressure sensor for plantar pressure measurement,” *Microelectron. Eng.*, vol. 99, pp. 1–5, Nov. 2012.

[133] S. Kamila, “Introduction, classification and applications of smart materials: An overview,” *Am. J. Appl. Sci.*, vol. 10, no. 8, pp. 876–880, 2013.

[134] G. Akhras, “Smart Materials and Smart Systems for the Future,” *Can. Mil. J.*, pp. 25–32, 2000.

[135] Y. J. Yan and L. H. Yam, “Online detection of crack damage in composite plates using embedded piezoelectric actuators/sensors and wavelet analysis,” *Compos. Struct.* vol. 58, no. 1, pp. 29–38, 2002.

[136] G. Dib, E. Koricho, O. Karpenko, M. Haq, and L. Udpa, “Feasibility of PZT Ceramics for Impact Damage Detection in Composite Structures,” *AIP Conf. Proc.*, vol. 1650, pp.1072–1080, 2015.

[137] M. Dziendzikowski, A. Kurnyta, K. Dragan, S. Klysz, and A. Leski, “In situ BarelyVisible Impact Damage detection and localization for composite structures using surface mounted and embedded PZT transducers: A comparative study,” *Mech. Syst. Signal Process.*, vol. 78, no. 2016, pp. 91–106, 2015.

[138] Y. Jiang, H. Hamada, S. Shiono, K. Kanda, T. Fujita, K. Higuchi and K. Maenaka, “A PVDF-based flexible cardiorespiratory sensor with independently optimized sensitivity to heartbeat and respiration,” *Proc. Eng.*, vol. 5, pp. 1466–1469, Jan. 2010.

[139] S. Choi and Z. Jiang, “A novel wearable sensor device with conductive fabric and PVDF film for monitoring cardiorespiratory signals,” *Sens. Actuators A, Phys.*, vol. 128, no. 2, pp. 317–326, 2006.

[140] J. A. Patterson, D. C. McIlwraith, and G.-Z. Yang, “A flexible, low noise reflective PPG sensor platform for ear-worn heart rate monitoring,” in *Proc. BSN*, Jun. 2009, pp. 286–291.

[141] W. Tao, T. Liu, R. Zheng, and H. Feng, “Gait analysis using wearable sensors,” *Sensors*, vol. 12, no. 12, pp. 2255–2283, 2012.

[142] A. Nag, S. C. Mukhopadhyay, and J. Kosel, “Flexible carbon nanotube nanocomposite sensor for multiple physiological parameter monitoring,” *Sens. Actuators A, Phys.*, vol. 251, pp. 148–155, Nov. 2016.

[143] S. Yao and Y. Zhu, “Wearable multifunctional sensors using printed stretchable conductors made of silver nanowires,” *Nanoscale*, vol. 6, no. 4, pp. 2345–2352, 2014.

[144] H. Kudo, T. Sawada, E. Kazawa, H. Yoshida, Y. Iwasaki, and K. Mitsubayashi, “A flexible and wearable glucose sensor based on functional polymers with Soft-MEMS techniques,” *Biosensors Bioelectron.*, vol. 22, no. 4, pp. 558–562, 2006.

[145] Y. H. Kwak, D.S. Choi, Y.N. Kim, H. Kim, D.H. Yoon, S.S. Ahn, J.W. Yang, W.S. Yang and S. Seo, “Flexible glucose sensor using CVD-grown graphene-based field effect transistor,” *Biosensors Bioelectron.*, vol. 37, no. 1, pp. 82–87, 2012.

[146] S. Iguchi, H. Kudo, T. Saito, M. Ogawo, H. Saito, K. Otsuka, A. Funakubo and K. Mitsubayashi., “A flexible and wearable biosensor for tear glucose measurement,” *Biomed. Microdevices*, vol. 9, no. 4, pp. 603–609, 2007.

[147] X. Wang, Y. Gu, Z. Xiong, Z. Cui, and T. Zhang, “Silk-molded flexible, ultrasensitive, and highly stable electronic skin for monitoring human physiological signals,” *Adv. Mater.*, vol. 26, no. 9, pp. 1336–1342, 2014.

[148] R. B. Katragadda and Y. Xu, “A novel intelligent textile technology based on silicon flexible skins,” *Sens. Actuators A, Phys.*, vol. 143, no. 1, pp. 169–174, 2008.

[149] S. Bauer, “Flexible electronics: Sophisticated skin,” *Nature Mater.*, vol. 12, no. 10, pp. 871–872, 2013.

[150] D. Son, J. Lee, S. Qiao, R. Ghaffari, J. Kim, J.E Lee, C. Song, S.J. Kim, D.L. Lee, S.W. Jun, S. Yang, M. Park, J. Shin, K. Do, M. Lee, K. Kang, C.S. Hwang, N. Lu, T. Hyeon and D.H. Kim “Multifunctional wearable devices for diagnosis and therapy of movement disorders,” *Nature Nanotechnol.*, vol. 9, no. 5, pp. 397–404, 2014.

[151] S. Choi, J. Park, W. Hyun, J. Kim, J. Kim, Y.B. Lee, C. Song, H.J. Hwang, J.H. Kim, T. Hyeon and D.H. Kim, "Stretchable heater using ligand-exchanged silver nanowire nanocomposite for wearable articular thermotherapy," *ACS Nano*, vol. 9, no. 6, pp. 6626–6633, 2015.

[152] I. R. Minev, P. Musienko, A. Hirsch, Q. Barrad, N. Wenger, E.M. Moraud, J. Gander, M. Capogrosso, T. Milekovic, L. Asboth, R.F. Torres, N. Vachicouras, Q. Liu, N. Pavlova, S. Dius, A. Larmagnac, J. Voros, S. Micera, Z. Suo, G. Courtine and S.P. Lacour., "Electronic dura mater for long-term multimodal neural interfaces," *Science*, vol. 347, no. 6218, pp. 159–163, 2015.

[153] J. Di, S. Yao, Y. Ye, Z. Cui, J. Yu, T.K. Ghosh, Y. Zhu and Z. Gu, "Stretch-triggered drug delivery from wearable elastomer films containing therapeutic depots," *ACS Nano*, vol. 9, no. 9, pp. 9407–9415, 2015.

[154] C. Pang, G.Y. Lee, T.I. Kim, S.M. Kim, H.N. Kim, S.H. Ahn and K.Y. Suh., "A flexible and highly sensitive strain-gauge sensor using reversible interlocking of nanofibres," *Nature Mater.*, vol. 11, no. 9, pp. 795–801, 2012.

[155] T. Yamada, Y. Hayamizu, Y. Yamamoto, Y. Yomogida, A. Izadi-Najafabadi, D.N.Futaba and K. Hata, "A stretchable carbon nanotube strain sensor for human-motion detection," *Nature Nanotechnol.*, vol. 6, pp. 296–301, Mar. 2011.

[156] J. J. Park, W. J. Hyun, S. C. Mun, Y. T. Park, and O. O. Park, "Highly stretchable and wearable graphene strain sensors with controllable sensitivity for human motion monitoring," *ACS Appl. Mater. Int.*, vol. 7, no. 11, pp. 6317–6324, 2015.

[157] Y. Zang, F. Zhang, C. Di, and D. Zhu, “Advances of flexible pressure sensors toward artificial intelligence and healthcare applications,” *Mater. Horizons*, vol. 2, no. 2, pp. 140–156, 2015.

[158] G. Schwartz, B.C.-K. Tee, J. Mei, A.L. Appleton, D.H. Kim, H. Wang and Z. Bao., “Flexible polymer transistors with high pressure sensitivity for application in electronic skin and health monitoring,” *Nature Commun.*, vol. 4, p. 1859, May 2013.

[159] Mohammad Ali Darabi, Ali Khosrozadeh, Quan Wang, Malcolm Xing, “Gum Sensor: A Stretchable, Wearable, and Foldable Sensor Based on Carbon Nanotube/Chewing Gum Membrane.” *ACS Applied Materials & Interfaces*, vol. 7 no.47, pp. 26195-26205, 2015.

[160] Yan, C.; Wang, J.; Kang, W.; Cui, M.; Wang, X.; Foo, C. Y.; Chee, K. J.; Lee, P. S. “Highly Stretchable Piezoresistive Graphene−Nanocellulose Nano paper for Strain Sensors.” *Adv. Mater.*, vol. 26, no. 13, pp. 2022-2027, 2014.

[161] Xiao, X.; Yuan, L.; Zhong, J.; Ding, T.; Liu, Y.; Cai, Z.; Rong, Y.; Han, H.; Zhou, J.; Wang, Z. L. “High-Strain Sensors Based on ZnO Nanowire/Polystyrene Hybridized Flexible Films." *Adv. Mater.* , vol. 23 no. 45, pp. 5440−5444, 2011.

[162] Zhao, J.; Zhang, G.-Y.; Shi, D.-X. Review of Graphene-Based Strain Sensors. *Chin. Phys. B*, vol. 22 no. 5, pp. 057701−057709, 2013.

[163] Herrmann, J.; Müller, K.-H.; Reda, T.; Baxter, G. R.; Raguse, B.; de Groot, G. J. J. B.; Chai, R.; Roberts, M.; Wieczorek, L. Nanoparticle Films as Sensitive Strain Gauges. *Appl. Phys. Lett.* , vol. 91, no. 18, pp. 183105−183107, 2007.

[164] Xu, F.; Zhu, Y. Highly Conductive and Stretchable Silver Nanowire Conductors. *Adv. Mater.*, vol. 24, no. 37, pp. 5117−5122, 2012.

[165] Osho S. “Design, Fabrication and Analysis of a Piezoelectric Nanocomposite Paint. (Published Master’s thesis), University of Manitoba, Winnipeg, Canada. 2017.

[166] Omer Guler. “ The effect of an excessive amount of Carbon nanotubes on the properties of Zinc oxide- Carbon nanotube nanocomposites”. Sci Eng Compos Mater., Vol. 23, pp. 1-5, 2014.

[167] Yu Kuronuma, Tomo Takeda, Yasuhide Shindo, Fumio Narita and Zhijuan Wei. “Electrical resistance-based strain sensing in Carbon nanotubes/polymer composites under tension: Analytical modelling and experiments.” *Composites Science and Technology*, vol 72, no. 14, pp. 1678-1682, 2012.

[168] Kara Evanoff, Javed Khan, Alexander A. Balandin, Alexandre Magasinko, W. Jud Ready, Thomas F. Fuller and Gleb Yushin, “Towards ultrathick battery electrodes: Aligned carbon nanotube-enabled architecture,” *Adv. Mater.*, vol. 24, no. 4, pp. 533–537, 2012.

[169] Chiaki Sotowa, Gaku Origi, Masataka Takeuchi, Yoshiyuki Nishimura, Kenji Takeuchi, In Young Jang, Yong Jung Kim, Takuya Hayashi, Yoong Ahm Kim, Morinobu Endo, and Mildred S. Dresselhaus ., “The Reinforcing Effect of Combined Carbon Nanotubes and Acetylene Blacks on the Positive Electrode of Lithium-Ion Batteries,” *ChemSucChem*, vol. 1, pp. 911–915, 2008.

[170] L. Dai, D. W. Chang, J.-B. Baek, and W. Lu, “Carbon nanomaterials for advanced energy conversion and storage.” *Small*, vol. 8, no. 8, pp. 1130–66, 2012.

[171] De Vivo B, Lamberti P, Spinelli G, Tucci V, Vertuccio L, Vittoria V. “Simulation and experimental characterization of polymer/carbon nanotubes composites for strain sensor applications.” *J Appl Phys*. vol. 116, no. 5, pp 054307-054321, 2014.

[172] Sheng P, Sichel EK, Gittleman JI. “Fluctuation-induced tunneling conduction in carbon-polyvinylchloride composites.” *Phys Rev Lett*, vol. 40, no. 18, pp. 1197-1200, 1978.

[173] Theodosiou TC, Saravanos DA. “Numerical investigation of mechanisms affecting the piezoresistive properties of CNT-doped polymers using multiscale models.” *Compos Sci Technol,* vol. 70, no. 9, pp. 1312-1320, 2010.

[174] Yang L, Han J. “Electronic structure of deformed carbon nanotubes.” *Phys Rev Lett.* Vol. 85, no. 1, pp. 154-157, 2000.

[175] Park M, Kim H, Youngblood JP. “Strain-dependent electrical resistance of multiwalled carbon nanotube/polymer composite films.” *Nanotechnology*. vol. 19, no. 5, pp. 1-7, 2008.

[176] Paleo-Vieto AJ, van Hattum F, Pereira J, Rocha JG, Silva J, Sencadas V, Lanceros- Mèndez S. “The piezoresistive effect in polypropylene the piezoresistive effect in polypropylene-carbon nanofibre composites obtained by shear extrusion.” *Smart Mater Struct*, vol. 19, no. 6, pp. 1-7, 2010.

[177] Wichmann MHG, Buschhorn ST, Gehrmann J, Schulte K. “Piezoresistive response of epoxy composites with carbon nanoparticles under tensile load.” *Phys Rev*. vol. 8, no. 24, 2009.

[178] Giovanni Spinelli, Patrizia Lamberti, Vincenzo Tucci, Luigi Vertuccio, and Liberata Guadagno. “Experimental and theoretical study on piezoresistive properties of a structural resin reinforced with carbon nanotubes for strain sensing and damage monitoring.” *Composite Part B*. vol. 145, pp. 90-99, 2018.

[179] Morteza Amjadi, Ki-Uk Kyung, Inkyu Park and Mentin Sitti. “Stretchable, Skin-Mountable, and Wearable Strain Sensors and Their Potential Applications: A review.” *Advanced Functional Materials*, vol. 25, no. 11, pp. 1678-1698, 2016.

[180] Jacob M. Wernik and Shaker A. Meguid. “Recent Developments in Multifunctional Nanocomposites using Carbon Nanotubes.” *Applied Mechanics Review*. Vol. 63, no. 5, pp. 050801-050841, 2010.

[181] Jin G., Qunfeng C., Ju L., Jianwen B., Shu L., Ying T., Zhiyong L., Chuck Z., and Chuck Z. “Thermal conductivity of MWCNT/epoxy Composites: The effects of length, alignment and functionalization.” J. Carbon, Volume 50, Issue 6, May 2012, Pages 2083-2090.

[182] Meyer J. “Glass transition temperature as a guide to selection of polymers suitable for PTC materials.” *Polym Eng Sci*, vol. 13, no. 6, pp. 462– 486, 1973.

[183] Meyer J. “Stability of polymer composites as positive-temperature coefficient resistors.” *Polym Eng Sci*, vol. 14, no 10, pp. 706-716, 1974.

[184] Ohe K, Naito Y. “A new resistor having an anomalously large positive temperature coefficient.” *Jpn J Appl Phys*, vol. 10, no. 1, pp. 99–108, 1971.

[185] Klason C, Kubat J. “Anomalous behavior of electrical conductivity and thermal noise in carbon black-containing polymers at Tg and Tm.” *J Appl Polym Sci*, vol. 19, no. 3, pp. 831–845, 1975.

[186] Voet A. “Temperature effect of electrical resistivity of carbon black filled polymers.” *Rubber Chem Technol*, vol. 54, no. 1, pp. 42–50, 1981.

[187] Allak HK, Brinkman AW, Woods J. “I–V characteristics of carbon black-loaded crystalline polyethylene.” *J Mater Sci*, vol. 28, no. 1, pp. 117– 20, 1993.

[188] X.J. He, J.H. Du, Z. Ying, H.M Cheng, and X.J. He. “Positive temperature coefficient effect in multiwalled carbon nanotube/ high-density polyethylene composite” American Institute of Physics, vol. 86, no. 3, pp 062112-062115, 2005.

[189] Feng J., Chan C-M. “Double positive temperature coefficient effects of carbon black-filled polymer blends containing two semi-crystalline polymers”. *Polymer*, vol.41, no. 12, pp. 4559–4565, 2000.

[190] Feng J., Chan C-M. “Positive and negative temperature coefficient effects of an alternating copolymer of tetrafluoroethylene-ethylene containing carbon black filled HDPE particles.” *Polymer*, vol. 41, no. 19, pp. 7279–7282, 2000.

[191] Hindermann-Bischoff M., Ehrburger-Dolle F. “Electrical conductivity of carbon black-polyethylene composites experimental evidence of the change of cluster connectivity in the PTC effect.” *Carbon*, vol. 39, no. 3, pp. 375–382, 2001.

[192] Zhang C., Ma C. A., Wang P., Sumita M. “Temperature dependence of electrical resistivity for carbon black filled ultra-high molecular weight polyethylene composites prepared by hot compaction.” *Carbon*, vol. 43, no. 12, pp. 2544–2553, 2005.

[193] Wernik JM, Meguid SA. “Recent developments in multifunctional nanocomposites using carbon nanotubes.” *ASME Appl Mech*, vol. 63, no. 5, pp. 050801, 2010.

[194] Gojny, F. H., Wichmann, M. H. G., Fiedler, B., and Schulte, K., 2005, “Influence of Different Carbon Nanotubes on the Mechanical Properties of Epoxy Matrix Composites-A Comparative Study,” *Compos. Sci. Technol.*, vol .65, no. 5-6, pp. 2300–2313, 2005.